A Dissertation for the Degree of Doctor of Philosophy

Study on the Functional Role of Glutathione Peroxidase 3 as a Tumor Suppressor in Prostate Cancer

전립선암에서 GPx3의 종양 억제 유전자로서의 기능에 관한 연구

Seo-Na Chang, D.V.M.

August 2017

Department of Veterinary Pathobiology and Preventive Medicine
(Major: Laboratory Animal Medicine)
Graduate School of Seoul National University

Study on the Functional Role of Glutathione Peroxidase 3 as a Tumor Suppressor in Prostate Cancer

By
Seo-Na Chang, D.V.M.

A dissertation submitted to the Graduate School in
Partial fulfillment of the requirement for the degree of
DOCTOR OF PHILOSOPHY

Supervisor: Prof. Jae-Hak Park, D.V.M., Ph.D.

Department of Veterinary Pathobiology and Preventive Medicine
(Major: Laboratory Animal Medicine)
Graduate School of Seoul National University

Seo-Na Chang

June 2017

Dissertation Committee:

Kang, Kyung-Sun
(Chairman)

Park, Jae-Hak	**Chae, Chanhee**
(Vice chairman)	**(Member)**
Ryu, Doug-Young	**Lee, Hui-Young**
(Member)	**(Member)**

ABSTRACT

Study on the Functional Role of Glutathione Peroxidase 3 as a Tumor Suppressor in Prostate Cancer

Seo-Na Chang, D.V.M.

Department of Veterinary Pathobiology and Preventive Medicine

(Major: Laboratory Animal Medicine)

Graduate School of Seoul National University

Supervisor: Prof. Jae-Hak Park, D.V.M., Ph.D.

Prostate cancer is the most frequently diagnosed cancer in Western men, and more men have been diagnosed at younger ages in recent years. A high-fat Western-style diet is a known risk factor for prostate cancer. Dietary fat increases oxidative stress and levels of reactive oxygen species (ROS) that interfere with cellular processes. Among the antioxidant enzymes, glutathione peroxidase 3 (GPx3) is an essential component of the cellular detoxification system. GPx3 is

involved in protecting cells from oxidative damage, and down-regulated levels of expression have been found in prostate cancer samples. However, it remains unknown whether GPx3 expression can regulate the development of prostate cancers and the role and mechanism of GPx3 in prostate tumorigenesis has never been directly tested. In addition, little is known about the effect of GPx3 expression on tumor invasion in prostate cancer. In this study, to study the functional role of GPx3 as a tumor suppressor in prostate cancer, I evaluated the expression and function of GPx3 during prostate cancer tumorigenesis in transgenic adenocarcinoma of the mouse prostate (TRAMP) mouse model and PC-3 human prostate cancer cells (Figure I).

Chapter I study evaluated the association between dietary animal fat and expression of antioxidant GPx3, in the early stages of transgenic adenocarcinoma of the mouse prostate (TRAMP) mice. Six-week-old male nontransgenic and TRAMP mice were placed on high animal-fat (45% Kcal fat) or control (10% Kcal fat) diets and sacrificed after 5 or 10 weeks. The histopathological score increased with age and high-fat diet consumption. TRAMP mice fed a high-animal fat diet showed decreased GPx3 expression both at the mRNA and protein levels. GPx3 decreased both at the mRNA and protein levels in mouse prostate. GPx3 mRNA expression decreased (~36.27% and ~23.91%, respectively) in the anterior and dorsolateral prostate of TRAMP mice fed a high-fat diet compared to TRAMP mice fed a control diet. Cholesterol treatment increased PC-3 human prostate cancer cell proliferation, decreased GPx3 mRNA and protein levels, and increased H_2O_2 levels

in culture medium. Moreover, increasing GPx3 mRNA expression by troglitazone (TGZ) in PC-3 cells decreased cell proliferation and lowered H_2O_2 levels. Overall, these results suggest that dietary fat enhances prostate cancer progression, possibly by suppressing GPx3 expression and increasing proliferation of prostate intraepithelial neoplasia (PIN) epithelial cells.

In Chapter II, I evaluated the tumorigenic role of the GPx3 *in vivo* by using GPx3 deficient TRAMP mice. TRAMP / GPx3 (–/–) KO mice were generated by cross-mating of TRAMP mutant mice and GPx3 mutant mice. Prostate cancer incidence and progression were determined in TRAMP, TRAMP / GPx3 (+/–) HET, and TRAMP / GPx3 (–/–) KO mice at 8, 16, and 20 weeks of age. GPx3 expression was decreased in TRAMP mice during progression of prostate cancer in a fashion that parallels observations in human prostate cancer. GPx3 was not detected in GPx3 KO mice both in mRNA and protein levels. Disruption of GPx3 expression in TRAMP mice increased the genitourinary tract weights and the histopathological scores in each lobe with increased proliferation rates. Moreover, deletion of one (+/–) or both (–/–) alleles of GPx3 gene resulted in increase in prostate cancer incidence with activated Wnt/β-catenin pathway. These results provide the first *in vivo* molecular genetic evidence that GPx3 does indeed function as a tumor suppressor during prostate carcinogenesis**.**

Chapter III study aimed to determine the inhibitory effect and mechanism of TGZ on cell growth, migration, and invasion using prostate cancer cell line PC-3. TGZ is a synthetic peroxisome proliferator-activated receptor γ (PPARγ) ligand

that exhibits potential antitumor effects on a broad range of cancers, including prostate cancer. Cell migration and invasion were assessed with wound healing assay and transwell assay, respectively. The expression levels of mRNA and protein were determined by quantitative reverse transcription-polymerase chain reaction and western blotting. TGZ dose-dependently inhibited cell migration and invasion of PC-3 cells. In addition, TGZ increased the mRNA and protein levels of E-cadherin and GPx3 in PC-3 human prostate cancer cells. In addition, GW9662, a PPARγ antagonist, attenuated the increased mRNA and protein levels of E-cadherin and GPx3, suggesting that PPARγ-dependent pathway was involved. Taken together, these results suggest that the anti-migration and anti-invasion effect of TGZ on PC-3 prostate cancer cells is, at least in part, mediated through upregulating E-cadherin and GPx3. I also conclude that PPARγ could be used as a potential therapeutic target for the prevention and treatment of prostate cancer cell invasion and metastasis.

These findings further support the important role that GPx3 plays as a tumor suppressor provide an insight into disease pathogenesis, and indicate that it may serve as a substrate for translational investigations in prostate cancer. Additionally, identification of mechanisms that cooperate with loss of GPx3 to promote tumorigenesis may provide additional therapeutic targets.

.

Keywords : prostate cancer, GPx3, TRAMP, tumor suppressor, tumorigenesis, dietary animal fat

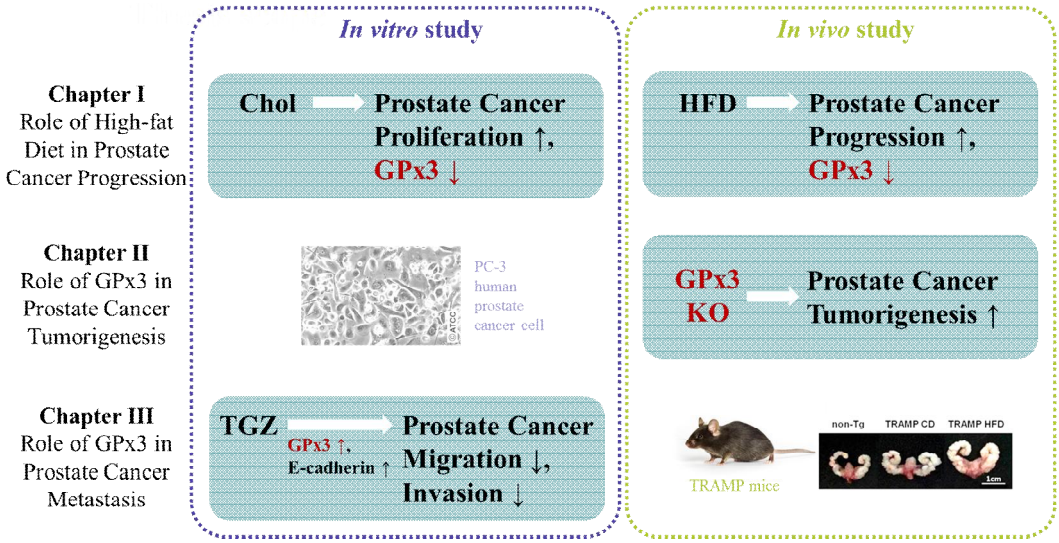

Figure I. Thesis scope. Summary of thesis findings on the functional role of glutathione peroxidase 3 (GPx3) as a tumor suppressor in prostate cancer.

Student Number : 2010-21652

LIST OF ABBREVIATION

AP	Anterior prostate
Axin2	Axis inhibition protein 2
CD	Control diet
Chol	Cholesterol
DLP	Dorsolateral prostate
EMT	Epithelial–mesenchymal transition
FoxA2	Forkhead box protein A2
GPx	Glutathione peroxidase
HET	Heterotype (+/–)
HFD	High-fat diet
HRP	Horse radish peroxidase
MD	Moderately differentiated adenocarcinoma
MMP7	Matrix metalloproteinase-7
PD	Poorly differentiated adenocarcinoma
PHY	Phyllodes-like tumor
PIN	Prostate intraepithelial neoplasia
PPARγ	Peroxisome proliferator-activated receptor γ

ROS	Reactive oxygen species
TGZ	Troglitazone
TRAMP	Transgenic adenocarcinoma of the mouse prostate
TZDs	Thiazolidinediones
VP	Ventral prostate
WD	Well-differentiated adenocarcinoma

TABLE OF CONTENTS

LITERATURE REVIEW

Obesity and prostate cancer

Obesity is associated with increased risk of various cancer types (1). There is consistent and convincing evidence for an association between obesity and increased incidence of high-risk or aggressive prostate cancer (2-4). Among numerous nutritional factors associated with obesity and prostate cancer risk, a number of epidemiological studies have reported that total fat intake was associated with the increased risk of advanced cancer and that this relationship was primarily related to animal fat consumption (Table I) (5-8).

Xue and co-workers have reported that Western-style diet induced epithelial cell proliferation in anterior and dorsal lobes of the C57BL/6J mouse prostate (9). In this study, which used wild-type mice, they suggested that dietary fat may have a role in human prostatic carcinogenesis, since the anterior and the dorsal lobes of the mouse prostate are homologous with the human prostate. Prostate cancer development also has been shown to be responsive to diet-induced obesity using transgenic mouse models. Llaverias and colleagues used the well-characterized TRAMP mouse model to examine the role of dietary fat and cholesterol in the progression of prostate cancer (10). For tumor studies, 8-week-old males were distributed into either a control diet (containing 4.5% fat and 0.002% cholesterol (wt/wt)) of Western diet (containing 21.2% fat and 0.2% cholesterol (wt/wt)) and sacrificed at 28 weeks of age. They conclude that consumption of a Western-type

diet accelerated prostate tumor incidence and tumor burden compared to mice fed a control diet, showing increased histological grade of prostate tumors (10). Blando *et al*. showed that high-fat diet enhanced but 30% calorie restriction diet reduced growth factor (Akt/mTORC1 and Stat3) and inflammatory (NFκB, cytokines) signaling, affecting prostate cancer progression in Hi-Myc mice (11). Kobayashi *et al*. also used Hi-Myc mice, which develop PIN to invasive adenocarcinoma due to the overexpression of human c-Myc in the mouse prostate. When placed on high-fat or low-fat diets with equal caloric intake, Hi-Myc mice showed delay in carcinogenesis of prostate cancer through suppression of the IGF-Akt pathway (12). In another study, high-fat diet promoted prostate cancer progression with increased inflammatory response in the PTEN haploinsufficient mouse model (13).

Dietary fat acts as an oxidant, which increases oxidative stress and levels of ROS that interfere with cellular process altering levels of key transcription factors (14, 15). The intricate interplay among dietary fat, antioxidant system, and genetic factors modulates prostate cancer risk.

Table I. Dietary fats in prostate cancer chemoprevention.

Dietary agent	Model system	Mechanism of action	References
Low-fat diet	Black and white men; randomized crossover studies	Decreased androgen levels	(16, 17)
Low-fat diet	Healthy men	Lower testosterone	(18-20)
Low-fat vs Western diet	Men with prostate cancer	Serum from men undergoing a low-fat diet reduced LNCaP prostate cancer cell growth	(21)
Low-fat diet	Healthy men	Serum from men undergoing a low-fat diet reduced PC-3 prostate cancer cell growth	(22)
High-fat and low-fat diet	Hi-Myc mouse transgenic	Delay in transition from PIN to carcinoma with low-fat diet; via IGF-Akt pathway	(12)
High-fat and 30% calorie restriction diet	Hi-Myc mouse transgenic	Reduction in prostate cancer progression; via growth factor (Akt/mTORC1 and Stat3) and inflammatory (NFκB, cytokines) signaling	(11)
High-fat diet	TRAMP mouse transgenic	Enhanced PIN development in early stages; via reducing GPx3	(23)
Western diet (High-fat and high-cholesterol)	TRAMP mouse transgenic	Accelerated prostate tumor incidence and tumor burden with Western-type diet	(24)
High-fat diet	PTEN haploinsufficient mouse	Promoted prostate cancer progression with increased inflammatory response	(13)

Oxidative stress and prostate cancer

Oxidative stress occurs following an imbalance between the production of ROS and the antioxidative capacity of a cell. In healthy cells, ROS are continuously formed in the cell and synchronously scavenged by antioxidant mechanisms (25). Several predisposing factors including an increase in the ROS production and/or a simultaneous impairment of antioxidative system have been postulated to contribute to prostate cancer carcinogenesis, progression and metastasis (26).

Prostate cancer cells contain higher amounts of ROS and oxidative DNA damage than normal prostate tissues, which is a hallmark of the aggressive phenotype of this disease (27-29). In prostate cancer, increased ROS production caused by various processes that lead to oxidative stress, including intrinsic conditions such as metabolic alterations, receptor activation and mitochondrial dysfunctions, and also extrinsic environmental factors such as inflammation, xenobiotic metabolism and hypoxia (14, 28). The impairment of enzymatic (such as superoxide dismutase, catalase, and glutathione peroxidase) and non-enzymatic antioxidative defence systems also cause oxidative stress in prostate cancer (15, 26, 28).

The elevated ROS levels in cells hyperactivate signaling pathways to promote tumorigenesis, leading to activation of NF-κB, PI3K, HIFs and MAP kinases, and others (30-32). It suggested to be related prostate cancer cell proliferation, apoptosis, angiogenesis, and metastasis (31, 33).

Levels of oxidative markers have been associated with prostate cancer. Patients with prostate cancer possess lower antioxidant enzyme levels in prostate tissues

compared to both healthy controls and men with benign prostatic hyperplasia (34, 35). For variations in genes involved in oxidative stress and antioxidative defense pathways modify prostate cancer, ROS-depletion with use of antioxidants scavenges ROS and results in blocking of ROS signaling and suppressing cancer development (36, 37).

Glutathione peroxidases family

GPx3 belongs to the family of glutathione peroxidases. It is well known that glutathione peroxidases are among the most important ROS scavengers that can protect cells from oxidative damage. In mammals, eight types of GPx (GPx1-GPx8) have been so far identified, and they are widely expressed in various tissues (38-40). According to phylogeny, the GPx family consists of three evolutionary groups arising from a Cys-containing ancestor: GPx1/GPx2, GPx3/GPx5/GPx6 and GPx4/GPx7/GPx8 (41). Selenium-containing GPxs are GPx1–4 and 6 (GPx6 is a selenoprotein only in humans), and their non-selenium congeners are GPx5, 7 and 8. Selenium-containing GPxs (cellular GPx (GPx1), gastrointestinal GPx (GPx2), extracellular GPx (GPx3), and phospholipid hydroperoxide GPx (GPx4)) have been studied to identify its role in different stages of carcinogenesis.

GPx1

GPx1 was the first mammalian identified as a selenoprotein in 1973 (42, 43). GPx1 is found in red cells, liver, lung, and kidney (44). Subcellularly, it is identified in the cytosol, nucleus, and mitochondria (45). GPx1 is a potent antioxidant enzyme, and cannot be replaced by any other selenoprotein in protecting from generalized oxidative stress (41). GPx1 KO mice were killed by severe oxidative stress regardless of selenium supplementation (46).

Related to neurodegenerative disease, GPx1 increased surrounding the damaged brain regions in Parkinson's disease patients (47). GPx1 KO increased vulnerability

to neurotoxins, whereas overexpression of GPx1 decreased neurotoxicity in mice (48-50). McClung *et al*. has been reported that GPx1-overexpressing mice showed hyperglycemia, hyperinsulinemia, and elevated plasma leptin. They showed the development of insulin resistance and obesity. GPx1 is thought to play a role in regulating diabetes disease (51).

GPx1 and cancer. GPx1 expression is decreased in prostate cancer (52, 53), in colorectal cancer (54), and in breast cancer cell lines (55). Overexpression of GPx1 in Ras-overexpressing pancreatic cancer cells reduced cell growth *in vitro*. When injected into nude mice, tumor growth was suppressed *in vivo* (56). Knockdown of GPx1 in human prostate cancer cells enhanced radiation-induced micronuclei formation (57). Inhibition of GPx1 promoted invasion and migration in esophageal cancer cells (58).

GPx2

GPx2 is mainly expressed in the whole gastrointestinal system and suggested to act as a barrier against absorption of food-born ROS (39). It subcellularly accumulates in the cytosol and nucleus (45). GPx2 has anti-inflammatory activity in the intestine (59, 60). GPx2 KO mice showed no obvious phenotype, but they showed increased apoptosis at colonic crypt bases, an area essential for the self-renewal of the intestinal epithelium, and increased mitosis in the middle parts of the crypts indicating an extension of the proliferative area (61). They were

predisposed to UV-induced squamous cell carcinoma formation (62). GPx2 is also identified as a major oxidative-stress inducible cellular GPx isoform in the lungs (63). GPx2 was expressed upon induction with allergic airway inflammation, suggesting important role in protection from allergen-induced disease (64). GPx2 has been revealed to be regulated by NF-E2-rebulated factor (Nrf2), a redox-sensitive basic leucine zipper transcription factor (65), and p63, a member of the p53 family (66).

GPx2 and cancer. GPx2 expressions in cancer cells are different depend on the developmental stage of malignant transformation. GPx2 is increased during squamous cell carcinoma development (67), in Barrett's esophagus (68), in breast cancer (69), and in colorectal cancer tissue (70-72). In contrast, GPx2 is decreased in prostatic intraepithelial neoplasia caused by loss of function of Nkx3.1 gene (73). Deficiency of GPx2 caused growth inhibition in vitro and in vivo. Patients with high GPx2 expression in biopsy specimen had lower survival than those with no GPx2, suggesting GPx2 as a prognostic marker in castration-resistant prostate cancer (74).

GPx3

GPx3 is a secreted protein also found in the cytosol (45). It is identified in various organs such as kidney, lung, epididymis, *vas deferens*, placenta, seminal vesicle, heart, and muscle (38-40, 44). GPx3 KO mice are viable, and tolerated

selenium deficiency without any ill effects (75). GPx3, a causal gene for obesity (76), was decreased in the adipose tissue of obese animal models (77). These reports suggested the role of GPx3 in regulating not only oxidative stress but also obesity-related metabolic diseases. Overexpression of GPx3 in adipocytes improved insulin resistance with decreased inflammatory gene expression (77). Similarly, plasma GPx3 levels were reduced in patients with type 2 diabetes and in obese mice (78).

GPx3 and cancer. GPx3 is highly expressed in the healthy tissues, and usually down-regulated in cancer tissues. GPx3 is strongly downregulated in prostate cancer (79), in thyroid cancer samples of different origin (80, 81), in colorectal cancer (82), and endometrial tumors (83). Downregulation of GPx3 by hypermethylation was found in breast, gastric, ovarian, esophagus, and other solid tumors (70, 84-94) including prostate cancer (23, 95, 96).

GPx3 KO enhances inflammation and injury, proliferation, and DNA damage in tumors of mice subjected to a colitis-associated carcinogenesis protocol, suggesting that GPx3 loss may lead to increased tumor promotion (97). Silencing GPx3 expression promoted tumor metastasis in human thyroid and gastric cancer (93, 94). Overexpression of GPx3 in prostate cancer cell lines suppressed colony formation and cell proliferation (23, 79, 98) and decreased invasiveness in a transmigration assay *in vitro* (79). Xenografted human prostate cancer cells expressing GPx3 showed reduction in tumor volume, prevention of metastasis, and reduction of

mortality *in vivo* (79). Its activity was significantly decreased in the blood of patients with breast cancer, gastric cancer and colorectal cancer (99). In prostate cancer, GPx3 has been shown to have a negative correlation with poor clinical outcomes (79, 100). Thus, GPx3 is suggested to be a novel tumor suppressor.

GPx4

GPx4 is broadly present in different tissues (44). It is subcellularly present in the nucleus, cytosol, mitochondria and bound to membranes (45). GPx4 is indispensable for mouse development and obviously has more important functions. For GPx4 has a crucial role during embryo development (101-103), GPx4 KO was finally lethal in mice (104, 105). Overexpression of GPx4 protected mice against oxidative insults (106). GPx4 heterozygous knockout mice showed longer life span compared to the wild-type mice, through increased sensitivity to oxidative stress-induced apoptosis (107). GPx4 has recently been revealed to have an essential function in neural development and neuropathological disease, protecting from injury and further cell damage (108, 109).

GPx4 and cancer. GPx4 expression has been reported to be decreased in pancreatic cancer cells (110) and in breast invasive ductal carcinoma (111). In hepatocellular carcinoma tissues, GPx4 had a overexpression compared to cirrhotic counterparts (non-tumor tissues) and GPx4 expression increased correlated positively with disease activity (112). Variant in GPx4 was detected in colorectal

cancer (113), in breast cancer (114), and in prostate cancer (115). These results propose its role in cancer development.

GPx5

GPx5 is androgen-regulated and seleno-independent epididymal GPx in mice, rats, pigs, monkey and humans (41). It is present in epithelial cells and in the lumen of the epididymis (116). GPx5 plays an important role in sperm maturation, protecting spermatozoa from oxidative injuries (117, 118). There are little reports concerning the expression and function of GPx5 in other tissues. In cancer research, GPx5 was identified to be associated with overall survival among patients with non-small cell lung cancer (119). In another study, the expression of GPx5 was shown to be downregulated in human breast cancer cells compared with non-cancerous breast cells on the basis of the ER status (120).

GPx6

GPx6 is a close homolog of plasma GPx3 and a selenoprotein in humans (121). GPx6 has not been purified and kinetic analyses remain to be investigated. GPx6 was downregulated by heat stress in the intestinal cells, suggesting its function in potential intestinal damage induced by heat stress (122). In a mouse model of Huntington's disease, GPx6 was demonstrated as a modulator of mutant toxicity and overexpression of GPx6 promoted both behavioral and molecular phenotype of this nervous disease (123). In one study, GPx6 variant was shown to be associated

with serious invasive epithelial ovarian cancer subtype (124).

GPx7

GPx7 is a non-selenocysteine containing phospholipid hydroperoxide GPx without GPx enzymatic activity (125). It is found in the lumen of the endoplasmic reticulum (126). GPx7 KO mice showed systemic oxidative stress, increased carcinogenesis, and shortened lifespan, suggesting essential role of GPx7 in physiological homeostasis (127). Otherwise, deficiency of GPx7 is thought to lead to obesity in mice and humans (128). GPx7 KO mice exhibited increased obesity with increased fat mass and adipocyte hypertrophy. Genetic variant of GPx7 with reduced expression in adipose tissue showed an association with higher body mass index in humans. Also, GPx7 has been suggested as a candidate gene directly affecting key biological process in pancreatic beta-cells, thus influencing diabetes risk (129).

GPx7 and cancer. GPx7 was downregulated in human breast cancer cells *in vitro* (120). Variant of a GPx7 gene was detected in primary lung cancer patients (130). Whereas, GPx7 showed an upregulated expression both in human hepatocellular carcinoma cells and tissues (112, 131). GPx7 deficiency has shown to promote the Barrett's carcinogenesis, inducing NF-κB activation through ROS independent manner (132).

GPx8

GPx8 has been detected in a phylogenetic analysis as a novel member belonging to the GPx family in mammalia and amphibia (133). It is an endoplasmic reticulum-resident protein (126). GPx8 is identified as a lung-abundant enzyme in the study using a mouse model of influenza (134). Influenza toxicity can be caused by oxidative stress, and this identification enables to understand the biology after infection. GPx8 recently has been identified as a cellular substrate of the Hepatitis C virus NS3-4A protease (135). Little is known about its regulation and biological function.

CHAPTER I

High Animal-Fat Intake Enhances Prostate Cancer Progression and Reduces Glutathione Peroxidase 3 Expression in Early Stages of TRAMP Mice

1.1 INTRODUCTION

Prostate cancer has long been considered a disease of older men. However, in recent years more men have been diagnosed with prostate cancer at younger ages; the proportion of men aged ≤ 55 years at diagnosis increased from 2.3% between 1988 and 1991 to 9.0% between 2002 and 2003 (136). In a recent analysis of US incidence trends during the last 20 years (1986–2005), the most dramatic growth in prostate incidence occurred in men aged 20–49 years (137). The most significant results of these analyses are the opposite of what might be expected with increasing comorbidity associated with age, because younger men have equivalent or worse outcomes compared with older men, suggesting a shorter latency and a different biology (136). In this respect, there is an urgent need to investigate the cause of early-onset prostate cancer.

Several studies have suggested that a Western diet is a major contributory factor to the early-onset of prostate cancer (138-141). Prostate cancer is the most commonly diagnosed cancer in Western men, and its incidence is rising rapidly in most countries, including low-risk populations (142, 143). These changes lagged ~10 years behind the inception of the nutrition transition toward a Westernized diet (144). Epidemiological studies have shown that when people move from a non-Western society (countries with low incidence) to a Western country (high incidence), such as the US, the incidence of prostate cancer increases, as they adopt new Western behaviors, such as changes in diet (145-148). Because 40% of total energy intake in a traditional Western diet is derived from fat (139), dietary fat has

been suggested as an important risk factor for prostate cancer, but this theory is controversial (15, 24, 149). Some studies have demonstrated that obesity is associated with a significantly increased risk of high-grade prostate cancer and in prostate cancer mortality, particularly in young men (140, 141).

Furthermore, several studies have observed an association between early-onset prostate cancer risk and a relatively high intake of animal fat (138, 139). These studies indicated that animal fat may be a promoter and may act by shortening the prostate cancer latency period. However, research is too limited to support strong conclusions regarding the role of animal fat in prostate cancer tumorigenesis, and the mechanisms remain unclear.

Dietary fat increases oxidative stress and levels of reactive oxygen species (ROS) that interfere with cellular processes (15). Healthy cells are attacked by free radicals, which cause peroxidation and eventually DNA damage. Oxidative stress-related markers are associated with prostate tissue in patients with prostate cancer (34). Among the antioxidant enzymes, glutathione peroxidase 3 (GPx3), also known as plasma or extracellular glutathione peroxidase, is an essential component of the cellular detoxification system. GPx3 belongs to the family of glutathione peroxidases that are among the most important ROS scavengers, as they catalyze the reduction of hydrogen peroxide, organic hydroperoxides, or lipid peroxides by reduced glutathione and protect cells from oxidative damage (150).

GPx3 is often downregulated in cancer including prostate cancer (79, 82, 151-153). It was recently reported that GPx3 expression is inversely related to prostate

cancer progression *in vivo* and that overexpression of GPx3 has tumor suppressing activity both *in vitro* and *in vivo* (79). GPx3 is downregulated in normal mouse prostate by a high-fat diet with increased oxidative stress (100). Yet, no studies have found that the decrease in GPx3 during progression of prostate cancer results from dietary fat intake. Thus, I investigated the association between dietary fat intake and GPx3 expression in prostate cancer tissue using transgenic adenocarcinoma of the mouse prostate (TRAMP) mice.

1.2 MATERIALS AND METHODS

1.2.1 Prostate cancer cell line

The human PC-3 prostate cancer cell line was obtained from the American Type Culture Collection (Manassas, VA, USA). The cells were cultured in RPMI (Gibco, Grand Island, NY, USA) with 10% fetal bovine serum (FBS) (Gibco) and 1% penicillin/streptomycin (Gibco) at 37°C in 95% air/5% CO_2. Cholesterol (Sigma, St. Louis, MO, USA) and troglitazone (Sigma) were dissolved in 100% ethanol (Merck and Co., Inc., Darmstadt, Germany) at 10 mM and 16 mM, respectively. The volumes were such that the final ethanol concentration was 0.25% (154). Ethanol alone at the same final concentration was added to the control.

1.2.2 Cell proliferation assay

The proliferation potential of cells was measured using the thiazolyl blue tetrazolium bromide (MTT; Sigma) assay, which is based on the ability of live cells to convert tetrazolium salt into purple formazan. Briefly, PC-3 cells were seeded in 96-well plates at a density of 4×10^3 per well in 200 μl media. After 24 h, the medium was changed to 1% FBS-RPMI for 24 h, and the cells were supplemented with cholesterol at concentrations of 2.5, 5, and 25 μM or vehicle (ethanol) for 48 h. The medium was then replaced with 100 μl of MTT (diluted to 1 mg/ml in FBS-free medium, from a stock solution of 10 mg/ml) for 3 h at 37°C. The supernatant

was removed, 100 μl of DMSO was added to each well to dissolve the formazan crystals, and the plates were agitated for 5 min at room temperature. The absorbance was read at 555 nm on an EL800 microplate reader (BIO-TEK Instruments, Winooski, VT, USA). All treatments were performed in triplicate.

1.2.3 Measurement of H_2O_2 level

H_2O_2 levels in culture medium were measured using the Amplex Red Hydrogen Peroxide/Peroxidase Assay kit (Invitrogen, Carlsbad, CA, USA). Briefly, 50 μl of 10-fold diluted culture medium was loaded into individual wells of a microplate. The working solution of 100 μM Amplex Red and 0.2 U/ml horse radish peroxidase (HRP) was added to each microplate well, and the absorbance was read at 560 nm after 30 min. H_2O_2 levels were expressed as fold change over the control. All treatments were performed in triplicate.

1.2.4 Western blot analysis

Cell lysates (40 μg) were resolved by sodium dodecyl sulfate polyacrylamide gel electrophoresis before transferring the proteins to nitrocellulose membranes and probing with mouse monoclonal anti-GPx3 primary antibody (Abcam, Inc., Cambridge, MA, USA) and rabbit polyclonal anti-β-actin primary antibody (Cell Signaling Technology, Inc., Danvers, MA, USA). Blots were then incubated with HRP-conjugated goat anti-mouse and anti-rabbit IgG secondary antibodies (Zymed, San Francisco, CA, USA), respectively. The blots were developed with

chemiluminescence using the Supersignal West Pico chemiluminescent substrate (Pierce, Rockford, IL, USA).

1.2.5 GPx assay

Cellular GPx activity was determined using an assay kit (Cayman Chemical Co., Ann Arbor, MI, USA) that measures GPx activity indirectly by a coupled reaction with glutathione reductase. The assay was performed according to the manufacturer's instructions.

1.2.6 Real-time reverse transcription-polymerase chain reaction (PCR)

Total RNA was isolated using TRIzol Reagent™ (Invitrogen) and cDNAs were synthesized using an M-MLV cDNA Synthesis kit (Enzynomics, Daejeon, South Korea) following the supplier's instructions. Real-time reverse transcription-PCR was performed using specific primers to human *GPx3* (GenBank accession no. NM_002084.3), mouse *GPx3* (GenBank accession no. NM_008161.3), human *GPx1* (GenBank accession no. NM_000581.2), human *GPx2* (GenBank accession no. NM_002083.3), human *Prdx6* (GenBank accession no. NM_004905.2), human *Mn SOD* (GenBank accession no. NM_000636.2), human *Cu/Zn SOD* (GenBank accession no. NM_000454.4), and human *catalase* (GenBank accession no. NM_001752.3) with iQ SYBR Green Supermix (Bio-Rad Laboratories, Hercules, CA, USA) on a CFX Connect Real-Time PCR Detection system (Bio-Rad). Human

beta-actin and mouse glyceraldehyde-3-phosphate dehydrogenase gene expression were used for cDNA normalization. mRNA fold changes were quantified using the comparative CT ($2^{-\Delta\Delta Ct}$) cycle (ΔCt) method (155). The primer sequences used in this study are shown in Table 1-1.

Table 1-1. Primer sequences used for RT-PCR.

Primer	Sequences
GPx3 (human)	<F> 5' – ACATGCCTACAGGTATGCGT – 3'
	<R> 5' – GAGCAGAACAATTGGACCTA – 3'
GPx3 (mouse)	<F> 5' – CTCCTGAGACCAGCCAAGAC – 3'
	<R> 5' – GAGCCTAAGCCTGAATGCAC – 3'
GPx1 (human)	<F> 5' – CGCTTCCAGACCATTGACATC – 3'
	<R> 5' – CGAGGTGGTATTTTCTGTAAGATCA – 3'
GPx2 (human)	<F> 5' – CAGTCTCAAGTATGTCCGT – 3'
	<R> 5' – AGGCTCAATGTTGATGGT – 3'
Prdx6 (human)	<F> 5' – GTGTGATGGTCCTTCCAACC – 3'
	<R> 5' – CTGACATCCTCTGGCTCACA – 3'
Mn SOD (human)	<F> 5' – GGAAGCCATCAAACGTGACT – 3'
	<R> 5' – CTGATTTGGACAAGCAGCAA – 3'
Cu/Zn SOD (human)	<F> 5' – AGGGCATCATCAATTTCGAG – 3'
	<R> 5' – TGCCTCTCTTCATCCTTTGG – 3'
Catalase (human)	<F> 5' – TTTCCCAGGAAGATCCTGAC – 3'
	<R> 5' – ACCTTGGTGAGATCGAATGG – 3'
Actin (human)	<F> 5' – CATGTACGTTGCTATCCAGGC – 3'
	<R> 5' – CTCCTTAATGTCACGCACGAT – 3'
Gapdh (mouse)	<F> 5' – TGACCACAGTCCATGCCATC – 3'
	<R> 5' – GACGGACACATTGGGGGTAG – 3'

1.2.7 Animals and diets

All animal studies were approved by the Institutional Animal Care and Use Committee of Seoul National University. Mice were kept on a 12-h light/dark cycle with *ad libitum* access to food and water. TRAMP mice expressing the SV40 large T-antigen under control of the prostate-specific rat probasin promoter were purchased from The Jackson Laboratory (Bar Harbor, ME, USA). At 6 weeks of age, TRAMP males and their nontransgenic littermates were randomly assigned to the control (10% Kcal fat) or high-fat (45% Kcal fat) diet (Research Diets Inc., New Brunswick, NJ, USA; D12450B and D12451, respectively). The compositions of the diets are listed in Table 1-2. Each group was divided into two subgroups depending on the age at the time of sacrifice (11 or 16 weeks old). The number of mice in each experimental group was 10–13. Body weight was measured weekly.

Table 1-2. Ingredients in the experimental diets.

Ingredient	Control diet		High fat diet	
	g	% of energy	g	% of energy
Casein	19.0	19.7	23.3	19.7
L-Cystine	0.3	0.3	0.3	0.3
Corn starch	29.9	31.1	8.5	7.2
Maltodextrin 10	3.3	3.5	11.7	9.9
Sucrose	33.2	34.5	20.1	17.0
Cellulose	4.7	0.0	5.8	0.0
Soybean oil	2.4	5.5	2.9	5.5
Lard	1.9	4.4	20.7	39.4
Mineral mix	0.9	0.0	1.2	0.0
DiCalcium phosphate	1.2	0.0	1.5	0.0
Calcium carbonate	0.5	0.0	0.6	0.0
Potassium citrate	1.6	0.0	1.9	0.0
Vitamin mix	0.9	1.0	1.2	1.0
Choline bitartrate	0.2	0.0	0.2	0.0
Total	100.0	100.0	100.0	100.0

1.2.8 Tissue excision and processing

At the time of sacrifice, epididymal white adipose tissue and the urogenital tract (UGT: prostate, bladder, seminal vesicle, and testicles) were quickly excised and weighed. The ventral, dorsal, lateral, and anterior prostate lobes were dissected under a stereoscope, from one side and frozen in liquid nitrogen for RT-PCR. The remainder of each prostate was fixed in 10% buffered formalin and processed for standard paraffin sections.

1.2.9 Histopathological analysis

Sections (3 μm) were obtained from the paraffin-embedded blocks and stained with hematoxylin and eosin (H&E). The mouse prostate lobes (ventral, dorsal, lateral, and anterior) were identified histopathologically in H&E-fixed sections using previously published criteria (156). Briefly, we evaluated each lobe of the prostate and assigned a prostate intraepithelial neoplasia (PIN) grade as PIN I (relative small foci with one or two layers of atypical cells), PIN II (larger foci with two or more layers of atypical cells that do not fill the lumen), PIN III (the foci of atypical cells fill, or almost fill, the lumen of the ducts), or PIN IV (the foci of atypical cells fill the lumen of the ducts), based on the most severe lesion within the lobe. The distribution of lesions within each individual lobe was also estimated as focal, multifocal, or diffuse. The distribution and lesion grade were then combined to calculate a distribution-adjusted PIN score ranging from 0 to 12 that could be used for statistical analysis. Sections were examined in a blinded manner

under light microscopy (Olympus AX70, Tokyo, Japan).

1.2.10 Immunohistochemistry

Sections (3 μm) were dewaxed with xylene, rehydrated through a graded ethanol series, and washed in distilled water. The sections were treated with Proteinase K for antigen retrieval and then endogenous peroxidase was blocked using 3% H_2O_2 in methanol for 10 min at room temperature. The tissue sections were then blocked with 1% bovine serum albumin for 30 min, and reacted with the mouse monoclonal anti-GPx3 primary antibody (Abcam) for 12–14 h at 4°C. Thereafter, sections were washed three times with PBS and incubated for 2 h with HRP-conjugated goat anti-mouse IgG secondary antibody (Zymed). Staining specificity was verified by omitting the primary antibody. Positive reactions were visualized with 3, 3′-diaminobenzidine and H_2O_2. Sections were counterstained lightly with hematoxylin. We evaluated each lobe of the prostate and assessed the intensity and pattern of the staining. A 6-point scale was used to assess the intensity of the staining from score 0 (absent expression) to score 5 (intense, wide spread expression).

1.2.11 Statistical analysis

All data are presented as mean ± standard error. Statistically significant ($P < 0.05$) data were further analyzed by Student's *t*-tests.

1.3 RESULTS

1.3.1 Cholesterol treatment increases human prostate cancer cell proliferation and decreases GPx3 expression in PC-3 human prostate cancer cells

PC-3 human prostate cancer cells were treated with different concentrations (2.5, 5, and 25 μM) of cholesterol. Cell proliferation was measured by the MTT assay after 48 h of treatment (Figure 1-1A). Cholesterol treatment enhanced cell proliferation in a dose-dependent manner and a 32.2% increase in growth rate was observed in cells treated with 25 μM cholesterol from that of vehicle-treated cells.

To determine if the cholesterol treatment affected GPx3 levels in prostate cancer cells, I measured GPx3 mRNA levels and found that GPx3 mRNA expression was reduced in a time- and dose-dependent manner (Figure 1-1B). Clearly, 25 μM cholesterol loading significantly downregulated the GPx3 mRNA levels by 0.5-fold at 12 h and 0.36-fold at 24 h. Once again, H_2O_2 levels in culture media increased significantly after cholesterol treatment in a time- and dose-dependent manner (Figure 1-1C). Cholesterol loading (25 μM) significantly increased the H_2O_2 levels by ~14.86% at 12 h and ~ 43.3% at 24 h.

A Western blot analysis with anti-GPx3 monoclonal antibody was performed to determine the amount of GPx3 expressed in the extracted protein preparation (Figure 1-1D). Unlike the GPx3 mRNA level, the protein immunoblotting analysis

did not show any significant difference in the expression of GPx3 in vehicle- and cholesterol-treated PC-3 cells at 12 h. However, particularly at 24 h, GPx3 expression decreased significantly in the 25 μM cholesterol treatment (by 0.5-fold).

Cellular GPx activity was also determined in the PC-3 cell line after 24 h of cholesterol treatment (Figure 1-1E). Cholesterol loading reduced GPx activity in a dose-dependent manner and significantly downregulated GPx activity by 0.49 fold at 25 μM of cholesterol.

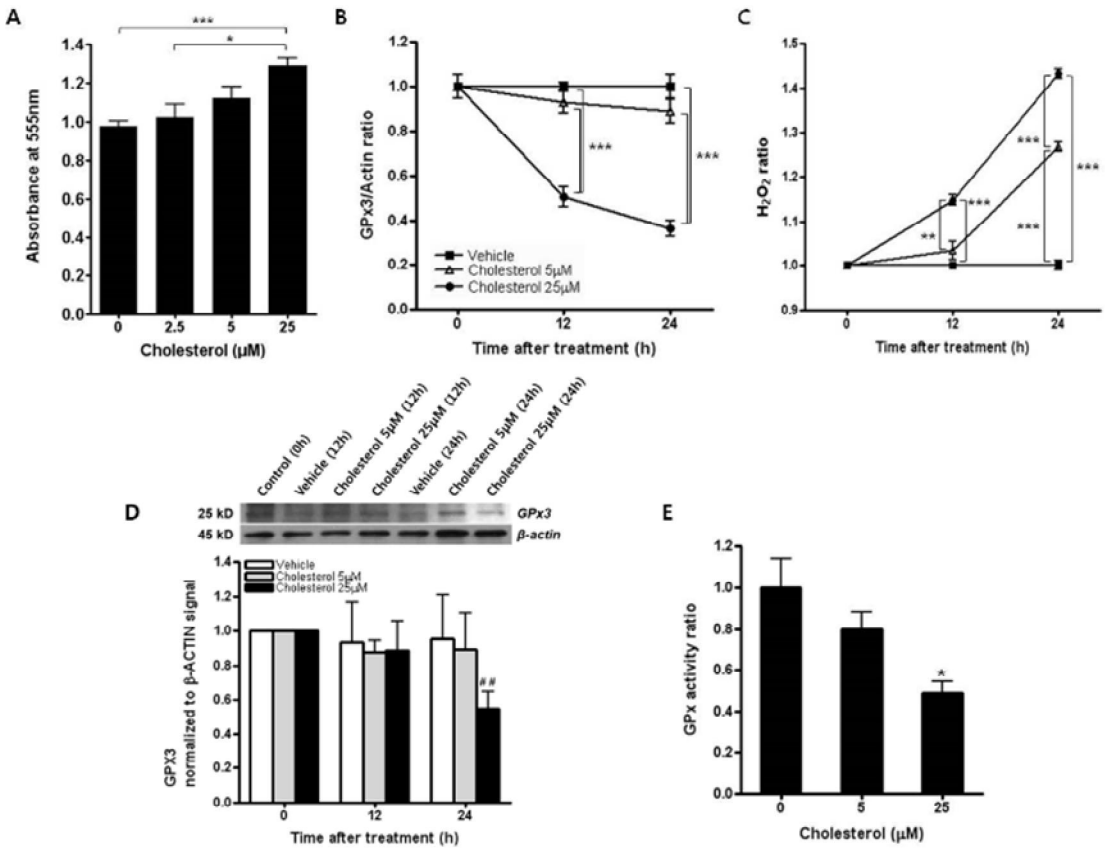

Figure 1-1. **Effect of cholesterol supplementation on PC-3 cells.** A, PC-3 growth increased with cholesterol supplementation and maximal effects occurred at 25 μM. *, $P < 0.05$; ***, $P < 0.001$. B, GPx3 mRNA levels in the PC-3 cell line were measured by quantitative reverse transcription polymerase chain reaction. ***, $P < 0.001$. C, Culture media were collected to measure H_2O_2 levels. **, $P < 0.01$; ***, $P < 0.001$. D, Representative Western blot analysis of the PC3 cell line. The intensities of the GPx3 bands corresponding to different concentrations of cholesterol were quantified and the values shown on the histogram. $^{\#\#}$, $P < 0.01$ vs.

control (0 h). E, Glutathione peroxidase activity ratio was determined after 24 h exposure to cholesterol. *, $P < 0.05$ vs. vehicle control. Values were expressed as the fold change compared to vehicle control at each time point. Results are given as mean ± SEM.

1.3.2 Troglitazone increases GPx3 expression and decreases cell proliferation in PC-3 human prostate cancer cells

PC-3 human prostate cancer cells were treated with different concentrations (1. 10, and 40 μM) of troglitazone (TGZ). Cell proliferation was measured by MTT assay after 24h of troglitazone treatment (Figure 1-2A). Troglitazone treatment decreased cell proliferation in a dose-dependent manner and a 95.54% decrease in growth rate was observed in cells treated with 40 μM Troligazone from that of vehicle-treated cells. Also, troglitazone increased GPx3 mRNA expression in a dose-dependent manner (Figure 1-2B). Troglitazone (40 μM) treatment significantly upregulated the GPx3 mRNA levels by 3.72-fold at 24h.

To determine if the troglitazone inhibited the effect of cholesterol on PC-3 cells, I added troglitazone to cholesterol supplemented media and measured cell proliferation, GPx3 mRNA expression and H_2O_2 levels (Figure 1-2C-E). Troglitazone (40 μM) inhibited the increase of cell proliferation observed after treatment with cholesterol (25 μM) in PC-3 cells (Figure 1-2C). Troglitazone treatment significantly increased the GPx3 mRNA levels by 1.85-fold at 12h and 2.67-fold at 24h from those of cholesterol-treated cells (Figure 1-2D). Moreover, troglitazone blocked cholesterol-induced H_2O_2 increase in cell culture medium of PC-3 cells (Figure 1-2E).

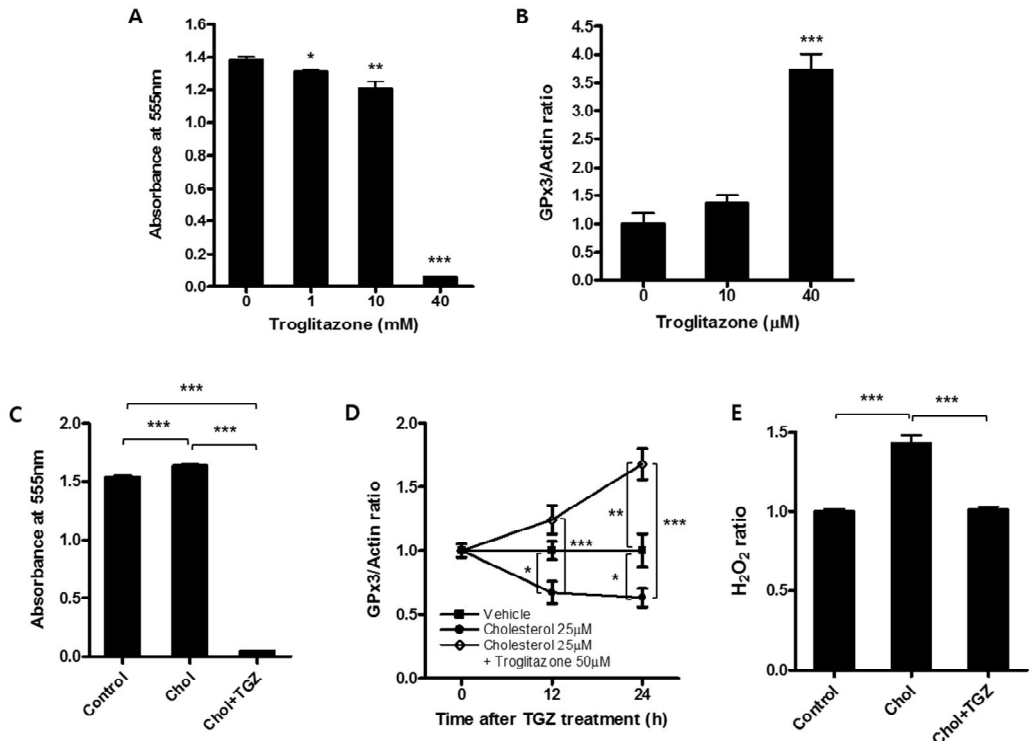

Figure 1-2. Effect of troglitazone on GPx3 expression in PC-3 cells. A, PC-3 growth decreased with troglitazone treatment for 24hr and maximal effects occurred at 40 μM. B, GPx3 mRNA levels in the PC-3 cell line after 24hr treatment of troglitazone 40 μM. C-E, PC-3 cells were incubated with medium containing 10% FBS for 24h, and medium changed to 1% FBS-RPMI for 24h. Then, the cells were supplemented with cholesterol (Chol) at concentration of 25 μM or vehicle (ethanol). After 24hr, troglitazone (TGZ) was added to Chol + TGZ group at 40 μM. Cell proliferation was measured after 24hr by MTT assay (C), and GPx3 mRNA levels after 12hr and 24hr (D) and H_2O_2 levels in culture media after 24hr

were measured. *, $P < 0.05$; **, $P < 0.01$; ***, $P < 0.001$. Results are given as mean ± SEM.

1.3.3 Obesity is induced after consumption of a high-animal fat diet

I then asked if a high-animal fat diet could enhance cancer progression in a spontaneous cancer model using TRAMP mice. Mice were switched onto the control or high-fat diets when they reached adulthood (6 weeks), and I found 10 weeks later that those consuming a high-fat diet were significantly heavier than those consuming a control diet even after 1 week on the diets (Figure 1-3A). Interestingly, with *ad libitum* access to food, weekly food intake averages were lower in mice fed the high-fat diet than in mice fed the control diet (data not shown). Additionally, weekly food intake averages were similar between the two control diet groups, whereas they were lower in TRAMP mice than that in non-Tg mice in the two high-fat diet groups. Because the dietary energy density of high-fat diet (4.73 Kcal/g) is higher than that of control diet (3.85 Kcal/g), the average weekly calorie intake of the high-fat diet groups were higher than that of the control diet groups, which affected the rates of body weight gain. Weights of epididymal fat were markedly higher in the high-fat diet group when compared to those in the control diet group (Figure 1-3B). High-fat diet increased body weight and epididymal fat weight and induced adiposity both in non-Tg and TRAMP mice.

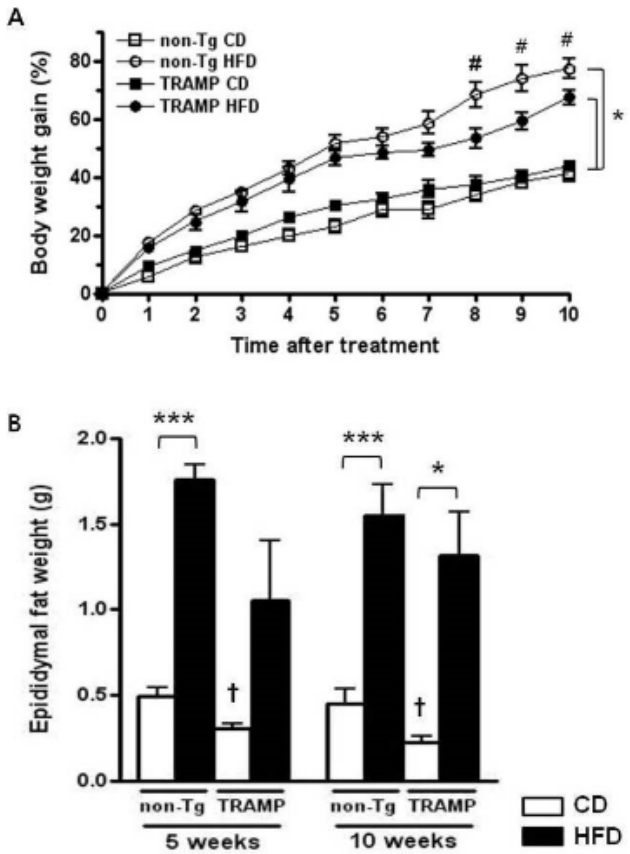

Figure 1-3. High-fat diet increased adiposity. A, The rates of body weight gain increased in high-fat diet groups over time. *, $P < 0.05$; #, $P < 0.05$ nontransgenic vs. transgenic adenocarcinoma of the mouse prostate (TRAMP) mice fed a high-fat diet. B, Epididymal fat was dissected and weighed for each mouse at the time of sacrifice. *, $P < 0.05$ and ***, $P < 0.001$ high-fat diet (HFD)-fed vs. control diet (CD)-fed animals; †, $P < 0.05$ TRAMP vs. nontransgenic males fed a control diet. Results are given as mean ± SEM.

1.3.4 Prostate cancer growth increases in TRAMP mice fed a high-animal fat diet

Consumption of a high-fat diet by TRAMP mice resulted in grossly larger prostate tumors (Figure 1-4A). Although UGT weight was not statistically different in the 5-week groups, it was significantly greater in TRAMP mice than in the corresponding nontransgenic mice in both 10-week control and high-fat diet fed mice (Figure 1-4B). Furthermore, UGT weight increased significantly in TRAMP mice fed a high-fat diet (0.89 ± 0.04 g) compared to TRAMP mice fed a control diet (0.72 ± 0.03 g). This weight was considered to be an indirect measure of the tumor burden in TRAMP mice.

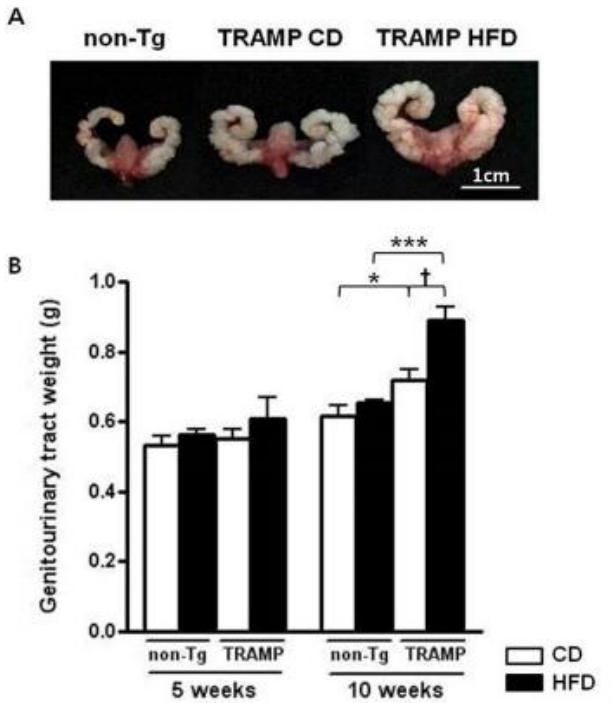

Figure 1-4. Hyperplasia of the genitourinary tract increased in transgenic adenocarcinoma of the mouse prostate (TRAMP) mice fed a high-fat diet. A, Genitourinary tracts from nontransgenic and TRAMP mice were carefully dissected *en bloc* at the time of sacrifice (16 weeks). Representative pictures of the genitourinary apparatus obtained from nontransgenic and TRAMP males fed a control (CD) or high fat diet (HFD) are shown. B, After dissection, genitourinary tracts were weighed. *, $P < 0.05$ TRAMP vs. nontransgenic males fed a control diet; ***, $P < 0.001$ TRAMP vs. nontransgenic males fed a high fat diet; †, $P < 0.05$ TRAMP males fed a high fat diet vs. TRAMP males fed a control diet. Results are given as mean ± SEM.

1.3.5 High-animal fat diet increases the histopathological score of prostate tumors

I then compared prostate tumor development in TRAMP mice on the high-fat vs. control diets. Representative histological sections are shown for anterior, lateral, dorsal, and ventral prostates and for each experimental condition (Figure 1-5A–L). The histopathological score increased with age and high-fat diet consumption (Figure 1-5M). I did not observe adenomas in any of the TRAMP mice prostates. For the anterior, lateral, dorsal, and ventral lobes, the average histopathological scores in the 5-week control diet group were 2.0 ± 0.8, 4.2 ± 0.5, 4.4 ± 0.6, and 1.0 ± 0.0, respectively, and those of each lobe in the 5-week high-fat diet group were 4.4 ± 0.9, 4.7 ± 0.9, 5.2 ± 0.2, and 1.6 ± 0.2, respectively. Although scores tended to increase with high-fat diet consumption, it was not statistically different. Similarly, the average histopathological scores in the 10-week control diet group for the anterior and ventral lobes were 4.8 ± 1.0 and 2.0 ± 0.0, respectively, and those of each lobe in the 10-week high-fat diet group were 5.6 ± 0.6 and 2.4 ± 0.2, respectively. However, in the lateral and dorsal lobes, the histopathological score increased significantly in the 10-week high-fat diet group (6.2 ± 0.2 and 6.2 ± 0.4, respectively) vs. the 10-week control diet group (5.3 ± 0.3 and 5.2 ± 0.2, respectively).

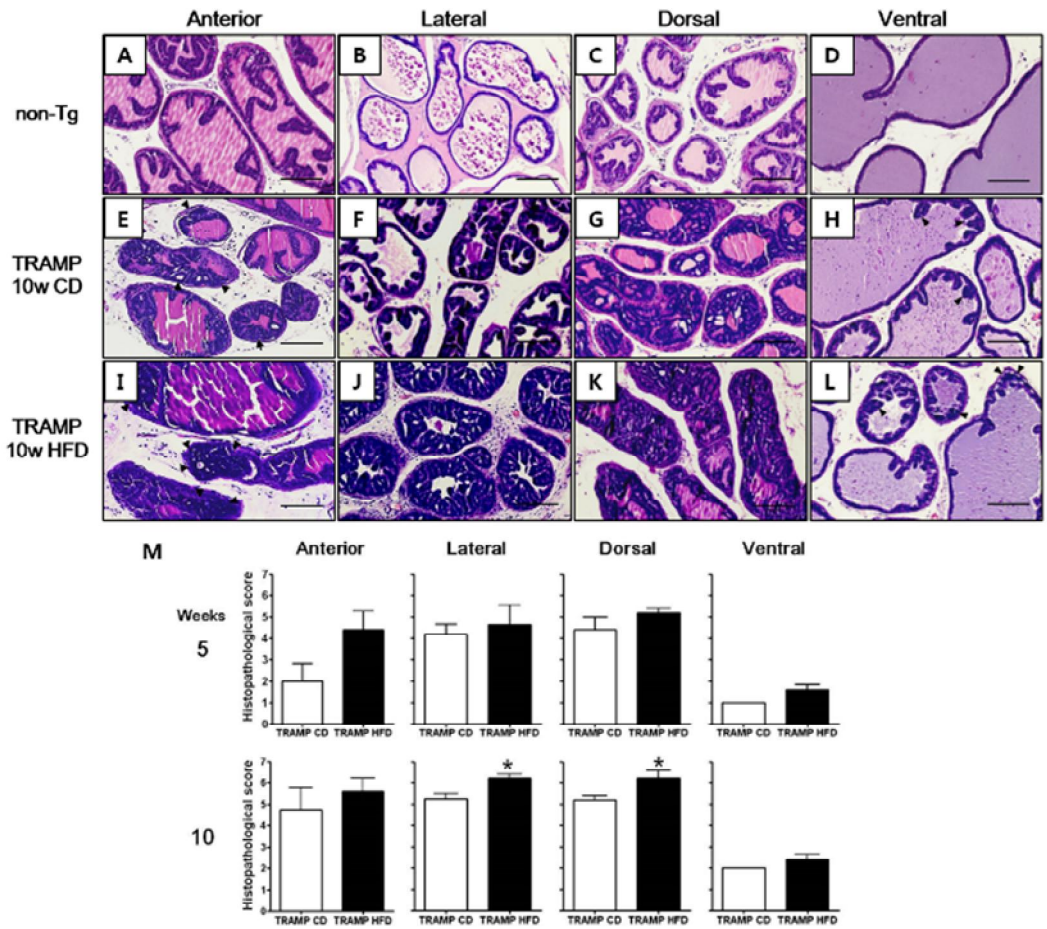

Figure 1-5. Transgenic adenocarcinoma of the mouse prostate (TRAMP) mice fed a high-fat diet show progressed prostate intraepithelial neoplasia (PIN) lesions. A–L, Histopathological sections of anterior (A, E, I), lateral (B, F, J), dorsal (C, G, K), and ventral (D, H, L) lobes of the prostate from non-transgenic mice (A–D), TRAMP mice fed a control diet (CD) (E–H), and TRAMP mice fed a high-fat diet (HFD) (I–L) stained with hematoxylin and eosin (H&E) (magnification, ×200). Scale bar = 100 μm. Arrowhead indicates PIN lesions in

anterior lobe (E, I) and ventral lobe (H, L). M, Histograms representing the histopathological score of prostate intraepithelial neoplasia (PIN) I to PIN IV in TRAMP males sacrificed at different ages. *, $P < 0.05$ TRAMP males fed a high fat diet vs. TRAMP males fed a control diet. Results are given as mean ± SEM.

1.3.6 TRAMP mice fed a high-animal fat diet show decreased GPx3 expression

To determine the possible relevance of the changes in GPx3 expression observed in PC-3 human prostate cancer cells, GPx3 mRNA levels were examined by real-time RT-PCR in each lobe of the prostate tissue samples, except for the ventral lobe which is too small to examine GPx3 mRNA level. GPx3 mRNA expression decreased significantly (~36.27% and ~23.91%, respectively) in the anterior and dorsolateral prostate of TRAMP mice fed a high-fat diet compared to TRAMP mice fed a control diet in the 10-week group (Figure 1-6A).

An immunohistochemistry assay was performed with the prostate samples from the 10-week group to determine GPx3 expression patterns (Figure 1-6B–D). The mean immunohistochemical score of GPx3 expression decreased significantly in all prostate lobes of TRAMP mice fed a high-fat diet compared to TRAMP mice fed a control diet in the 10-week group (Figure 1-6E). GPx3 was highly expressed in the normal prostate tissues of non-Tg mice. In contrast, GPx3 immunoreactivity in the prostate tissue of TRAMP mice was very weak in control animals and not detectable when fed they were a high-fat diet. I observed a GPx3 positive reaction in the cytoplasm and cell membranes of prostate tissue with reduced or absent nuclear staining.

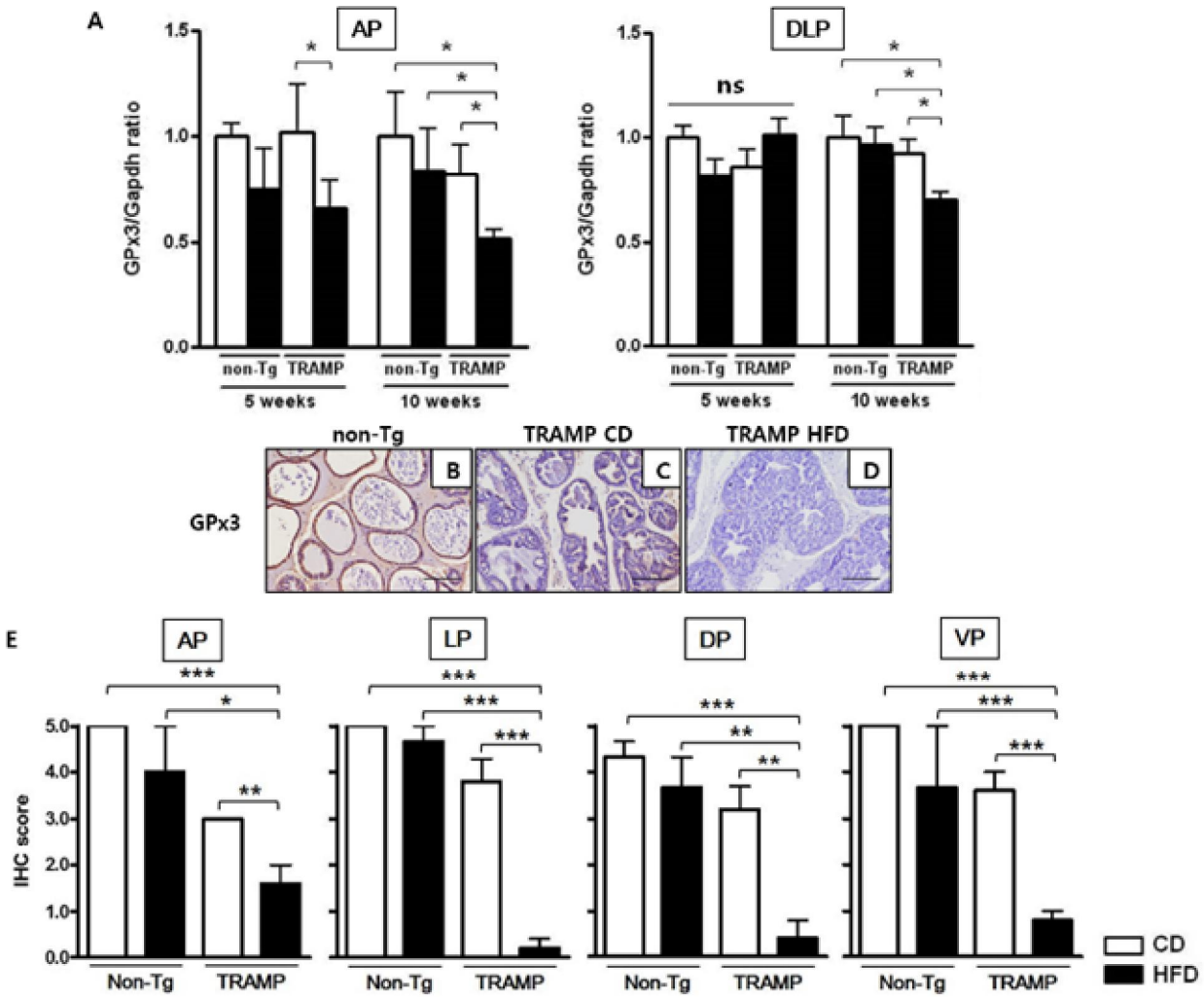

Figure 1-6. High-animal fat diet decreases glutathione peroxidase 3 (GPx3) expression in the prostate of transgenic adenocarcinoma of the mouse prostate (TRAMP) mice. A, mRNA expression of GPx3 in the anterior (AP) and dorsolateral prostate (DLP) of all groups was evaluated by real-time reverse transcription polymerase chain reaction. Expression values were expressed as the fold change compared to non-Tg control. B–D, Immunohistochemical staining of

GPx3 in the lobes of the prostate from non-transgenic mice (B), TRAMP mice fed a control diet (CD) (C), and TRAMP mice fed a high-fat diet (HFD) (D) (magnification, ×200). Scale bar = 100 μm. E, Intensity of GPx3 expression (IHC score) in the prostate tissues. AP; anterior prostate, LP; lateral prostate, DP; dorsal prostate, VP; ventral prostate. *, $P < 0.05$; **, $P < 0.01$; ***, $P < 0.001$. Results are given as mean ± SEM.

1.4 DISCUSSION

The main findings from this study are the following: (1) cholesterol treatment increased proliferation of PC-3 human prostate cancer cells, decreased GPx3 expression both at the mRNA and protein levels, and decreased GPx activity, which was associated with increased H_2O_2 in cell culture media, (2) troglitazone increased GPx3 mRNA expression in PC-3 human prostate cancer cells, decreased cell proliferation and attenuated cholesterol-induced H_2O_2 increase in cell culture media, and (3) a high-fat diet enhanced prostate cancer tumorigenesis in early-stage TRAMP mice and decreased GPx3 expression both at the mRNA and protein levels in prostates of TRAMP mice. Overall, these results suggest that dietary fat may reduce GPx3 expression and increase prostate cancer tumorigenesis.

Transgenic mouse models are more appropriate to study the mechanisms related to early tumor development. TRAMP transgenic mice represent a suitable model for human prostate cancer. These mice develop spontaneous multistage prostate carcinogenesis that exhibits both histological and molecular features recapitulating many salient aspects of human prostate cancer (157). As well, they display elevated levels of nuclear p53 and a decreased heterogeneous pattern of androgen-receptor expression; thus, mimicking human prostate cancer (158). These transgenic mice have a 100% chance of advanced prostate tumors by 28–32 weeks (157). In the TRAMP model, the PIN lesions are characterized by epithelial tufting, hyperchromatic nuclei, elongated nuclei, nuclear stratification, micropapillary

projections, cribriform structures, increased mitoses, and increased apoptosis (159). PIN lesions appear to arise from dorsal and lateral lobes, and those lobes are the major lesions at early stages of prostate cancer progression in the TRAMP mice model (159). TRAMP mice fed a Western diet (containing 21.2% fat and 0.2% cholesterol) for 20 weeks also show increased histopathological scores compared to those eating a chow diet (containing 4.5% fat and 0.002% cholesterol) (24). I previously reported that TRAMP mice fed a high-fat (45% Kcal fat) diet produce consistent results compared to TRAMP mice fed a control (16% Kcal fat) diet when mice were fed each diet for 10 weeks (160). In the present study, the histopathological score increased with age and high-fat diet consumption. The lateral and dorsal lobes of 10-week high-fat diet group showed significantly increased histopathological scores compared to those in the 10-week control diet group.

Interestingly, the rates of body weight gain in non-Tg and TRAMP mice fed a control diet were not statistically different. However, in the two high-fat diet groups, TRAMP mice had lower weekly food intake, body weight gain, and epididymal fat weights than those in non-Tg mice. Similar to what I observed in TRAMP mice, progressive wasting in patients with cancer could be attributed to changes in dietary intake and/or energy expenditure, mediated by metabolic alterations (161, 162). Moreover, clinical studies have revealed that a decrease in body weight is explained by loss of body fat, preferentially from the trunk (161). Transgenic mice ate less, expended more energy, and stored fewer calories as fat.

Hypermethylation and downregulation of the GPx3 promoter are frequently observed in a wide spectrum of human cancers (79, 82, 151-153). Decreased GPx3 expression by promoter hypermethylation is found in head and neck, lung, cervical, thyroid, and gastric cancers, as well as in melanoma (151, 153). The GPx3 gene is widely methylated or deleted in prostate cancer, resulting in low expression (79). Furthermore, removing GPx3 enhances inflammation and injury, proliferation, and DNA damage in tumors of mice subjected to a colitis-associated carcinogenesis protocol, suggesting that GPx3 loss may lead to increased tumor promotion (97). Although GPx3 expression was recently reported to decrease in the prostates of normal mice fed a high-fat diet (100), it was unknown whether dietary high-fat could affect GPx3 expression during prostate cancer tumorigenesis. In this study, I confirmed that dietary high-fat reduced GPx3 expression during prostate cancer tumorigenesis. This finding in TRAMP transgenic mice prostate and the prostate cancer cell line is plausible to decrease GPx3 because the microenvironment and biology of prostate cancer are fundamentally different from a normal prostate gland (163). I did detect GPx3 expression and also observed decreased GPx3 expression with cholesterol treatment in the PC-3 cell line, although previous studies have reported that GPx3 mRNA is undetectable in several human prostate cancer cell lines (100). I increased the mRNA concentration in the initial step of the RT-PCR to detect GPx3 gene expression in the prostate cancer cell line. Cholesterol-treated cells also revealed increased H_2O_2 levels in cell culture media and decreased mRNA expression of other antioxidant enzymes (data not shown). These data

suggest that oxidative stress, which increases with dietary fat, may induce proliferation of prostate cancer cells and dietary fat reduces the expression of GPx3 and other anti-oxidant enzymes, supporting previous reports on the association between dietary fat and oxidative stress (15, 34).

Thiazolidinediones (TZDs), such as troglitazone and ciglitazone, are agonists for the peroxisome proliferator-activated receptor γ (PPARγ) and exhibit antitumor activities in many cancers (164, 165), including prostate cancer (166). It has been reported that troglitazone induced GPx3 expression in human skeletal muscle cells (78) and prostate cells (100). In this study, I found that troglitazone also increased GPx3 expression and decreased cell proliferation in PC-3 human prostate cancer cells, blunting the effect of cholesterol on PC-3 cells.

GPx3 mRNA expression in the anterior and dorsolateral prostate were also significantly lower in TRAMP mice fed a high-fat diet than that in all other groups, consistent with the *in vitro* results. It suggests that dietary fat enhanced prostate cancer progression and that GPx3 may provide a potential mechanistic link between dietary fat and prostate cancer. This study presents some new evidence on the following hypothesis: (1) when there is genetic predisposition to prostate cancer, decreased GPx3 expression due to a high-fat diet before diagnosis may advance the disease to a clinically detectable stage and shorten the latency period of prostate carcinogenesis and (2) dietary high-fat may act as a tumor promoting factor during the early-stage of prostate cancer, leading to more rapidly downregulated expression of GPx3 gene and more advanced prostate cancer.

In conclusion, this is the first report to investigate the association between dietary fat intake and GPx3 expression in prostate cancer tissue using TRAMP mice. GPx3 seemed to serve as a potent tumor suppressor during prostate cancer tumorigenesis, likely by reducing oxidative stress and ROS that lead to tumor initiation and progression. More *in vivo* animal studies focusing on the effect of downregulation of GPx3 on prostate cancer tumorigenesis and development will be needed by modulating GPx3 expression using genetic manipulation. Additional studies will be required to further elucidate the precise mechanism by which GPx3 could act as a tumor suppressor during prostate cancer development. If the role of GPx3 in prostate cancer is clearly established, GPx3 may become an attractive target for the design of therapeutic and chemopreventive strategies in patients with prostate cancer.

CHAPTER II

Glutathione Peroxidase 3 Inhibits Prostate Tumorigenesis in TRAMP Mice

2.1 INTRODUCTION

The U.S. annual report (1975–2011) indicates that prostate cancer remains the most common cancer among men and the rates were substantially higher than any other type of cancer (167). Internationally, prostate cancer is the second most common cause of cancer and the sixth leading cause of cancer death among men (168). As prostate cancer is remarkably age-related, reactive oxygen species (ROS) signaling may play an important role in the development and progression of this malignancy. Evidence from epidemiological, experimental, and clinical studies suggest that prostate cancer cells with increased exposure to oxidative stress are associated with the development of prostate cancer (14, 27). Under normal physiological conditions, healthy cells are equipped with adequate antioxidant defense mechanisms to protect against ROS (25, 169). A chronic state of oxidative stress exists in cells because of either increased ROS generation or a loss of antioxidant defense mechanisms.

The glutathione peroxidase (GPx) families, widely expressed in various tissues (38-40), are the most important ROS scavengers. Four types of GPx (cellular GPx (GPx1), gastrointestinal GPx (GPx2), extracellular GPx (GPx3), and phospholipid hydroperoxide GPx (GPx4)) have been identified, and each enzyme is antigenetically, structurally, and enzymatically different (170). GPx3 plays a critical role in the detoxification of ROS. Some studies have demonstrated that silencing GPx3 expression promotes tumor metastasis in human thyroid and gastric cancer cells (93, 94). It was recently reported that removal of GPx3 enhanced

inflammation and injury, proliferation, and DNA damage in tumors of mice subjected to an inflammatory carcinogenesis and chronic colitis protocols (171). These studies suggest that functional inactivation of this ROS scavenger may play a role in cancer development. Down-regulation of GPx3 by hypermethylation was found in breast, gastric, ovarian, esophagus, and other solid tumors (70, 84-94) including prostate cancer (23, 95, 96). GPx3 is emerging as a potential tumor suppressor in these cancers. Nevertheless, the exact mechanisms of GPx3 in cancer remain unclear. Several signaling pathways have been suggested to be associated with GPx3 expression in cancer, such as Wnt/β-catenin (94, 171) and p53-induced gene 3 (172) signaling.

In terms of prostate, GPx3 has been shown in clinical studies to have a negative correlation with poor clinical outcomes (96, 173). Molecular studies involving GPx3 with prostate cancer progression and metastasis to date have focused on *in vitro* and xenografting model. These studies have shown that overexpression of GPx3 in prostate cancer cell lines suppressed colony formation and cell proliferation (23, 96, 172). Xenografted PC3 human prostate cancer cells expressing GPx3 have shown reduction in tumor volume, elimination of metastasis, and reduction of animal death (96). However, it remains unknown whether GPx3 expression can regulate the development of prostate cancers *in vivo* and the role and mechanism of GPx3 in prostate tumorigenesis has never been directly tested.

To elucidate the role of the GPx3 in prostate tumorigenesis *in vivo*, I generated transgenic adenocarcinoma of the mouse prostate (TRAMP) mice that are deficient

in GPx3 (TRAMP / GPx3 (–/–) KO mice). Here, I show that disruption of GPx3 in the TRAMP model increases prostate cancer growth leading to an overall larger average genito-urinary (GU) tract weight among these mice compared to TRAMP mice. Histopathologically, TRAMP / GPx3 KO mice showed more severe prostate cancer compared to the age-matched TRAMP mice, influencing β-catenin pathway.

2.2 MATERIALS AND METHODS

2.2.1 Animals and PCR genotyping

All animal studies were approved by the Institutional Animal Care and Use Committee of Seoul National University. Mice were kept on a 12-h light/dark cycle with *ad libitum* access to food and water. TRAMP mice expressing the SV40 large T-antigen under control of the prostate-specific rat probasin promoter were purchased from The Jackson Laboratory (Bar Harbor, ME, USA). Parental GPx3 KO mice created in a C57BL/6 background were previously described (75). GPx3 KO mice obtained from Dr. Raymond F. Burk (Department of Medicine, Vanderbilt University School of Medicine, Nashville, TN, USA). GPx3 (–/–) KO males were bred with TRAMP females to generate GPx3 (+/–) HET and TRAMP / GPx3 (+/–) HET mice. Then, GPx3 (+/+) WT, GPx3 (+/–) HET, GPx3 (–/–) KO, TRAMP / GPx3 (+/+) WT, TRAMP / GPx3 (+/–) HET, and TRAMP / GPx3 (–/–) KO mice were generated through backcross and sibling breeding. PCR genotyping was performed as described previously (23, 75). The number of mice in each experimental group was 3–10 (Table 2-1). Genetic authenticities of all strains were monitored by KRiBB (Daejeon, Korea) using single nucleotide polymorphism (SNP)-based marker set previously developed by The Jackson Laboratory (174).

Table 2-1. Average genito-urinary (GU) weight at 8, 16 and 20 weeks (mean ± SEM).

Genotype	Age (weeks)	Sample size, N	Body weight (g)	GU weight (g)	Relative GU weight (%)
WT	8	3	18.6 ± 0.8	0.090 ± 0.013	0.480 ± 0.054
GPx3 HET	8	3	20.1 ± 0.4	0.195 ± 0.003	0.969 ± 0.031
GPx3 KO	8	3	20.7 ± 1.6	0.157 ± 0.016	0.759 ± 0.017
TRAMP	8	3	19.6 ± 0.3	0.143 ± 0.009	0.732 ± 0.035
TRAMP / GPx3 HET	8	3	21.3 ± 0.7	0.225 ± 0.009	1.060 ± 0.075
TRAMP / GPx3 KO	8	3	19.8 ± 0.8	0.117 ± 0.002	0.590 ± 0.034
WT	16	3	28.5 ± 1.0	0.410 ± 0.006	1.440 ± 0.045
GPx3 HET	16	5	29.0 ± 0.9	0.420 ± 0.018	1.445 ± 0.052
GPx3 KO	16	4	27.1 ± 0.2	0.312 ± 0.015	1.150 ± 0.065
TRAMP	16	10	27.8 ± 0.4	0.531 ± 0.033	1.916 ± 0.125
TRAMP / GPx3 HET	16	9	26.4 ± 0.4	0.577 ± 0.085	2.173 ± 0.303
TRAMP / GPx3 KO	16	4	26.4 ± 1.7	0.469 ± 0.044	1.776 ± 0.150
WT	20	4	33.1 ± 0.8	0.381 ± 0.018	1.153 ± 0.061
GPx3 HET	20	5	23.4 ± 0.8	0.331 ± 0.011	1.415 ± 0.023
GPx3 KO	20	5	31.8 ± 0.9	0.389 ± 0.026	1.229 ± 0.092
TRAMP	20	10	30.0 ± 1.1	0.646 ± 0.049	2.166 ± 0.163
TRAMP / GPx3 HET	20	10	28.7 ± 0.6	0.671 ± 0.050	2.328 ± 0.140
TRAMP / GPx3 KO	20	8	27.4 ± 0.7	0.653 ± 0.053	2.378 ± 0.184

2.2.2 Tissue excision and processing

Mice were sacrificed at approximately 8, 16, and 20 weeks and the GU tract (prostate, bladder, and seminal vesicle) was quickly excised and weighed. The ventral, dorsal, lateral, and anterior prostate lobes were dissected under a stereoscope, from one side and frozen in liquid nitrogen for RT-PCR and western blot. The remainder of each prostate was fixed in 10% buffered formalin and processed for standard paraffin sections.

2.2.3 Histopathological analysis

Sections (3 μm) were obtained from the paraffin-embedded blocks and stained with hematoxylin and eosin (H&E). The mouse prostate lobes (ventral, dorsal, lateral, and anterior) were identified histopathologically in H&E-fixed sections using previously published criteria (156, 175, 176). Briefly, I evaluated each lobe of the prostate and assigned a prostate intraepithelial neoplasia (PIN), phyllodes-like tumor (PHY), well-differentiated adenocarcinoma (WD), moderately differentiated adenocarcinoma (MD), or poorly differentiated adenocarcinoma (PD) grade as PIN I (relative small foci with one or two layers of atypical cells), PIN II (larger foci with two or more layers of atypical cells that do not fill the lumen), PIN III (the foci of atypical cells fill, or almost fill, the lumen of the ducts), PIN IV (the foci of atypical cells fill the lumen of the ducts), PHY (staghorn luminal patterns containing papillary projections of loose stroma with loosely arranged stellate mesenchymal cells), WD (increased of quantity of small glands that have round

nuclei with fewer hyperchromatic nuclei than in PIN lesions), MD (anaplastic sheets of cells that may contain remnants of glandular architecture), or PD (anaplastic sheets of cells containing pleomorphic cells with irregular nuclei), based on the most severe lesion within the lobe. The distribution of lesions within each individual lobe was also estimated as focal, multifocal, or diffuse. The distribution and lesion grade were then combined to calculate a distribution-adjusted histopathological score ranging from 0 to 24 that could be used for statistical analysis. Sections were examined in a blinded manner under light microscopy (Olympus AX70, Tokyo, Japan).

2.2.4 Western blot analysis

Cell lysates (40 μg) were resolved by sodium dodecyl sulfate polyacrylamide gel electrophoresis before transferring the proteins to nitrocellulose membranes and probing with mouse monoclonal anti-GPx3 primary antibody (Abcam, Inc., Cambridge, MA, USA), mouse monoclonal anti-SV40T Ag primary antibody (Santa Cruz Biotechnology, Santa Cruz, CA, USA), and rabbit polyclonal anti-β-actin primary antibody (Cell Signaling Technology, Inc., Danvers, MA, USA). Blots were then incubated with HRP-conjugated goat anti-mouse and anti-rabbit IgG secondary antibodies (Zymed, San Francisco, CA, USA), respectively. The blots were developed using a chemiluminescent substrate (DoGEN, Seoul, South Korea).

2.2.5 Real-time reverse transcription-polymerase chain reaction (PCR)

Total RNA was isolated using a Hybrid-R RNA extraction kit (GeneAll Biotechnology, Seoul, South Korea) and cDNAs were synthesized using an M-MLV cDNA Synthesis kit (Enzynomics, Daejeon, South Korea) following the supplier's instructions. Real-time reverse transcription-PCR was performed using specific primers to mouse *GPx3* (GenBank accession no. NM_008161.3), mouse *Twist1* (GenBank accession no. NM_ 011658.2), mouse *β-catenin* (GenBank accession no. NM_ 007614.3), mouse *Cyclin D1* (GenBank accession no. NM_ 007631.2), mouse *C-Myc* (GenBank accession no. NM_ 010849.4), mouse *FoxA2* (GenBank accession no. NM_ 001291065.1), mouse *MMP7* (GenBank accession no. NM_ 010810.4), mouse *Axin2* (GenBank accession no. NM_ 015732.4), and mouse *β-actin* (GenBank accession no. NM_ 007393.3) with TOPreal™ qPCR 2X PreMIX (Enzynomics) on a CFX Connect Real-Time PCR Detection system (Bio-Rad). Mouse beta-actin gene expression were used for cDNA normalization. mRNA fold changes were quantified using the comparative CT ($2^{-\Delta\Delta Ct}$) cycle (ΔCt) method (155). The primer sequences used in this study are shown in Table 2-2.

Table 2-2. Primer sequences used for RT-PCR.

Primer	Sequences
GPx3 (mouse)	<F> 5' – CTCCTGAGACCAGCCAAGAC – 3'
	<R> 5' – GAGCCTAAGCCTGAATGCAC – 3'
Twist1 (mouse)	<F> 5' – CACGCTGCCCTCGGACAA – 3'
	<R> 5' – GGGACGCGGACATGGACC – 3'
β-catenin (mouse)	<F> 5' – GATATTGACGGGCAGTATGCAA – 3'
	<R> 5' – AACTGCGTGGATGGGATCTG – 3'
Cyclin D1 (mouse)	<F> 5' – AGCAGAAGTGCGAAGAGG – 3'
	<R> 5' – GCAGTCAAGGGAATGGTC – 3'
C-Myc (mouse)	<F> 5' – AAGGGAAGACGATGACGG – 3'
	<R> 5' – TGAGAAACCGCTCCACATA – 3'
FoxA2 (mouse)	<F> 5' – GAGCACCATTACGCCTTCAAC – 3'
	<F> 5' – AGGCCTTGAGGTCCATTTTGT – 3'
MMP7 (mouse)	<F> 5' – ACTTCAGACTTACCTCGGATCG – 3'
	<F> 5' – TCCCCCAACTAACCCTCTTGA – 3'
Axin2 (mouse)	<F> 5' – GAGAGTGAGCGGCAGAGC – 3'
	<F> 5' – CGGCTGACTCGTTCTCCT – 3'
β-actin (mouse)	<F> 5' – GTCCCTCACCCTCCCAAAAG – 3'
	<R> 5' – GCTGCCTCAACACCTCAACCC – 3'

2.2.6 Immunohistochemistry

Sections were deparaffinised, rehydrated and antigen retrieval performed. Endogenous peroxidase was blocked using 3% H_2O_2 in methanol for 20 min at room temperature. The tissue sections were then treated with blocking solution (5% BSA/ 0.3% Triton-X 100 in TBS) for 30 min, and reacted with the mouse monoclonal anti-GPx3 primary antibody (Abcam), mouse monoclonal anti-SV40T Ag primary antibody (Santa Cruz), rabbit polyclonal anti-Ki67 primary antibody (Novocastra, Newcastle, UK), and rabbit polyclonal anti-active caspase-3 primary antibody (Cell Signaling) for 12–14 h at 4°C. Thereafter, remaining steps were carried out using appropriate Vectastain Elite ABC kits (Vector Laboratories, Burlingame, CA, USA) and DAB Peroxidase Substrate (Vector Laboratories), with hematoxylin counterstaining. Staining specificity was verified by omitting the primary antibody. Ki-67 and active caspase-3 staining were quantified by counting the number of positively stained cells in 6 randomly chosen fields at ×400. Image analysis was conducted using IHC profiler plugin in ImageJ 1.48v software (National Institutes of Health, Bethesda, MD, USA).

2.2.7 Statistical analysis

All data are presented as mean ± standard error. Statistically significant ($P < 0.05$) data were further analyzed by Student's *t*-tests.

2.3 RESULTS

2.3.1 GPx3 mRNA expression is down-regulated in prostate lobes of TRAMP mice

Initially, I wanted to determine the endogenous level of GPx3 in the TRAMP prostate; therefore, I performed a quantitative RT-PCR and compared relative GPx3 mRNA expression levels in TRAMP mice to age-matched nontransgenic littermates. Overall, a significant decrease in GPx3 mRNA levels was evident in the anterior (AP), dorsolateral (DLP), and ventral prostate (VP) of TRAMP mice as disease progressed (Figure 2-1). In the AP of 8-week-old TRAMP mice, GPx3 mRNA expression was similar to wild-type (Figure 2-1). However, by 16 weeks a 6-fold decrease (relative expression= 0.2 ± 0.1) in mRNA was observed, followed by a significant decrease at 20 weeks of age (Figure 2-1). In the DLP, the GPx3 mRNA expression was considerably lower in TRAMP mice compared to normal littermates at 8 and 16 weeks of age (Figure 2-1). However, at 20 weeks, a significant increase in GPx3 mRNA was observed (Figure 2-1). In the VP, the GPx3 mRNA levels was significantly reduced at 8 weeks and remained below normal until 20 weeks of age (Figure 2-1). These results indicate that GPx3 mRNA expression in indeed altered in TRAMP mice, in a lobe-specific pattern.

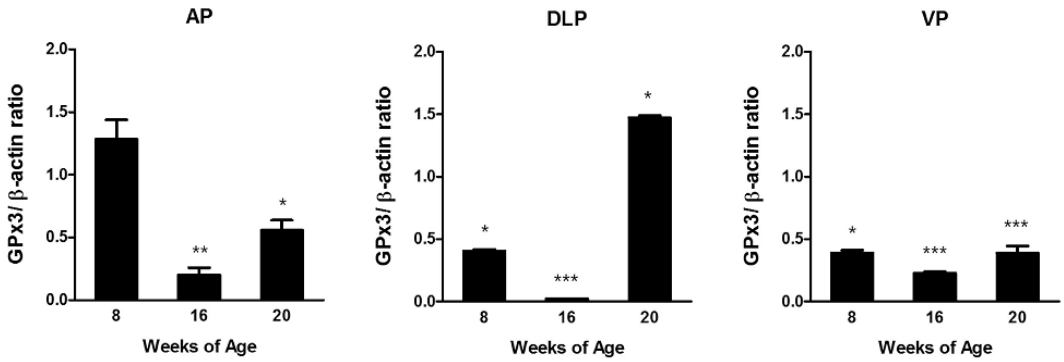

Figure 2-1. Relative expression of GPx3 mRNA in the transgenic adenocarcinoma of the mouse prostate (TRAMP) mice. The anterior (AP), dorsolateral (DLP), and ventral prostate (VP) of mice at 8, 16, and 20 weeks of age were analyzed. GPx3 mRNA levels in the TRAMP mice were measured by quantitative reverse transcription polymerase chain reaction. Values were expressed as the fold change compared to age-matched nontransgenic mice at each time point. *, $P < 0.05$; **, $P < 0.01$; ***, $P < 0.001$ vs. age-matched nontransgenic mice. Results are given as mean ± SEM.

2.3.2 Prostate cancer growth is increased in TRAMP mice by inactivation of one or both alleles of GPx3

In order to determine whether GPx3 levels contribute to prostate cancer progression, I cross-bred male GPx3 KO mice with female TRAMP mice and generated TRAMP / GPx3 KO mice. Any difference in GU weight among the TRAMP versus the TRAMP / GPx3 KO mice can be attributed to changes in GPx3 expression. I monitored tumor growth in each genotype, collecting tissue samples at 8, 16, and 20 weeks of age. At each time point, I assessed total body weight and individual weights of GU tract. Interestingly, inactivation of one allele of GPx3 in HET mice was also sufficient to result in substantial increase in both absolute (organ weight, g) and relative GU weights (organ weight/body weight, %). As a consequence, results from HET and KO cohorts were combined. A trend is present suggesting that the average TRAMP / GPx3 HET & KO GU weights are larger than TRAMP at all-time points (Table 2-1 and Figure 2-2). This weight was considered to be an indirect measure of the tumor burden in TRAMP mice.

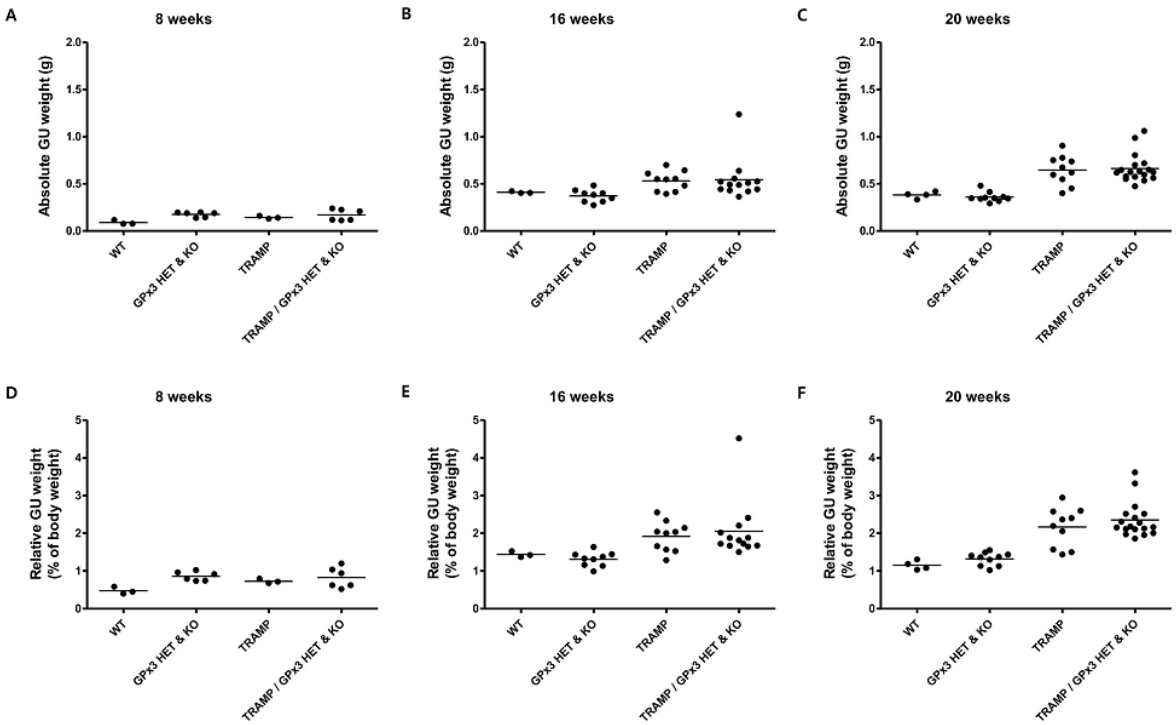

Figure 2-1. Distribution of genito-urinary (GU) tract weights. A-F, GU tracts from all genotypes were carefully dissected *en bloc* at the time of sacrifice. After dissection, GU tract weights were recorded for WT, combined GPx3 (+/–) HET and (–/–) KO, TRAMP, and combined TRAMP / GPx3 (+/–) HET and (–/–) KO cohorts at 8, 16, and 20 weeks of age. The average of both relative GU weight (D–F) and absolute GU weight (A–C) increased in TRAMP / GPx3 HET and KO mice compared to the age-matched TRAMP mice.

2.3.3 Genetic ablation of GPx3 increases the histopathological score of prostate cancer

Results of the histopathological examination of prostatic lobes are shown in Table 2-3 with lesions in each lobe listed both by grade (PIN I - PD) and distribution (focal, multifocal, and diffuse). The mean distribution-adjusted lesion grades for the TRAMP groups, TRAMP / GPx3 HET groups and TRAMP / GPx3 KO groups are shown in Figure 2-3. At 20 weeks, in the lateral, dorsal, and ventral lobes, the histopathological score increased significantly in the TRAMP / GPx3 KO group vs. the TRAMP group. The histopathological scores tended to increase with age and genetic ablation of GPx3. This suggest that the partial or complete loss of GPx3 affects the early transformative steps in the establishment of prostate cancer.

Table 2-3. Grade and distribution of prostate lesions at 8, 16, and 20 weeks.

Lobe and Genotype		PIN I			PIN II			PIN III			PIN IV			WD			PD		
		Focal	Multifocal	Diffuse	Focal	Multifocal	Diffuse	Focal	Multifocal	Diffuse	Focal	Multifocal	Diffuse	Focal	Multifocal	Diffuse	Focal	Multifocal	Diffuse
AP Week 8	TRAMP	1			2														
	TRAMP / GPx3 HET		1		1	1													
	TRAMP / GPx3 KO				2														
AP Week 16	TRAMP				1	3		1	1		4								
	TRAMP / GPx3 HET							3	1		5								
	TRAMP / GPx3 KO							2			2								
AP Week 20	TRAMP							3	2		4	1							
	TRAMP / GPx3 HET								4		1	5							
	TRAMP / GPx3 KO							1			4	2	1						
LP Week 8	TRAMP			2			1												
	TRAMP / GPx3 HET						1		2										
	TRAMP / GPx3 KO								2	1									
LP Week 16	TRAMP								3	2	1	3							1
	TRAMP / GPx3 HET									2		7							
	TRAMP / GPx3 KO										1	3							
LP Week 20	TRAMP								1	2	4	3							
	TRAMP / GPx3 HET									1	2	6	1						
	TRAMP / GPx3 KO										1	3	4						

Table continues

Table 2-3. Continued

Lobe and Genotype		PIN I			PIN II			PIN III			PIN IV			WD			PD		
		Focal	Multifocal	Diffuse	Focal	Multifocal	Diffuse	Focal	Multifocal	Diffuse	Focal	Multifocal	Diffuse	Focal	Multifocal	Diffuse	Focal	Multifocal	Diffuse
DP Week 8	TRAMP				2	1													
	TRAMP / GPx3 HET				2	1													
	TRAMP / GPx3 KO				1	2													
DP Week 16	TRAMP							1	1	5	3								
	TRAMP / GPx3 HET									2	1	6							
	TRAMP / GPx3 KO									1	1	2							
DP Week 20	TRAMP								1	1	2	6							
	TRAMP / GPx3 HET									1	1	8							
	TRAMP / GPx3 KO											4	1	1	1				1
VP Week 8	TRAMP		2		1														
	TRAMP / GPx3 HET		1	1					1										
	TRAMP / GPx3 KO			2	1														
VP Week 16	TRAMP					3		5	2										
	TRAMP / GPx3 HET				1	2		1	3			1							1
	TRAMP / GPx3 KO																		
VP Week 20	TRAMP				3	2	1	3	1										
	TRAMP / GPx3 HET							4	6										
	TRAMP / GPx3 KO							1	2	1	2	1							1

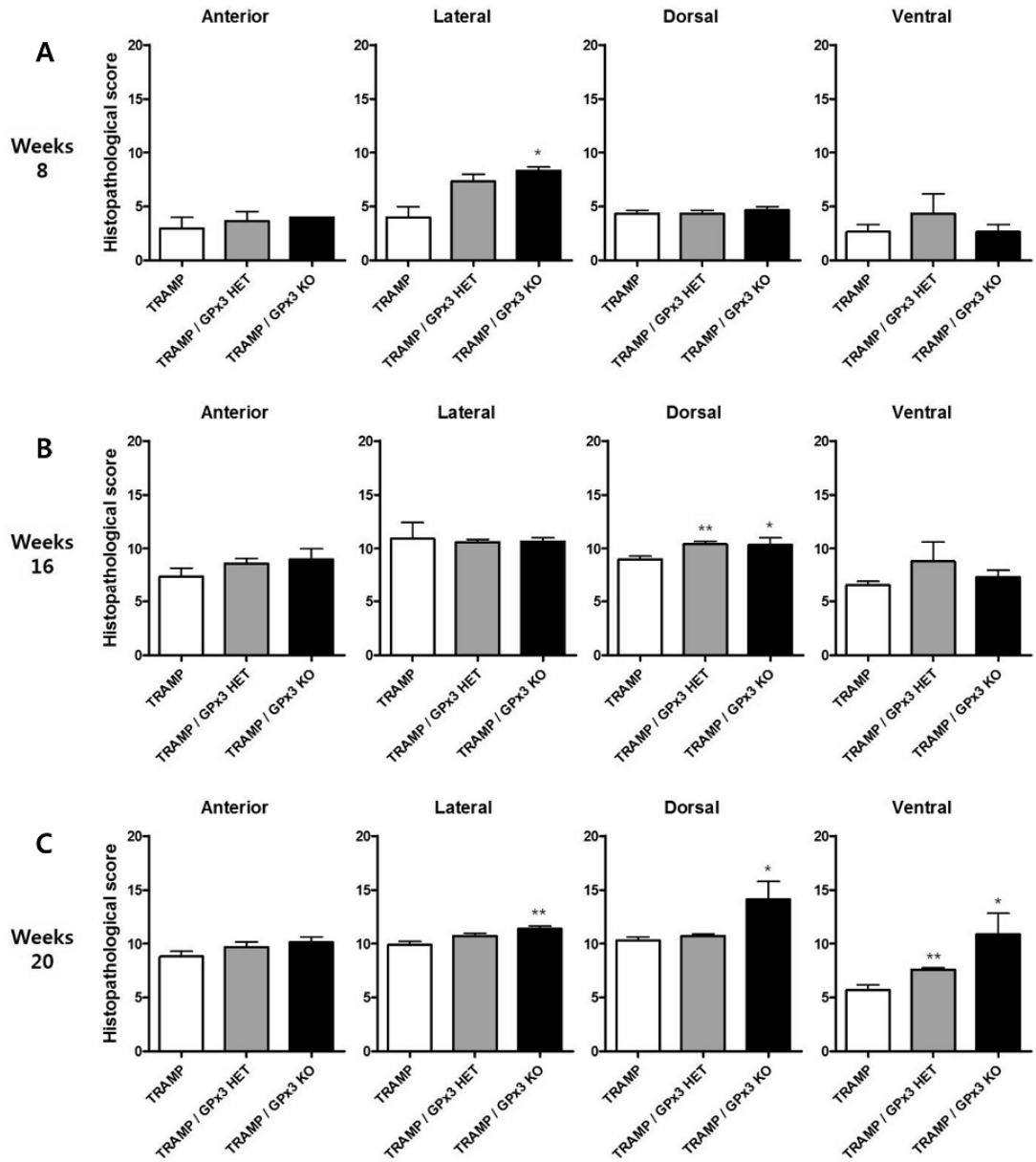

Figure 2-3. Distribution of histopathological score per prostatic lobe in TRAMP mice with age. A-C, Histograms representing the histopathological score

of prostate intraepithelial neoplasia (PIN) to poorly differentiated adenocarcinoma (PD) in TRAMP, TRAMP / GPx3 HET, and TRAMP / GPx3 KO males sacrificed at 8 (A), 16 (B), and 20 (C) weeks of age. *, $P < 0.05$; **, $P < 0.01$ vs. TRAMP. Results are given as mean ± SEM.

2.3.4 Loss of GPx3 affects prostate cancer incidence in TRAMP mice

The TRAMP / GPx3 KO group had a greater percentage of mice with prostate adenocarcinoma present in their prostates than the TRAMP group (Table 2-4 and Figure 2-4). By 16 weeks of age, prostate cancers were detected in only one of 10 mice of TRAMP genotype and only one of 9 mice of TRAMP / GPx3 HET genotype. At the same age, 4 mice of TRAMP / GPx3 KO genotype showed no cancers. Prostate cancer incidence in TRAMP / GPx3 KO mice approached 50% by 20 weeks, while TRAMP and TRAMP / GPx3 HET mice didn't developed prostate cancer at this age. Metastases were scored by macroscopic observation during necropsy and microscopic analysis of organs. By 16 weeks, the number of TRAMP/GPx3 HET mice with lymph node metastases was similar to that of TRAMP mice (11% vs. 10%, respectively, Table 2-5). At the same age, four mice with TRAMP/GPx3 KO genotype showed no metastases. By 20 weeks, the percentages of TRAMP/GPx3 HET and TRAMP/GPx3 KO mice developed lymph node metastases were 10% and 13%, respectively. In addition, the number of TRAMP/GPx3 HET mice with organ metastases by 16 weeks was similar to that of TRAMP mice (11% vs. 10%, respectively, Table 2-6). The incidence of organ metastasis at 20 weeks in TRAMP/GPx3 KO mice was slightly greater than that in TRAMP mice (38% vs. 30%, respectively).

Table 2-4. Number of mice presenting with prostate cancer along with GU weight (mean ± SEM).

Genotype	Age (weeks)	N	Incidence (%)	GU weight (g)
TRAMP	16	1	10	0.700
TRAMP / GPx3 HET	16	1	11	1.238
TRAMP / GPx3 KO	20	4	50	0.727 ± 0.089

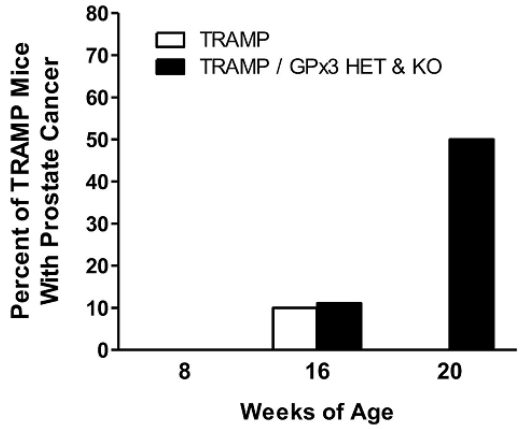

Figure 2-4. GPx3 protection against prostate cancer development in TRAMP mice. The percentage of TRAMP and combined TRAMP / GPx3 HET and KO mice with prostate cancers was determined at 8, 16, and 20 weeks of age. Note that prostate cancer at 20 weeks are only from TRAMP / GPx3 KO mice (50%, N = 8).

Table 2-5. Incidence of mice with lymph node metastasis (percent).

Genotype	8 weeks	16 weeks	20 weeks
TRAMP	0 / 3 (0)	1 / 10 (10)	0 / 10 (0)
TRAMP / GPx3 HET	0 / 3 (0)	1 / 9 (11)	1 / 10 (10)
TRAMP / GPx3 KO	0 / 3 (0)	0 / 4 (0)	1 / 8 (13)

Table 2-6. Incidence of mice with organ metastasis (percent).

Genotype	8 weeks	16 weeks	20 weeks
TRAMP	0 / 3 (0)	1 / 10 (10)	3 / 10 (30)
TRAMP / GPx3 HET	0 / 3 (0)	1 / 9 (11)	0 / 10 (0)
TRAMP / GPx3 KO	0 / 3 (0)	0 / 4 (0)	3 / 8 (38)

2.3.5 GPx3 is disturbed in generated GPx3 deficient TRAMP mice with unchanged SV40T expression

To further ensure that prostate GPx3 expression reflected the genotypes, I evaluated prostate GPx3 mRNA and protein expression in the different prostate lobes of the mice at 8, 16, and 20 weeks of age. GPx3 mRNA and protein expression were absent in lysates and intact tissues of the prostates of TRAMP / GPx3 KO mice and also show dramatic reductions in the prostates of TRAMP / GPx3 HET mice (Figure 2-5A-D and Figure 2-6D-F). I also assessed whether the expression of SV40T Ag alters GPx3 expression in prostate epithelium. No difference in SV40T Ag mRNA (data not shown) and protein expression (Figure 2-5E and Figure 2-6A-C) was observed among the different groups of TRAMP mice and the SV40T Ag expression was abundant within the nuclei of prostate epithelium (Figure 2-6A-C). Therefore, these findings demonstrate that phenotypes mediated by disruption of GPx3 expression are not due to changes in SV40T Ag expression and that TRAMP / GPx3 KO mice have been successfully created.

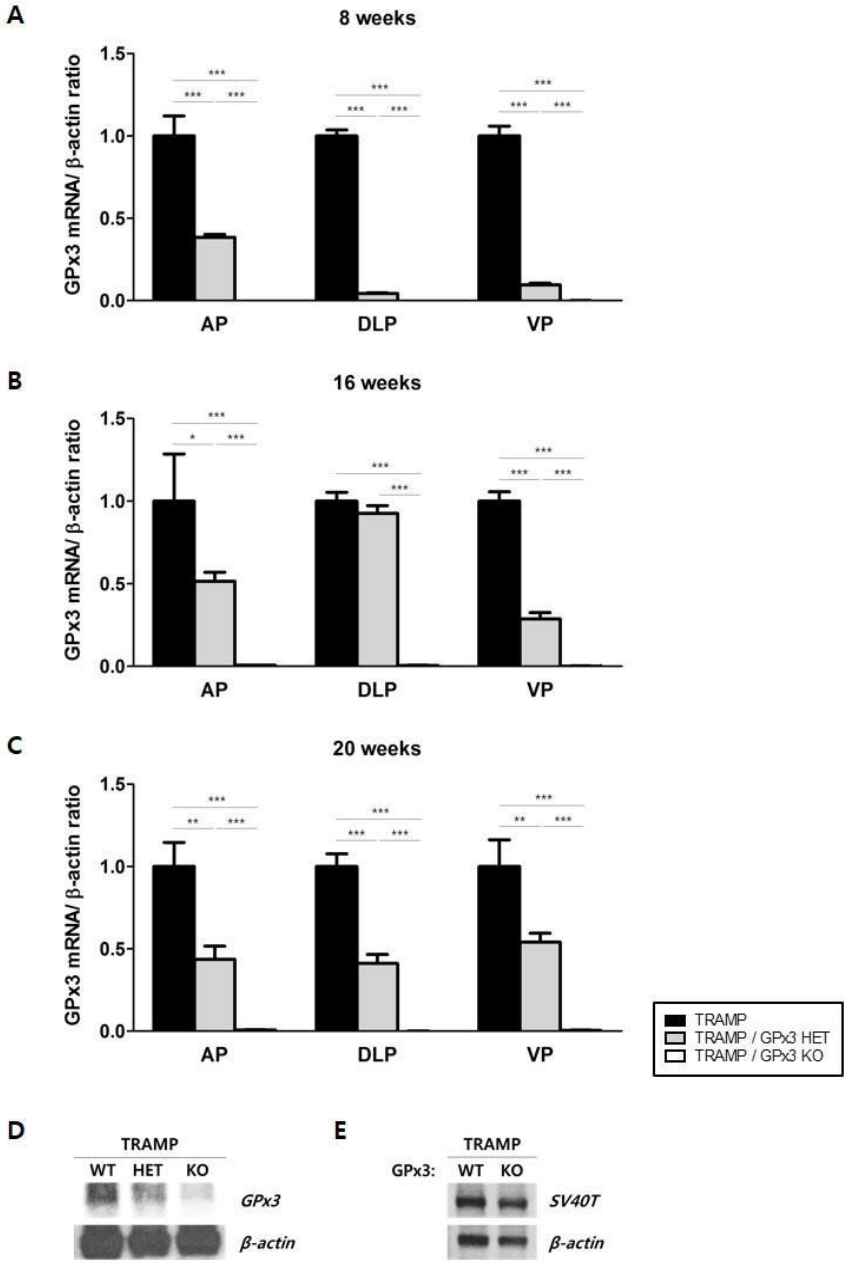

Figure 2-5. Absent GPx3 expression in TRAMP / GPx3 KO prostates. A-C,

Relative expression of GPx3 mRNA in the TRAMP, TRAMP / GPx3 HET, and TRAMP / GPx3 KO mice. The AP, DLP, and VP of mice at 8 (A), 16 (B), and 20 (C) weeks of age were analyzed. In each lobe, values were expressed as the fold change compared to age-matched TRAMP mice at each time point. *, $P < 0.05$; **, $P < 0.01$; ***, $P < 0.001$. Results are given as mean ± SEM. D, Representative Western blot analysis of GPx3 in the DLP at 20 weeks of age. Note that GPx3 expression in TRAMP / GPx3 KO prostate is absent. GPx3 expression in TRAMP / GPx3 HET prostate is also reduced greatly compared to TRAMP prostate. β-actin was used as a loading control. E, Representative Western blot analysis of SV40T antigen in the DLP at 20 weeks of age. Note that levels of the SV40T antigen are not altered because of loss of GPx3. β-actin was used as a loading control.

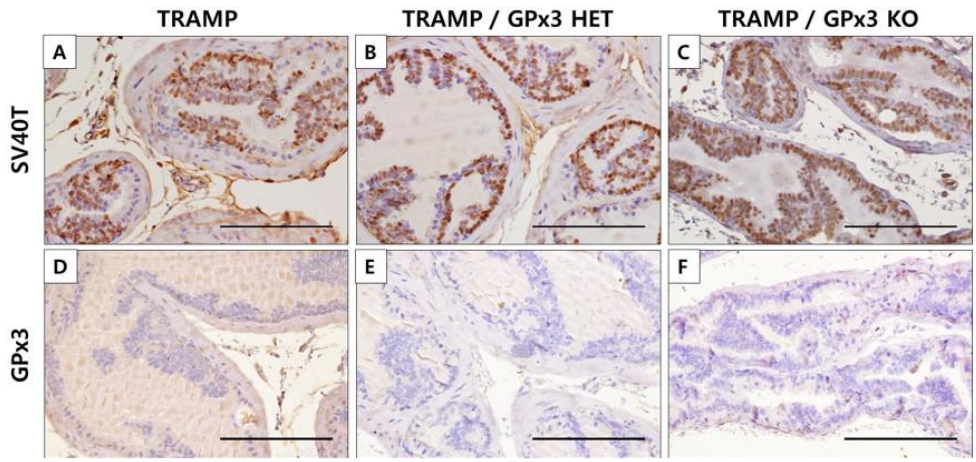

Figure 2-6. Representative immunohistochemical (IHC) analyses of SV40T antigen and GPx3 in dorsal prostate at 8 weeks of age. A-C, IHC for SV40T, brown color, in the TRAMP (A), TRAMP / GPx3 HET (B), and TRAMP / GPx3 KO (C). D-F, IHC for GPx3, brown color, in the TRAMP (D), TRAMP / GPx3 HET (E), and TRAMP / GPx3 KO (F). Magnification, ×400. Scale bar = 100 μm.

2.3.6 Ablation of GPx3 increases proliferation and decreases apoptosis in prostate tissues

To identify how the loss of GPx3 results in enhanced prostate tumorigenesis, I evaluated TRAMP prostates for Ki67, a marker of proliferation, and for active caspase-3, as an index of apoptosis at 20 weeks of age (Figure 2-7). TRAMP / GPx3 KO prostates demonstrated an average of 29.20 ± 1.56 % Ki67-positive cells as compared with 18.71 ± 1.21 % Ki67-positive cells in TRAMP prostates (Figure 2-7A-C). Quantitative analysis also determined the numbers of active caspase-3-positive cells were significantly decreased in TRAMP / GPx3 KO prostate sections as compared with TRAMP (Figure 2-7D-F). These results suggest that proliferative and survival advantage may exist in the GPx3 deficient TRAMP prostate cancer cells.

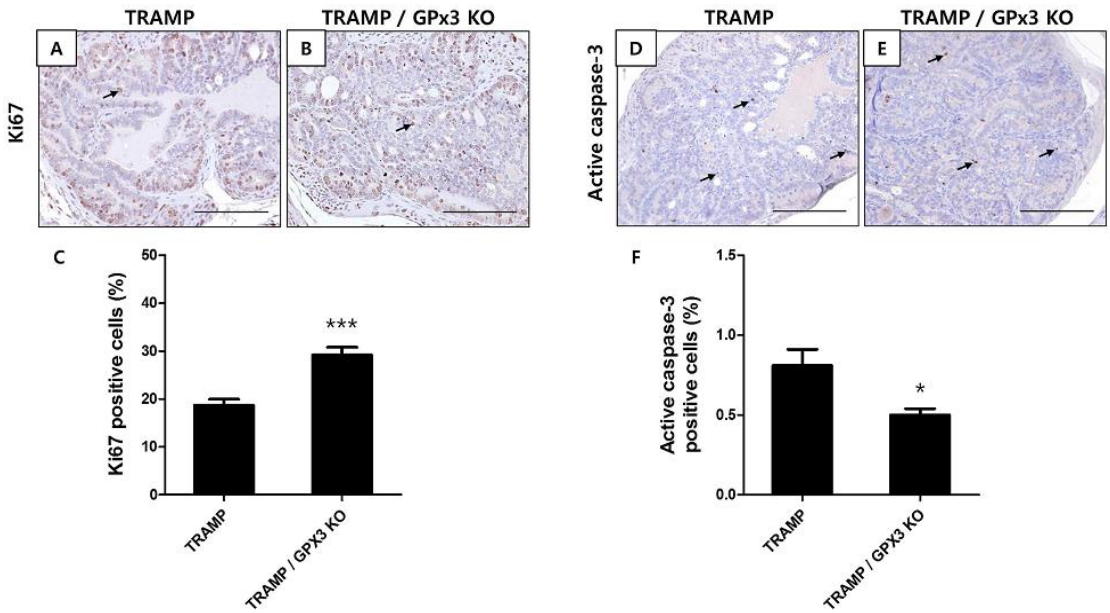

Figure 2-7. Prostate cell proliferation and apoptosis in TRAMP and TRAMP / GPx3 KO mice at 20 weeks. A-C, Ki67 immunostaining was performed to determine proliferation rates in the TRAMP prostates (A) and TRAMP / GPx3 KO prostates (B). Prostates from TRAMP / GPx3 KO mice exhibited significantly increased proportion of Ki-67-positive cells compared to prostates from TRAMP mice (C). D-F, an apoptosis marker, active caspase-3-positive cells in prostate tissues were determined in the TRAMP prostates (D) and TRAMP / GPx3 KO prostates (E). Proportion of apoptotic prostate cells decreased significantly in TRAMP / GPx3 KO prostates compared to TRAMP prostates (F). *, $P < 0.05$; ***, $P < 0.001$ vs. TRAMP. Results are given as mean ± SEM. Arrows depict a few of the positive staining cells (magnification, ×400). Scale bar = 100 μm.

2.3.7 GPx3 deficiency activates Wnt/β-catenin signaling in prostate cancer

To explore the function of GPx3 on Wnt signaling in prostate cancer, the key components of Wnt signaling were determined by quantitative real-time RT-PCR in the AP, DLP, and VP of the mice at 16 and 20 weeks of age (Figure 2-8). Overall, the levels of β-catenin, c-Myc, cyclin D1, forkhead box protein A2 (FoxA2), and matrix metalloproteinase-7 (MMP7) were increased, whereas the level of axis inhibition protein 2 (Axin2) decreased in TRAMP / GPx3 HET and KO mice when compared with the TRAMP mice. These results suggest that the Wnt pathway is up-regulated in GPx3 deficient TRAMP mice. Moreover, one of a transcription factor activated by oxidative stress, Twist1, demonstrated reduced levels in TRAMP / GPx3 WT prostates (Figure 2-8). Taken together, the increased expression levels of β-catenin, c-Myc, cyclin D1, FoxA2, MMP7, and Twist1 but decreased expression of axin2 observed TRAMP prostates lacking GPx3 expression provides further molecular evidence that these GPx3 KO prostate cancers are more prone to cancer development.

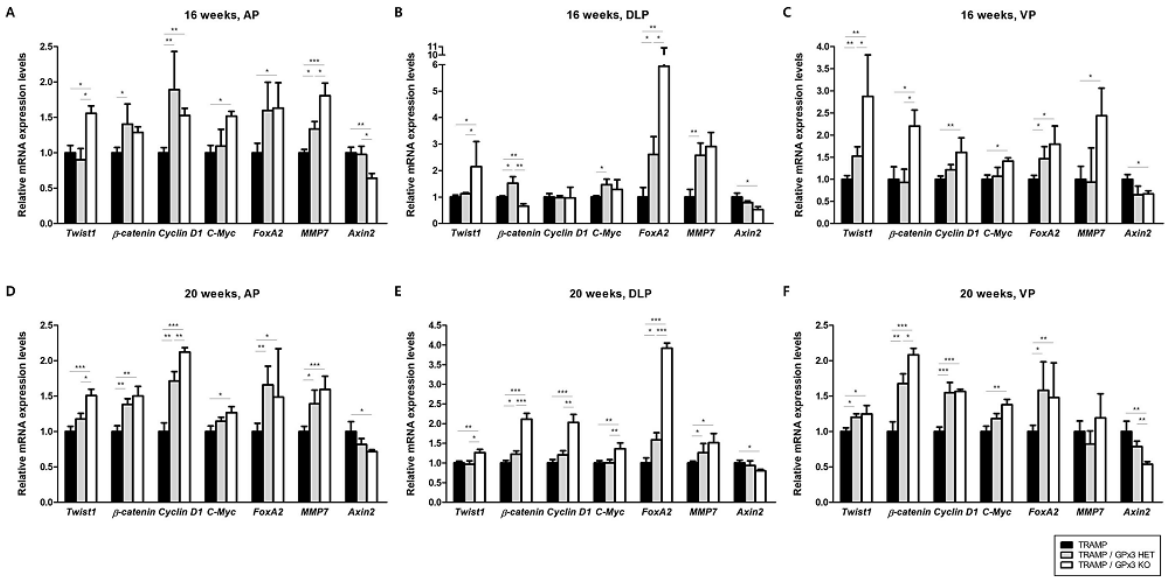

Figure 2-8. Effect of GPx3 genotype and age on Twist1, β-catenin, cyclin D1, c-Myc, FoxA2, MMP7, and axin2 expression in TRAMP mice prostates. A-F, Relative expression of Twist1, β-catenin, cyclin D1, c-Myc, FoxA2, MMP7, and axin2 mRNA in the TRAMP, TRAMP / GPx3 HET, and TRAMP / GPx3 KO mice. The AP (A, D), DLP (B, E), and VP (C, F) of mice at 16 (A-C) and 20 (D-F) weeks of age were analyzed. In each lobe, values were expressed as the fold change compared to age-matched TRAMP mice at each time point. *, $P < 0.05$; **, $P < 0.01$; ***, $P < 0.001$. Results are given as mean ± SEM.

2.4 DISCUSSION

The main findings from this study are the following: (1) GPx3 is down-regulated in prostates of TRAMP mice, (2) alterations in GPx3 expression are associated with and may influence disease progression and ultimately increase prostate tumor outgrowth and histopathological score in prostates of TRAMP mice, (3) ablation of GPx3 increases proliferation and decreases apoptosis in prostate tissues, and (4) GPx3 inhibits prostate cancer development with suppressing Wnt/β-catenin signaling. Overall, these results suggest that GPx3 seems to serve as a tumor suppressor in prostate cancer.

In TRAMP mice, prostate cancer occurs as a consequence of the expression of oncoprotein SV40 large T-antigen under the control of prostate-specific rat probasin promoter (177). Disease pathogenesis in this model mirrors closely that observed in humans, evolving through the early PIN lesion between 8 and 12 weeks of age, WD at 12 weeks of age, MD by 18 weeks of age, and PD by 24 to 30 weeks of age (157, 178, 179). The major advantages of using TRAMP mice for prostate cancer research are that the cancer arises autochthonously within the appropriate microenvironment, mice possess an intact immune system, and heterogenous cancer arises *de novo* and has well-defined course of disease progression (176, 180).

To determine the effect of GPx3 disruption in prostate cancer progression and development, I generated GPx3 deficient TRAMP mice and compared with other genotypes at various ages (8, 16, and 20 weeks) considering the pathogenesis of

prostate cancer in TRAMP model. At 16 weeks of age, only two mice had prostate cancers and all mice in TRAMP / GPx3 KO group had only PIN lesions. This might be because the number of samples in TRAMP / GPx3 KO group is limited to four mice. At 20 weeks of age, only in TRAMP / KO group presented prostate cancers, showing 50% incidence rate (four mice from eight mice), even though the other groups has enough sample size (10 mice in each group). Resultantly, I found that disruption of GPx3 affects prostate cancer incidence in TRAMP mice under 24 weeks of age accordingly, focusing on the effect of disruption of GPx3 on prostate cancer tumorigenesis. GPx3-deficient TRAMP mice also showed a tendency of increasing metastasis compared to TRAMP mice. However, under 20 weeks of age, the incidences of metastasis in the two groups were below ~38% in this study, which is difficult to obtain a meaningful comparison. Therefore, further study is ongoing in our laboratory to investigate the effect of GPx3 genetic modulation on prostate cancer metastasis using TRAMP mice over 28 weeks of age.

GPx3 mRNA and protein expression were absent in the prostate of TRAMP / GPx3 KO mice and they also decreased dramatically in TRAMP / GPx3 HET mice. These findings explain why prostate tumorigenesis in TRAMP / GPx3 HET and TRAMP / GPx3 KO mice behaves similarly. With this disruption of GPx3 levels, β-catenin, c-Myc, cyclin D1, FoxA2, MMP7, and Twist1 expression increased and axin2 expression decreased. β-catenin is a key player in the signal transduction of the Wnt pathway. It can regulate the downstream targets, c-Myc, cyclin D1, FoxA2, MMP7, and axin2. My results suggest that the up-regulation of c-Myc, cyclin D1,

FoxA2, and MMP7 and the down-regulation of axin2 in prostates of GPx3-deficient TRAMP mice may be due to the increased β-catenin expression. There have been a limited number of investigations on the potential role of Wnt/β-catenin signaling in cancer. In thyroid cancer cells, the expression of β-catenin, c-Myc and cyclin D1 is reduced and the level of p-β-catenin was increased after restoration of GPx3 expression (94). Also, GPx3 KO tumors show a significant increase in both nuclear and total β-catenin in colitis-associated carcinoma *in vivo* (171). Activation of the Wnt/β-catenin pathway has effects on prostate cell proliferation, differentiation and the epithelial–mesenchymal transition (EMT) (181, 182). Collectively, these findings suggest that GPx3 inhibits Wnt/β-catenin signaling pathway in these cancers including prostate cancer. Wnt/β-catenin signaling pathway directly controls Foxa2 levels (183, 184). Constitutive activation of β-catenin during prostate development can cause PIN, inducing Foxa2 expression in the mouse prostate (183). FoxA2 is an indicator of active β-catenin signaling in the prostate. Another target gene of Wnt/β-catenin is MMP7, a membrane-type MMP associated with cancer initiation and progression that can cause hyperplastic growths (31, 185). Axin2 is a negative regulator of the Wnt/β-catenin signaling (29, 30, 33). In prostate cancer, dysregulation of axin2 whether from low expression or mutation can disrupt β-catenin degradation and increase nuclear translocation and transcriptional activity (30, 32, 186). Depletion of axin2 can significantly promote the invasiveness, proliferation, and tumor growth. However, these phenotypes are attenuated by axin2 overexpression *in vitro* and *in vivo* (30). High expression levels

of β-catenin are correlated with low expression levels of axin2 in malignant tumors, including prostate cancer (30, 33). One of the factor which could induce β-catenin activation (183), Twist1 increased in the prostates of the GPx3-deficient TRAMP mice. Twist1 regulates cell proliferation, apoptosis inhibition, invasion, and metastasis (183), and its overexpression predicts poor prognosis in various kinds of cancers (184, 185). Twist1 was highly expressed in prostate cancer tissues and positively correlated with pathological grade and metastasis (185). Furthermore, down-regulation of Twist1 induced apoptosis and suppressed migration and invasion in human prostate cancer cells (185). The impact of GPx3 loss on tumorigenesis is likely mediated by increased proliferation and decreased apoptosis that probably results from an increase in β-catenin and Twist1 expressions.

Most cancer cells have higher than normal ROS levels (29, 31) and it suggested to be related cell proliferation, apoptosis, angiogenesis, and metastasis (31, 33). The elevated ROS levels hyperactivate signaling pathways to promote tumorigenesis, leading to activation of NF-κB, PI3K, HIFs and MAP kinases, and others (30-32). Because the balance between pro-oxidant reactions and antioxidant defense is important in prostate cancer treatment, ROS-depleting antioxidative agent may more effectively abrogate activated ROS signaling and suppress tumor growth compared to hormonal therapy alone (30, 186). Furthermore, antioxidants, such as vitamins and glutathione as well as antioxidative enzymes, not only selectively enhance the effect of therapeutic agents on tumor cells but also reduce its toxicity on normal cells, protecting against its adverse effects (187, 188).

Combinational chemotherapy with ascorbic acid and paclitaxel, for example, showed to alleviate the cytotoxicity of paclitaxel but ameliorate the side-effects caused by paclitaxel *in vivo* and *in vitro* (189). Thus, particularly in prostate cancer, chemotherapy and/or radiation and antioxidants are expected to work effectively when used appropriately.

In this study, I show that disruption of GPx3 enhances prostate cancer progression and development, proliferation, and β-catenin and Twist1 expression in the prostates of autochthonous TRAMP mice. The net effect of these changes leads to an increase in cancer promotion in response to GPx3 loss. These findings further support the important role that GPx3 plays as a tumor suppressor, provide an insight into disease pathogenesis, and indicate that it may serve as a substrate for translational investigations in prostate cancer. Additionally, identification of signaling pathways that cooperate with loss of GPx3 to promote tumorigenesis may provide additional therapeutic targets.

CHAPTER III

Troglitazone Inhibits the Migration and Invasion of PC-3 Human Prostate Cancer Cells by Upregulating E-cadherin and Glutathione Peroxidase 3

3.1 INTRODUCTION

Prostate cancer is the most commonly diagnosed noncutaneous cancer. It is also the second leading cause of cancer death in men in the western world (190). Androgen-deprivation therapy, a standard-of-care treatment for prostate cancer, can efficiently control the growth of androgen-dependent cancers. Many patients with localized disease have excellent long-term survival and high cure rates with standard approaches. However, their cancers eventually become resistant to hormone deprivation and progress to castration-resistant prostate cancer. These patients with locally advanced and metastatic disease have poor prognosis, leading to significant morbidity and mortality (191, 192). Therefore, understanding the mechanisms underlying cancer invasion and subsequent metastasis are urgently needed to develop therapies for combating metastatic prostate cancer.

Thiazolidinediones (TZDs) such as troglitazone and ciglitazone are synthetic ligands of peroxisome proliferator-activated receptor γ (PPARγ). They exhibit potential antitumor effects on a broad range of cancers (193-199), including prostate cancer (23, 200, 201). My previous studies performed in prostate cancer cell lines have demonstrated that troglitazone (TGZ) can decrease cell proliferation which is associated with increased expression of glutathione peroxidase 3 (GPx3) (23). TGZ has been tested in clinical trials against breast cancer, colorectal cancer, and prostate cancer (202-204). Treatment with TGZ in patients with advanced prostate cancer has been associated with long periods of stable disease characterized by the absence of new symptoms without new metastases (202),

suggesting that TGZ could have clinical value in suppressing cancer metastasis. However, the role of TGZ in metastasis and the precise molecular mechanisms involved in its action have not been fully elucidated.

During cancer progression, epithelial–mesenchymal transition (EMT) is the major mechanism responsible for mediating the invasiveness and metastasis of cancer cells. EMT is a process that converts immotile epithelial cells to motile mesenchymal cells (205-207). Downregulation of epithelial marker E-cadherin expression is the hallmark of the EMT process. E-cadherin is a tumor suppressor that plays crucial roles in cell-cell adhesion (207). Loss of E-cadherin expression or function is associated with cancer cell invasion and metastasis (208).

In this report, I aimed to investigate the anti-invasive and anti-metastatic activities of TGZ. I hypothesized that TGZ could act on a variety of stages of the metastatic process to prevent cancer cells from metastasizing. I therefore determined the effect of TGZ on the reduction of cell invasive activity. I also examined the effect of TGZ on the expression levels of E-cadherin and GPx3 in PC-3 human prostate cancer cells.

3.2 MATERIALS AND METHODS

3.2.1 Prostate cancer cell line

Human PC-3 prostate cancer cell line was obtained from the American Type Culture Collection (Manassas, VA, USA). These cells were cultured in RPMI (Gibco, Grand Island, NY, USA) supplemented with 10% fetal bovine serum (FBS) (Gibco) and 1% penicillin/streptomycin (Gibco) at 37°C in 95% air/5% CO_2. TGZ (Sigma, St. Louis, MO, USA) and GW9662 (Cayman, Ann Arbor, MI, USA) were dissolved in 100% ethanol (Merck and Co., Inc., Darmstadt, Germany) to obtain concentration of 16 mM. The final ethanol concentration in the solution was 0.25%. Ethanol alone at the same final concentration of 0.25% was used as control.

3.2.2 Cell proliferation assay

The proliferation potential of cells was measured using thiazolyl blue tetrazolium bromide (MTT; Sigma) assay based on the ability of live cells to convert tetrazolium salt into purple formazan. Briefly, PC-3 cells were seeded into 96-well cell culture plates at a density of 8×10^3 per well in 200 μl media. After 24 h of culturing, the medium was changed to 1% FBS-RPMI for 24 h. Cells were supplemented with TGZ at concentrations of 1, 10, 40 μM or vehicle (ethanol) control and cultured for 48 h. The medium was then replaced with 100 μl of MTT (diluted to 1 mg/ml in FBS-free medium, from a stock solution of 10 mg/ml) and

incubated at 37°C for 3 h. The supernatant was removed and 100 µl of DMSO was added to each well to dissolve the formazan crystals. Plates were agitated at room temperature for 5 min. The absorbance was read at 540 nm on an Epoch BioTek microplate reader (BioTek, Winooski, VT, USA). All treatments were performed in triplicates.

3.2.3 Cell migration assay

Cell motility was assessed using an *in vitro* wound healing assay. PC-3 cells were seeded into six-well cell culture plate and grown until confluent. Monolayers of confluent PC-3 cells were then scarred. Cell repair was monitored using an inverted microscope (Olympus IX70, Tokyo, Japan) following 24 h exposure to TGZ at concentrations of 1, 10, 40 µM, or vehicle (ethanol) control. All treatments were performed in triplicates.

3.2.4 Cell invasion assay

Cell invasion was measured using a Transwell insert. Briefly, 8-µm transwell inserts (SPL, Pocheon, Korea) were coated with Matrigel (Gibco) and incubated at 37°C for 2 h to become gelatinous. Cells were grown to subconfluence, detached by trypsinization, washed, resuspended in serum free RPMI, and added to the transwell insert (2×10^4 cells/insert) at a final concentration of 1×10^5 cells/ml together with TGZ at concentrations of 1, 10, 40 µM, or vehicle (ethanol) control.

Cell-free RPMI medium was added to the lower chamber. Assays were incubated at 37°C for 30 h. Non-invasive cells in the upper surface of the membrane were removed with a cotton swab. The remaining cells on the membrane were fixed in methanol for 10 min, stained with Hematoxylin, and washed with PBS. Invaded cells were counted under a light microscope.

3.2.5 Real-time reverse transcription-polymerase chain reaction (PCR)

Total RNA was isolated using a Hybrid-R RNA extraction kit (GeneAll Biotechnology, Seoul, South Korea). First strand cDNAs were synthesized using an M-MLV cDNA Synthesis kit (Enzynomics, Daejeon, South Korea) following the supplier's instructions. Real-time reverse transcription-PCR was performed with TOPreal™ qPCR 2X PreMIX (Enzynomics) on a CFX Connect Real-Time PCR Detection system (Bio-Rad). Primers used were 5'–ACATGCCTACAGGTATGCGT–3 (sense) and 5'–GAGCAGAACAATTGGACCTA–3' (antisense) for human GPx3; 5'–TTGCTACTGGAACAGGGACACT–3' (sense) and 5'–GGAGATGTATTGGGAGGAAGGTC–3' (antisense) for human E-cadherin; and 5'–CATGTACGTTGCTATCCAGGC–3' (sense) and 5'–CTCCTTAATGTCACGCACGAT–3' (antisense) for human beta-actin. Human beta-actin gene expression were used for cDNA normalization. Changes in mRNA expression (fold) were quantified using comparative CT ($2^{-\Delta\Delta Ct}$) method.

3.2.6 Western blot analysis

Cell lysates were resolved by sodium dodecyl sulfate polyacrylamide gel electrophoresis (SDS-PAGE) before transferring the proteins to nitrocellulose membranes and probing with mouse monoclonal anti-E-cadherin primary antibody (Santa Cruz Biotechnology, Santa Cruz, CA, USA), mouse monoclonal anti-GPx3 primary antibody (Abcam, Inc., Cambridge, MA, USA), and goat polyclonal anti-actin primary antibody (Santa Cruz). Blots were then incubated with HRP-conjugated secondary antibodies (Zymed, San Francisco, CA, USA). Blots were developed with a chemiluminescent substrate (DoGEN, Seoul, South Korea).

3.2.7 Statistical analysis

All data are presented as mean ± standard error. Statistically significance ($P < 0.05$) was further analyzed with Student's *t*-test.

3.3 RESULTS

3.3.1 Effect of TGZ on cell proliferation of PC-3 cells

To examine the effect of TGZ on cell viability of PC-3 cells, I treated these cells with 1, 10, or 40 μM of TGZ for 0, 24, or 48 h and determined the rate of cell survival with MTT assay. Results are shown in Figure 3-1. TGZ treatment decreased cell proliferation in a dose-dependent manner. Compared to control cells, cells treated with 10 and 40 μM of TGZ for 24 h showed decreased cell growth rate by 20.49% and 34.69%, respectively.

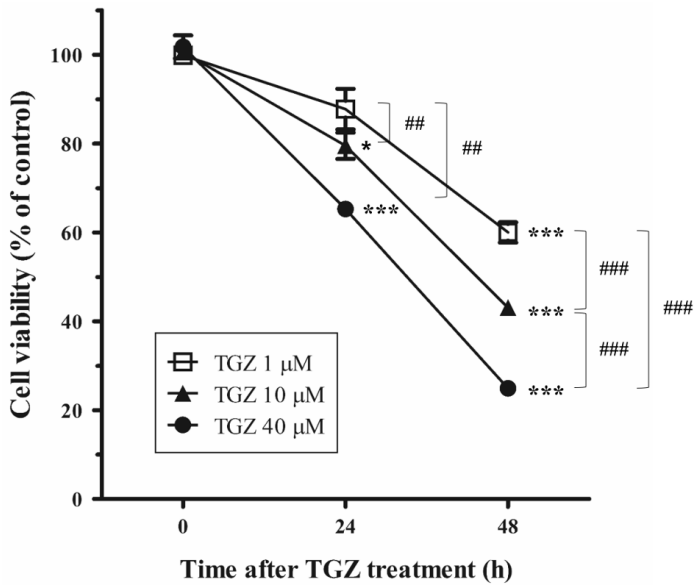

Figure 3-1. Effect of TGZ on the proliferation of PC-3 cells. TGZ inhibited the proliferation of PC-3 cells. The absorbance values of PC-3 cells treated with 1, 10, and 40 μM TGZ for different times were read at 540 nm using a plate reader. The cell viability of cells was calculated based on the proliferation of PC-3 cells compared to the proliferation of the vehicle control group. *, $P < 0.05$; ***, $P < 0.001$, vs. vehicle control. $^{\#\#}$, $P < 0.01$; $^{\#\#\#}$, $P < 0.001$, compared to each other. Results are presented as mean ± SEM.

3.3.2 TGZ inhibits cell migration and invasion of PC-3 cells

I measured cell migration and invasion of PC-3 cells treated with TGZ with *in vitro* wound healing assay and Transwell assay. Results are shown in Figure 3-2 and Figure 3-3, respectively. Following incubation with different concentrations of TGZ for 24 h, the migration of PC-3 cells to the denuded zone was suppressed in a dose-dependent manner (Figure 3-2), indicating that TGZ significantly inhibited the motility of PC-3 cells.

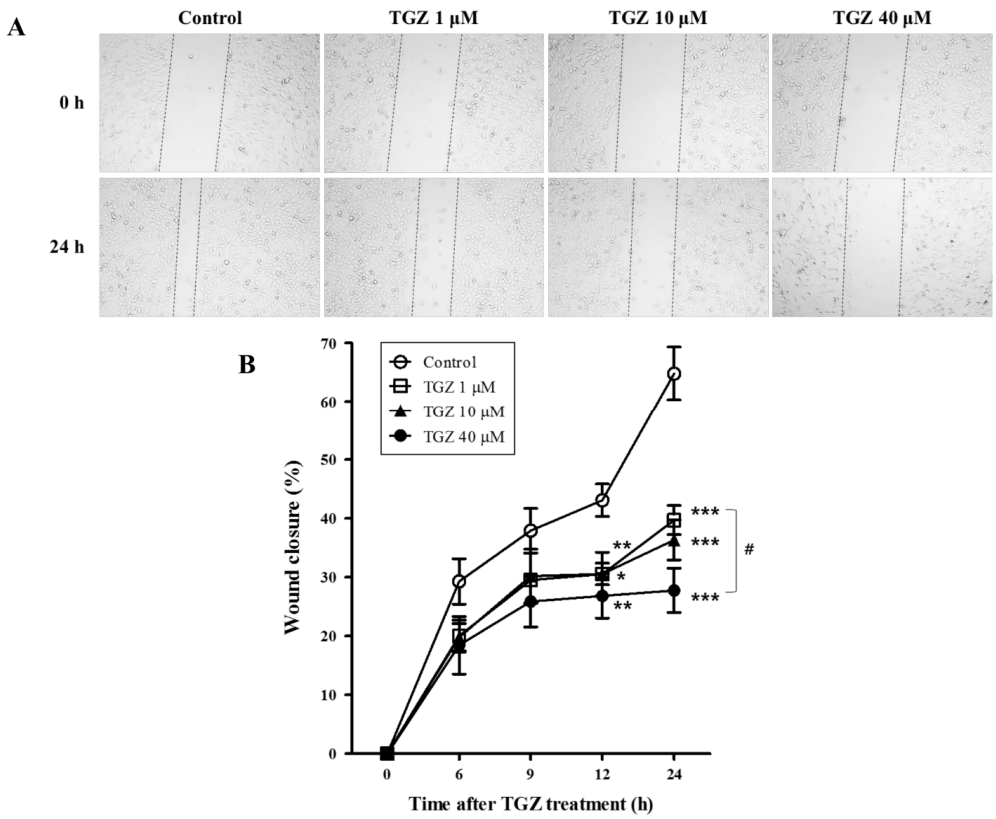

Figure 3-2. Effect of TGZ on the migration of PC-3 cells. TGZ suppressed the migration of PC-3 human prostate cancer cells. (A) Cells that migrated to the wounded region were photographed (magnification, x40). (B) Migration ability of PC-3 cells treated with 1, 10, and 40 μM TGZ for different time period was measured by wound healing assay. *, $P < 0.05$; **, $P < 0.01$, ***, $P < 0.001$, compared to vehicle control at each time point. $^{\#}$, $P < 0.05$, compared to each other. Results are presented as mean ± SEM.

Results of transwell assay revealed that TGZ suppressed the invasion of PC-3 cells across Matrigel-coated filter in a dose-dependent manner (Figure 3-3). Treatment with 1, 10, and 40 μM of TGZ inhibited 54.27, 65.63, and 73.70% of cell invasion, respectively. These results revealed that TGZ significantly inhibited the invasion of PC-3 cells. Taken together, these data demonstrate that TGZ can inhibit both cell migration and invasion of PC-3 cells.

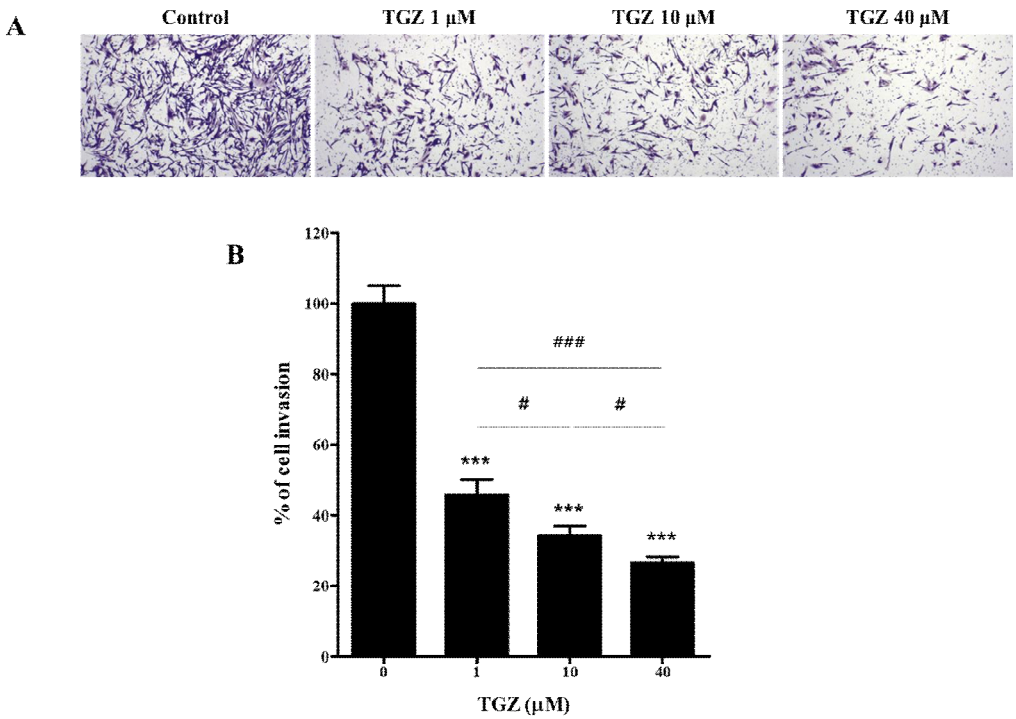

Figure 3-3. Effect of TGZ on the invasion of PC-3 cells. TGZ suppressed the invasion of PC-3 human prostate cancer cells. (A) Invaded cells were photographed (magnification, x100). (B) Invasion capacity was examined using a Transwell insert coated with matrigel. ***, $P < 0.001$, vs. vehicle control. $^{\#}$, $P < 0.05$; $^{\#\#\#}$, $P < 0.001$, compared to each other. Results are presented as mean ± SEM.

3.3.3 TGZ increases the mRNA levels of E-cadherin and GPx3 in PC-3 human prostate cancer cells

To investigate whether TGZ could enhance the transcriptional levels of E-cadherin and GPx3 genes in PC-3 cells, RT-qPCR was performed. Results are shown in Figure 4. TGZ at 1 and 10 μM significantly increased the mRNA levels of E-cadherin in a dose-dependent manner (Figure 3-4A). TGZ at 10 μM also significantly increased the mRNA levels of GPx3 (Figure 3-4B).

Although TGZ was able to affect the transcriptional levels of E-cadherin and GPx3, the mechanisms underlying these events remain to be elucidated. To confirm whether these effects were dependent on the activation of PPARγ, GW9662 (a PPARγ antagonist) was used to inhibit the function of PPARγ in PC-3 cells. TGZ-induced upregulation of E-cadherin and GPx3 mRNAs in PC-3 cells were attenuated upon the addition of GW9662 (Figure 3-4). Taken together, these results showed that TGZ increased the transcriptional levels of both E-cadherin and GPx3 in PC-3 cells in a PPARγ-dependent manner.

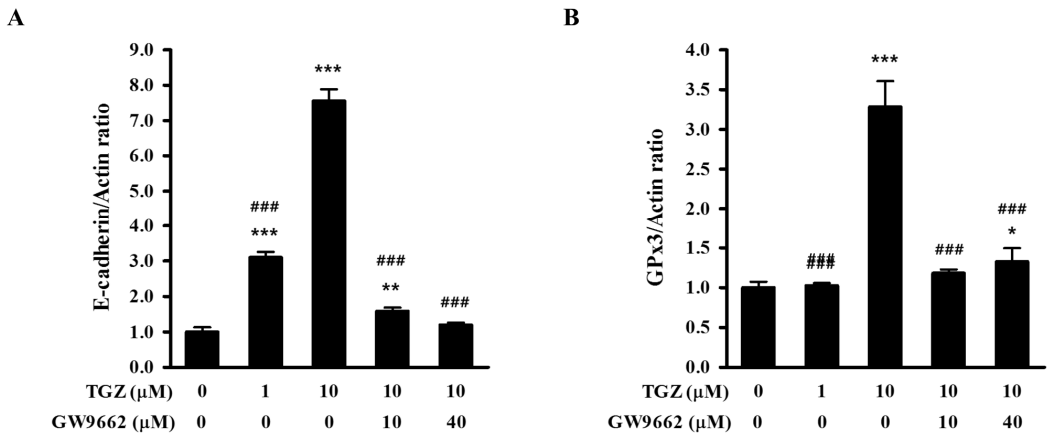

Figure 3-4. Effect of TGZ on mRNA expression levels of E-cadherin and GPx3 in PC-3 cells. TGZ upregulated the mRNA expression levels of E-cadherin and GPx3 in PC-3 cells. PC-3 cells were treated with various concentration of TGZ (0, 1, or 10 μM) for 24 h prior to harvest. Total RNA was extracted and the expression of E-cadherin (A) and GPx3 (B) was measured by real-time reverse transcription-PCR reaction. (A) TGZ at 1 and 10 μM increased the mRNA levels of E-cadherin in a dose-dependent manner. (B) TGZ at 10 μM increased the mRNA levels of GPx3. *, $P < 0.05$; **, $P < 0.01$; ***, $P < 0.001$, vs. vehicle control. $^{###}$, $P < 0.001$, vs. 10 μM TGZ treatment group. Results are given as mean ± SEM.

3.3.4 TGZ increases the protein levels of E-cadherin and GPx3 in PC-3 human prostate cancer cells

I next determined the protein levels of E-cadherin and GPx3 in PC-3 cells by western blot analysis following 48 h treatment with 0, 1, or 10 μM TGZ. Results are shown in Figure 3-5. TGZ at 1 and 10 μM significantly increased the protein levels of E-cadherin in a dose-dependent manner (Figure 3-5A and Figure 3-5B). TGZ at 10 μM also significantly increased the protein levels of GPx3 (Figure 3-5A and Figure 3-5C). TGZ-induced upregulation of E-cadherin and GPx3 protein levels in PC-3 cells were attenuated upon the addition of GW9662 (Figure 3-5). Thus, TGZ upregulated E-cadherin and GPx3 protein levels in a PPARγ-dependent manner, which was consistent with its upregulating effect on E-cadherin and GPx3 mRNA levels.

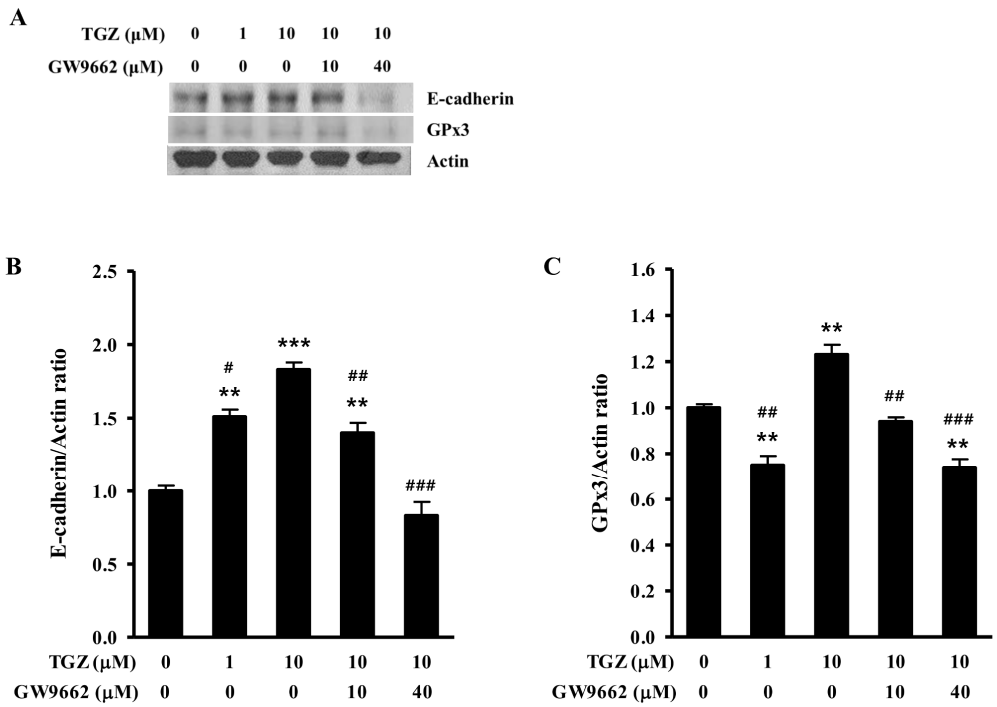

Figure 3-5. Effect of TGZ on protein expression levels of E-cadherin and GPx3 in PC-3 cells. TGZ increased the protein expression levels of E-cadherin and GPx3 in PC-3 cells. (A) Representative Western blot analysis of the PC3 cell line. (B, C) Protein expression levels of E-cadherin (B) and GPx3 (C) were quantified using actin as a normalization control. **, $P < 0.01$; ***, $P < 0.001$, vs. vehicle control. $^{\#}$, $P < 0.05$; $^{\#\#}$, $P < 0.01$; $^{\#\#\#}$, $P < 0.001$, vs. 10 μM TGZ treatment group. Results are given as mean ± SEM.

3.4 DISCUSSION

TZDs are a new class of antidiabetics. They are specific ligands for PPARγ. The level of PPARγ expression is known to be varied depending on the types of tissues and carcinomas (209). PPARγ has been investigated as a therapeutic target for cancer treatment. Some studies have reported that PPARγ can induce anti-proliferative, anti-angiogenic, and pro-differentiation pathways in several tissue types, thus playing role in the pathogenesis and progression of cancers including prostate cancer (210, 211). Using TZDs as PPARγ ligands, some studies have investigated the effect of PPARγ on the metastatic potential and explored its underlying mechanisms. TZDs have been shown to be able to suppress cell migration, invasion, and metastasis of cancers in the colon, liver, breast, lung, bladder, prostate, and other organs (212-220). For example, in colon cancer, TZD can inhibit the growth and metastasis of HT-29 human colon cancer cells through its differentiation-promoting effects both *in vivo* and *in vitro* by involving the modulation of E-cadherin/β-catenin system (212). In hepatocellular carcinoma, the suppression of cell invasion and migration mediated by PPARγ has been demonstrated to be mediated via downregulation of MMPs and increased expression levels of TIMP3 and E-cadherin (214, 215).

However, the mechanisms behind the inhibitory action of TZDs on cell invasion in prostate cancer remain unclear. To better understand the molecular mechanisms involved in TGZ-induced inhibition of cell invasion, I examined the effect of TGZ on the expression of E-cadherin and GPx3 in the present study. Both E-cadherin

and GPx3 might be involved in cancer cell invasion. The present study clearly demonstrated that TGZ reduced cell migration and invasion of PC-3 cells. Consistently, TGZ positively regulated the mRNA and protein levels of E-cadherin and GPx3 in PPARγ-dependent manner. This study might provide preliminary evidence for further research to determine the mechanisms underlying the inhibition of metastasis by TZDs.

A great majority of human solid tumors are carcinomas originating from various epithelial cell types throughout the body (206, 207). The most apparent morphological change that occurs during the transition from a benign tumor to a malignant and metastatic one is that tumor cells change from a highly differentiated epithelial morphology to a migratory and invasive phenotype (206). This process of EMT can lead to the loss of cell–cell contacts and the gain of cell motility (206, 221). It also causes the dissemination of single carcinoma cells from primary epithelial tumors (207). These changes are necessary for invasion. During the execution of EMT, many genes involved in cell adhesion, mesenchymal differentiation, cell migration, and invasion are transcriptionally regulated (207). Among these genes, loss of adhesive function of E-cadherin in epithelial cell has been considered a hallmark of EMT and metastatic carcinoma (205, 207, 208, 221).

E-cadherin production is maintained in most differentiated tumors, including carcinomas of the skin, head and neck, breast, lung, liver, colon, and prostate. However, there seems to be an inverse correlation between E-cadherin levels and cancer grade or patient survival (205). Partial loss of E-cadherin has been

associated with carcinoma progression and poor prognosis in various human and mouse tumors (207). In both tumor cell cultures and *in vivo* mouse tumor models, forced expression of E-cadherin in certain invasive carcinoma cells can inhibit their ability to invade and metastasize. Conversely, blocking E-cadherin function in noninvasive tumor cells can activate their invasiveness and metastatic powers (206, 207). In the present study, an increase in E-cadherin might explain the increased cell to cell interactions and deceased capacity for the motility of PC-3 cells following TGZ treatment. Thus, reversing the functional protein levels of E-cadherin might be an alternative strategy to develop cancer therapy.

GPx3 belongs to the family of glutathione peroxidases. It is well known that glutathione peroxidases are among the most important ROS scavengers that can protect cells from oxidative damage. Down-regulation of GPx3 by hypermethylation has been found in many cancers (82, 88, 94, 153, 222-226), including prostate cancer (23, 79, 152). In prostate cancer, GPx3 has been shown to have a negative correlation with poor clinical outcomes (79, 100). Overexpression of GPx3 in prostate cancer cell lines can suppress colony formation and cell proliferation *in vitro* (23, 79, 98). Xenografted PC3 human prostate cancer cells expressing GPx3 have shown reduction in tumor volume, elimination of metastasis, and reduction of animal death (79). My previous work using transgenic adenocarcinoma of mouse prostate (TRAMP) has shown that GPx3 is down-regulated in prostates of TRAMP mice and that disruption of GPx3 expression in TRAMP mice can increase prostate cancer development and metastasis (227). It

has been demonstrated that silencing GPx3 expression will promote cancer metastasis in human thyroid and gastric cancer cells (94, 222). In this study, it was noteworthy that GPx3 expression was upregulated by treatment with TGZ in human prostate cancer cells. This induction was closely associated with the anti-invasion effect of TGZ. All these results suggest that GPx3 can act as a negative regulator of prostate tumor growth and invasion, providing further evidence for its potential as a tumor suppressor.

In conclusion, the present study indicated that TGZ effectively abrogated the migration and invasion of PC-3 cells *in vitro* by increasing the expression levels of E-cadherin and GPx3. Upregulated expression of E-cadherin and GPx3 is one of possible mechanism involved in the anti-migration and anti-invasion effects of TGZ. Changed expression caused by TGZ might explain the mechanisms underlying the invasion inhibition ability of TZDs and its mode of action.

GENERAL CONCLUSION

High intake of animal fat has been linked to prostate cancer development. However, research is too limited to support strong conclusions regarding the role of animal fat in prostate cancer tumorigenesis, and the mechanisms remain unclear. No studies have found that the decrease in GPx3 during progression of prostate cancer results from dietary fat intake. I therefore determined the role of GPx3 in prostate cancer progression using PC-3 human prostate cancer cells and TRAMP mouse model in Chapter I. Cholesterol treatment increased proliferation of PC-3 human prostate cancer cells, decreased GPx3 expression both at the mRNA and protein levels, and decreased GPx activity, which was associated with increased H_2O_2 in cell culture media. TGZ increased GPx3 mRNA expression in PC-3 human prostate cancer cells, decreased cell proliferation and attenuated cholesterol-induced H_2O_2 increase in cell culture media. A high-fat diet enhanced prostate cancer tumorigenesis in early-stage TRAMP mice and decreased GPx3 expression both at the mRNA and protein levels in prostates of TRAMP mice.

The role of GPx3 in prostate cancer tumorigenesis is not determined precisely. So I used TRAMP mouse model to study the molecular mechanism related to the effect of modulating GPx3 expression using genetic manipulation in Chapter II. GPx3 was down-regulated in prostates of TRAMP mice. Alterations in GPx3 expression were associated with and may influence disease progression and ultimately increase prostate tumor outgrowth and histopathological score in

prostates of TRAMP mice. Ablation of GPx3 increased proliferation and decreases apoptosis in prostate tissues. GPx3 inhibited prostate cancer development with suppressing Wnt/β-catenin signaling. I showed that disruption of GPx3 enhances prostate cancer progression and development, proliferation, and β-catenin and Twist1 expression in the prostates of autochthonous TRAMP mice. The net effect of these changes leads to an increase in cancer promotion in response to GPx3 loss.

I was observed that TGZ decreased cell proliferation which is associated with increased expression of GPx3 in Chapter I. Yet, the role of TGZ in metastasis and the molecular mechanisms involved in its action have not been fully elucidated. So I determined the effect of TGZ on the reduction of cell invasive activity and examined the effect of TGZ on the expression levels of E-cadherin and GPx3 in PC-3 human prostate cancer cells in Chapter III. TGZ effectively abrogated the migration and invasion of PC-3 cells *in vitro* by increasing the expression levels of E-cadherin and GPx3. Upregulated expression of E-cadherin and GPx3 is one of possible mechanism involved in the anti-migration and anti-invasion effects of TGZ.

The result of this study can help to understand the role of GPx3 as a potent tumor suppressor in prostate cancer, likely by reducing oxidative stress and ROS that lead to tumor initiation, progression and metastasis. GPx3 may become an attractive target for the design of therapeutic and chemopreventive strategies in patients with prostate cancer.

REFERENCES

1. McMichael AJ. Food, nutrition, physical activity and cancer prevention. Authoritative report from World Cancer Research Fund provides global update. Public health nutrition. 2008;11(7):762-3.

2. Zhang X, Zhou G, Sun B, Zhao G, Liu D, Sun J, et al. Impact of obesity upon prostate cancer-associated mortality: A meta-analysis of 17 cohort studies. Oncology letters. 2015;9(3):1307-12.

3. Discacciati A, Orsini N, Wolk A. Body mass index and incidence of localized and advanced prostate cancer--a dose-response meta-analysis of prospective studies. Annals of oncology : official journal of the European Society for Medical Oncology. 2012;23(7):1665-71.

4. Rodriguez C, Freedland SJ, Deka A, Jacobs EJ, McCullough ML, Patel AV, et al. Body mass index, weight change, and risk of prostate cancer in the Cancer Prevention Study II Nutrition Cohort. Cancer epidemiology, biomarkers & prevention : a publication of the American Association for Cancer Research, cosponsored by the American Society of Preventive Oncology. 2007;16(1):63-9.

5. Pelser C, Mondul AM, Hollenbeck AR, Park Y. Dietary fat, fatty acids, and risk of prostate cancer in the NIH-AARP diet and health study. Cancer epidemiology, biomarkers & prevention : a publication of the American Association for Cancer Research, cosponsored by the American Society of Preventive Oncology. 2013;22(4):697-707.

6. Ma RW, Chapman K. A systematic review of the effect of diet in prostate cancer prevention and treatment. Journal of human nutrition and dietetics : the official journal of the British Dietetic Association. 2009;22(3):187-99; quiz 200-2.

7. Gathirua-Mwangi WG, Zhang J. Dietary factors and risk for advanced prostate cancer. Eur J Cancer Prev. 2014;23(2):96-109.

8. Giovannucci E, Rimm EB, Colditz GA, Stampfer MJ, Ascherio A, Chute CG, et al. A prospective study of dietary fat and risk of prostate cancer. J Natl Cancer Inst. 1993;85(19):1571-9.

9. Xue L, Yang K, Newmark H, Lipkin M. Induced hyperproliferation in epithelial cells of mouse prostate by a Western-style diet. Carcinogenesis. 1997;18(5):995-9.

10. Llaverias G, Danilo C, Wang Y, Witkiewicz AK, Daumer K, Lisanti MP, et al. A Western-type diet accelerates tumor progression in an autochthonous mouse model of prostate cancer. Am J Pathol. 2010;177(6):3180-91.

11. Blando J, Moore T, Hursting S, Jiang G, Saha A, Beltran L, et al. Dietary energy balance modulates prostate cancer progression in Hi-Myc mice. Cancer prevention research. 2011;4(12):2002-14.

12. Kobayashi N, Barnard RJ, Said J, Hong-Gonzalez J, Corman DM, Ku M, et al. Effect of low-fat diet on development of prostate cancer and Akt phosphorylation in the Hi-Myc transgenic mouse model. Cancer Res. 2008;68(8):3066-73.

13. Liu J, Ramakrishnan SK, Khuder SS, Kaw MK, Muturi HT, Lester SG, et

al. High-calorie diet exacerbates prostate neoplasia in mice with haploinsufficiency of Pten tumor suppressor gene. Molecular metabolism. 2015;4(3):186-98.

14. Bostwick DG, Burke HB, Djakiew D, Euling S, Ho SM, Landolph J, et al. Human prostate cancer risk factors. Cancer. 2004;101(10 Suppl):2371-490.

15. Venkateswaran V, Klotz LH. Diet and prostate cancer: mechanisms of action and implications for chemoprevention. Nat Rev Urol. 2010;7(8):442-53.

16. Fleshner N, Zlotta AR. Prostate cancer prevention: past, present, and future. Cancer. 2007;110(9):1889-99.

17. Hill P, Wynder EL, Garbaczewski L, Garnes H, Walker AR. Diet and urinary steroids in black and white North American men and black South African men. Cancer Res. 1979;39(12):5101-5.

18. Rosenthal MB, Barnard RJ, Rose DP, Inkeles S, Hall J, Pritikin N. Effects of a high-complex-carbohydrate, low-fat, low-cholesterol diet on levels of serum lipids and estradiol. Am J Med. 1985;78(1):23-7.

19. Hamalainen EK, Adlercreutz H, Puska P, Pietinen P. Decrease of serum total and free testosterone during a low-fat high-fibre diet. J Steroid Biochem. 1983;18(3):369-70.

20. Hamalainen E, Adlercreutz H, Puska P, Pietinen P. Diet and serum sex hormones in healthy men. J Steroid Biochem. 1984;20(1):459-64.

21. Aronson WJ, Barnard RJ, Freedland SJ, Henning S, Elashoff D, Jardack PM, et al. Growth inhibitory effect of low fat diet on prostate cancer cells: results of a prospective, randomized dietary intervention trial in men with prostate cancer.

The Journal of urology. 2010;183(1):345-50.

22. Soliman S, Aronson WJ, Barnard RJ. Analyzing serum-stimulated prostate cancer cell lines after low-fat, high-fiber diet and exercise intervention. Evid Based Complement Alternat Med. 2011;2011:529053.

23. Chang SN, Han J, Abdelkader TS, Kim TH, Lee JM, Song J, et al. High Animal Fat Intake Enhances Prostate Cancer Progression and Reduces Glutathione Peroxidase 3 Expression in Early Stages of TRAMP Mice. Prostate. 2014;74(13):1266-77.

24. Llaverias G, Danilo C, Wang Y, Witkiewicz AK, Daumer K, Lisanti MP, et al. A Western-Type Diet Accelerates Tumor Progression in an Autochthonous Mouse Model of Prostate Cancer. Am J Pathol. 2010;177(6):3180-91.

25. Droge W. Free radicals in the physiological control of cell function. Physiological reviews. 2002;82(1):47-95.

26. Udensi UK, Tchounwou PB. Oxidative stress in prostate hyperplasia and carcinogenesis. J Exp Clin Cancer Res. 2016;35(1):139.

27. Khandrika L, Kumar B, Koul S, Maroni P, Koul HK. Oxidative stress in prostate cancer. Cancer Lett. 2009;282(2):125-36.

28. Paschos A, Pandya R, Duivenvoorden WC, Pinthus JH. Oxidative stress in prostate cancer: changing research concepts towards a novel paradigm for prevention and therapeutics. Prostate Cancer Prostatic Dis. 2013;16(3):217-25.

29. Tong L, Chuang CC, Wu S, Zuo L. Reactive oxygen species in redox cancer therapy. Cancer Lett. 2015;367(1):18-25.

30. Gupta SC, Hevia D, Patchva S, Park B, Koh W, Aggarwal BB. Upsides and downsides of reactive oxygen species for cancer: the roles of reactive oxygen species in tumorigenesis, prevention, and therapy. Antioxidants & redox signaling. 2012;16(11):1295-322.

31. Liou GY, Storz P. Reactive oxygen species in cancer. Free radical research. 2010;44(5):479-96.

32. Schieber M, Chandel NS. ROS function in redox signaling and oxidative stress. Current biology : CB. 2014;24(10):R453-62.

33. Waris G, Ahsan H. Reactive oxygen species: role in the development of cancer and various chronic conditions. Journal of carcinogenesis. 2006;5:14.

34. Rao AV, Fleshner N, Agarwal S. Serum and tissue lycopene and biomarkers of oxidation in prostate cancer patients: A case-control study. Nutr Cancer. 1999;33(2):159-64.

35. Choi JY, Neuhouser ML, Barnett M, Hudson M, Kristal AR, Thornquist M, et al. Polymorphisms in oxidative stress-related genes are not associated with prostate cancer risk in heavy smokers. Cancer epidemiology, biomarkers & prevention : a publication of the American Association for Cancer Research, cosponsored by the American Society of Preventive Oncology. 2007;16(6):1115-20.

36. Conklin KA. Dietary antioxidants during cancer chemotherapy: impact on chemotherapeutic effectiveness and development of side effects. Nutr Cancer. 2000;37(1):1-18.

37. Seifried HE, McDonald SS, Anderson DE, Greenwald P, Milner JA. The

antioxidant conundrum in cancer. Cancer Res. 2003;63(15):4295-8.

38. Burk RF, Olson GE, Winfrey VP, Hill KE, Yin DP. Glutathione peroxidase-3 produced by the kidney binds to a population of basement membranes in the gastrointestinal tract and in other tissues. Am J Physiol-Gastr L. 2011;301(1):G32-G8.

39. Chu FF, Doroshow JH, Esworthy RS. Expression, characterization, and tissue distribution of a new cellular selenium-dependent glutathione peroxidase, GSHPx-GI. The Journal of biological chemistry. 1993;268(4):2571-6.

40. Chu FF, Esworthy RS, Doroshow JH, Doan K, Liu XF. Expression of plasma glutathione peroxidase in human liver in addition to kidney, heart, lung, and breast in humans and rodents. Blood. 1992;79(12):3233-8.

41. Brigelius-Flohe R, Maiorino M. Glutathione peroxidases. Biochimica et biophysica acta. 2013;1830(5):3289-303.

42. Flohe L, Gunzler WA, Schock HH. Glutathione peroxidase: a selenoenzyme. FEBS Lett. 1973;32(1):132-4.

43. Rotruck JT, Pope AL, Ganther HE, Swanson AB, Hafeman DG, Hoekstra WG. Selenium: biochemical role as a component of glutathione peroxidase. Science. 1973;179(4073):588-90.

44. Brown KM, Pickard K, Nicol F, Beckett GJ, Duthie GG, Arthur JR. Effects of organic and inorganic selenium supplementation on selenoenzyme activity in blood lymphocytes, granulocytes, platelets and erythrocytes. Clin Sci (Lond). 2000;98(5):593-9.

45. Herbette S, Roeckel-Drevet P, Drevet JR. Seleno-independent glutathione peroxidases. More than simple antioxidant scavengers. FEBS J. 2007;274(9):2163-80.

46. Cheng WH, Ho YS, Valentine BA, Ross DA, Combs GF, Jr., Lei XG. Cellular glutathione peroxidase is the mediator of body selenium to protect against paraquat lethality in transgenic mice. J Nutr. 1998;128(7):1070-6.

47. Damier P, Hirsch EC, Zhang P, Agid Y, Javoy-Agid F. Glutathione peroxidase, glial cells and Parkinson's disease. Neuroscience. 1993;52(1):1-6.

48. Bensadoun JC, Mirochnitchenko O, Inouye M, Aebischer P, Zurn AD. Attenuation of 6-OHDA-induced neurotoxicity in glutathione peroxidase transgenic mice. Eur J Neurosci. 1998;10(10):3231-6.

49. Zhang J, Graham DG, Montine TJ, Ho YS. Enhanced N-methyl-4-phenyl-1,2,3,6-tetrahydropyridine toxicity in mice deficient in CuZn-superoxide dismutase or glutathione peroxidase. J Neuropathol Exp Neurol. 2000;59(1):53-61.

50. Klivenyi P, Andreassen OA, Ferrante RJ, Dedeoglu A, Mueller G, Lancelot E, et al. Mice deficient in cellular glutathione peroxidase show increased vulnerability to malonate, 3-nitropropionic acid, and 1-methyl-4-phenyl-1,2,5,6-tetrahydropyridine. J Neurosci. 2000;20(1):1-7.

51. McClung JP, Roneker CA, Mu W, Lisk DJ, Langlais P, Liu F, et al. Development of insulin resistance and obesity in mice overexpressing cellular glutathione peroxidase. Proc Natl Acad Sci U S A. 2004;101(24):8852-7.

52. Gladyshev VN, Factor VM, Housseau F, Hatfield DL. Contrasting

patterns of regulation of the antioxidant selenoproteins, thioredoxin reductase, and glutathione peroxidase, in cancer cells. Biochem Biophys Res Commun. 1998;251(2):488-93.

53. Zachara BA, Szewczyk-Golec K, Tyloch J, Wolski Z, Szylberg T, Stepien S, et al. Blood and tissue selenium concentrations and glutathione peroxidase activities in patients with prostate cancer and benign prostate hyperplasia. Neoplasma. 2005;52(3):248-54.

54. Nalkiran I, Turan S, Arikan S, Kahraman OT, Acar L, Yaylim I, et al. Determination of gene expression and serum levels of MnSOD and GPX1 in colorectal cancer. Anticancer research. 2015;35(1):255-9.

55. Esworthy RS, Baker MA, Chu FF. Expression of selenium-dependent glutathione peroxidase in human breast tumor cell lines. Cancer Res. 1995;55(4):957-62.

56. Liu J, Hinkhouse MM, Sun W, Weydert CJ, Ritchie JM, Oberley LW, et al. Redox regulation of pancreatic cancer cell growth: role of glutathione peroxidase in the suppression of the malignant phenotype. Hum Gene Ther. 2004;15(3):239-50.

57. Baliga MS, Diwadkar-Navsariwala V, Koh T, Fayad R, Fantuzzi G, Diamond AM. Selenoprotein deficiency enhances radiation-induced micronuclei formation. Mol Nutr Food Res. 2008;52(11):1300-4.

58. Gan X, Chen B, Shen Z, Liu Y, Li H, Xie X, et al. High GPX1 expression promotes esophageal squamous cell carcinoma invasion, migration, proliferation and cisplatin-resistance but can be reduced by vitamin D. Int J Clin Exp Med.

2014;7(9):2530-40.

59. Esworthy RS, Binder SW, Doroshow JH, Chu FF. Microflora trigger colitis in mice deficient in selenium-dependent glutathione peroxidase and induce Gpx2 gene expression. Biol Chem. 2003;384(4):597-607.

60. Esworthy RS, Yang L, Frankel PH, Chu FF. Epithelium-specific glutathione peroxidase, Gpx2, is involved in the prevention of intestinal inflammation in selenium-deficient mice. J Nutr. 2005;135(4):740-5.

61. Florian S, Krehl S, Loewinger M, Kipp A, Banning A, Esworthy S, et al. Loss of GPx2 increases apoptosis, mitosis, and GPx1 expression in the intestine of mice. Free Radic Biol Med. 2010;49(11):1694-702.

62. Walshe J, Serewko-Auret MM, Teakle N, Cameron S, Minto K, Smith L, et al. Inactivation of glutathione peroxidase activity contributes to UV-induced squamous cell carcinoma formation. Cancer Res. 2007;67(10):4751-8.

63. Singh A, Rangasamy T, Thimmulappa RK, Lee H, Osburn WO, Brigelius-Flohe R, et al. Glutathione peroxidase 2, the major cigarette smoke-inducible isoform of GPX in lungs, is regulated by Nrf2. Am J Respir Cell Mol Biol. 2006;35(6):639-50.

64. Dittrich AM, Meyer HA, Krokowski M, Quarcoo D, Ahrens B, Kube SM, et al. Glutathione peroxidase-2 protects from allergen-induced airway inflammation in mice. Eur Respir J. 2010;35(5):1148-54.

65. Banning A, Deubel S, Kluth D, Zhou Z, Brigelius-Flohe R. The GI-GPx gene is a target for Nrf2. Mol Cell Biol. 2005;25(12):4914-23.

66. Yan W, Chen X. GPX2, a direct target of p63, inhibits oxidative stress-induced apoptosis in a p53-dependent manner. The Journal of biological chemistry. 2006;281(12):7856-62.

67. Serewko MM, Popa C, Dahler AL, Smith L, Strutton GM, Coman W, et al. Alterations in gene expression and activity during squamous cell carcinoma development. Cancer Res. 2002;62(13):3759-65.

68. Mork H, Scheurlen M, Al-Taie O, Zierer A, Kraus M, Schottker K, et al. Glutathione peroxidase isoforms as part of the local antioxidative defense system in normal and Barrett's esophagus. Int J Cancer. 2003;105(3):300-4.

69. Naiki-Ito A, Asamoto M, Hokaiwado N, Takahashi S, Yamashita H, Tsuda H, et al. Gpx2 is an overexpressed gene in rat breast cancers induced by three different chemical carcinogens. Cancer Res. 2007;67(23):11353-8.

70. Murawaki Y, Tsuchiya H, Kanbe T, Harada K, Yashima K, Nozaka K, et al. Aberrant expression of selenoproteins in the progression of colorectal cancer. Cancer Lett. 2008;259(2):218-30.

71. Lin YM, Furukawa Y, Tsunoda T, Yue CT, Yang KC, Nakamura Y. Molecular diagnosis of colorectal tumors by expression profiles of 50 genes expressed differentially in adenomas and carcinomas. Oncogene. 2002;21(26):4120-8.

72. Mork H, al-Taie OH, Bahr K, Zierer A, Beck C, Scheurlen M, et al. Inverse mRNA expression of the selenocysteine-containing proteins GI-GPx and SeP in colorectal adenomas compared with adjacent normal mucosa. Nutr Cancer.

2000;37(1):108-16.

73. Ouyang X, DeWeese TL, Nelson WG, Abate-Shen C. Loss-of-function of Nkx3.1 promotes increased oxidative damage in prostate carcinogenesis. Cancer Res. 2005;65(15):6773-9.

74. Naiki T, Naiki-Ito A, Asamoto M, Kawai N, Tozawa K, Etani T, et al. GPX2 overexpression is involved in cell proliferation and prognosis of castration-resistant prostate cancer. Carcinogenesis. 2014;35(9):1962-7.

75. Olson GE, Whitin JC, Hill KE, Winfrey VP, Motley AK, Austin LM, et al. Extracellular glutathione peroxidase (Gpx3) binds specifically to basement membranes of mouse renal cortex tubule cells. American journal of physiology Renal physiology. 2010;298(5):F1244-53.

76. Yang X, Deignan JL, Qi H, Zhu J, Qian S, Zhong J, et al. Validation of candidate causal genes for obesity that affect shared metabolic pathways and networks. Nat Genet. 2009;41(4):415-23.

77. Lee YS, Kim AY, Choi JW, Kim M, Yasue S, Son HJ, et al. Dysregulation of adipose glutathione peroxidase 3 in obesity contributes to local and systemic oxidative stress. Mol Endocrinol. 2008;22(9):2176-89.

78. Chung SS, Kim M, Youn B-S, Lee NS, Park JW, Lee IK, et al. Glutathione peroxidase 3 mediates the antioxidant effect of peroxisome proliferator-activated receptor γ in human skeletal muscle cells. Molecular and cellular biology. 2009;29(1):20-30.

79. Yu YP, Yu GY, Tseng G, Cieply K, Nelson J, Defrances M, et al.

Glutathione peroxidase 3, deleted or methylated in prostate cancer, suppresses prostate cancer growth and metastasis. Cancer Res. 2007;67(17):8043-50.

80. Hasegawa Y, Takano T, Miyauchi A, Matsuzuka F, Yoshida H, Kuma K, et al. Decreased expression of glutathione peroxidase mRNA in thyroid anaplastic carcinoma. Cancer Lett. 2002;182(1):69-74.

81. Schmutzler C, Mentrup B, Schomburg L, Hoang-Vu C, Herzog V, Kohrle J. Selenoproteins of the thyroid gland: expression, localization and possible function of glutathione peroxidase 3. Biol Chem. 2007;388(10):1053-9.

82. Murawaki Y, Tsuchiya H, Kanbe T, Harada K, Yashima K, Nozaka K, et al. Aberrant expression of selenoproteins in the progression of colorectal cancer. Cancer Lett. 2008;259(2):218-30.

83. Karlsson S, Klinga-Levan K. Expression analysis of human endometrial adenocarcinoma in an inbred rat model. Adv Exp Med Biol. 2008;617:503-9.

84. Zhang X, Yang JJ, Kim YS, Kim KY, Ahn WS, Yang S. An 8-gene signature, including methylated and down-regulated glutathione peroxidase 3, of gastric cancer. International journal of oncology. 2010;36(2):405-14.

85. Agnani D, Camacho-Vanegas O, Camacho C, Lele S, Odunsi K, Cohen S, et al. Decreased levels of serum glutathione peroxidase 3 are associated with papillary serous ovarian cancer and disease progression. Journal of ovarian research. 2011;4:18.

86. Brigelius-Flohe R, Kipp A. Glutathione peroxidases in different stages of carcinogenesis. Biochimica et biophysica acta. 2009;1790(11):1555-68.

87. Chen B, Rao X, House MG, Nephew KP, Cullen KJ, Guo Z. GPx3 promoter hypermethylation is a frequent event in human cancer and is associated with tumorigenesis and chemotherapy response. Cancer letters. 2011;309(1):37-45.

88. Lee OJ, Schneider-Stock R, McChesney PA, Kuester D, Roessner A, Vieth M, et al. Hypermethylation and loss of expression of glutathione peroxidase-3 in Barrett's tumorigenesis. Neoplasia. 2005;7(9):854-61.

89. He Y, Wang Y, Li P, Zhu S, Wang J, Zhang S. Identification of GPX3 epigenetically silenced by CpG methylation in human esophageal squamous cell carcinoma. Digestive diseases and sciences. 2011;56(3):681-8.

90. Falck E, Karlsson S, Carlsson J, Helenius G, Karlsson M, Klinga-Levan K. Loss of glutathione peroxidase 3 expression is correlated with epigenetic mechanisms in endometrial adenocarcinoma. Cancer cell international. 2010;10:46.

91. Yang ZL, Yang L, Zou Q, Yuan Y, Li J, Liang L, et al. Positive ALDH1A3 and negative GPX3 expressions are biomarkers for poor prognosis of gallbladder cancer. Disease markers. 2013;35(3):163-72.

92. Mohamed MM, Sabet S, Peng DF, Nouh MA, El-Shinawi M, El-Rifai W. Promoter hypermethylation and suppression of glutathione peroxidase 3 are associated with inflammatory breast carcinogenesis. Oxidative medicine and cellular longevity. 2014;2014:787195.

93. Peng DF, Hu TL, Schneider BG, Chen Z, Xu ZK, El-Rifai W. Silencing of glutathione peroxidase 3 through DNA hypermethylation is associated with lymph node metastasis in gastric carcinomas. PloS one. 2012;7(10):e46214.

94. Zhao H, Li J, Li X, Han C, Zhang Y, Zheng L, et al. Silencing GPX3 Expression Promotes Tumor Metastasis in Human Thyroid Cancer. Current protein & peptide science. 2015;16(4):316-21.

95. Lodygin D, Epanchintsev A, Menssen A, Diebold J, Hermeking H. Functional epigenomics identifies genes frequently silenced in prostate cancer. Cancer research. 2005;65(10):4218-27.

96. Yu YP, Yu G, Tseng G, Cieply K, Nelson J, Defrances M, et al. Glutathione peroxidase 3, deleted or methylated in prostate cancer, suppresses prostate cancer growth and metastasis. Cancer research. 2007;67(17):8043-50.

97. Barrett CW, Ning W, Chen X, Smith JJ, Washington MK, Hill KE, et al. Tumor suppressor function of the plasma glutathione peroxidase gpx3 in colitis-associated carcinoma. Cancer Res. 2013;73(3):1245-55.

98. Wang H, Luo K, Tan LZ, Ren BG, Gu LQ, Michalopoulos G, et al. p53-induced Gene 3 Mediates Cell Death Induced by Glutathione Peroxidase 3. Journal of Biological Chemistry. 2012;287(20):16890-902.

99. Pawlowicz Z, Zachara BA, Trafikowska U, Maciag A, Marchaluk E, Nowicki A. Blood selenium concentrations and glutathione peroxidase activities in patients with breast cancer and with advanced gastrointestinal cancer. J Trace Elem Electrolytes Health Dis. 1991;5(4):275-7.

100. Sekine Y, Osei-Hwedieh D, Matsuda K, Raghavachari N, Liu DL, Furuya Y, et al. High Fat Diet Reduces the Expression of Glutathione Peroxidase 3 in Mouse Prostate. Prostate. 2011;71(14):1499-509.

101. Conrad M. Transgenic mouse models for the vital selenoenzymes cytosolic thioredoxin reductase, mitochondrial thioredoxin reductase and glutathione peroxidase 4. Biochimica et biophysica acta. 2009;1790(11):1575-85.

102. Ufer C, Wang CC. The Roles of Glutathione Peroxidases during Embryo Development. Front Mol Neurosci. 2011;4:12.

103. Borchert A, Wang CC, Ufer C, Schiebel H, Savaskan NE, Kuhn H. The role of phospholipid hydroperoxide glutathione peroxidase isoforms in murine embryogenesis. The Journal of biological chemistry. 2006;281(28):19655-64.

104. Yant LJ, Ran Q, Rao L, Van Remmen H, Shibatani T, Belter JG, et al. The selenoprotein GPX4 is essential for mouse development and protects from radiation and oxidative damage insults. Free Radic Biol Med. 2003;34(4):496-502.

105. Imai H, Hirao F, Sakamoto T, Sekine K, Mizukura Y, Saito M, et al. Early embryonic lethality caused by targeted disruption of the mouse PHGPx gene. Biochem Biophys Res Commun. 2003;305(2):278-86.

106. Ran Q, Liang H, Gu M, Qi W, Walter CA, Roberts LJ, 2nd, et al. Transgenic mice overexpressing glutathione peroxidase 4 are protected against oxidative stress-induced apoptosis. The Journal of biological chemistry. 2004;279(53):55137-46.

107. Ran Q, Liang H, Ikeno Y, Qi W, Prolla TA, Roberts LJ, 2nd, et al. Reduction in glutathione peroxidase 4 increases life span through increased sensitivity to apoptosis. J Gerontol A Biol Sci Med Sci. 2007;62(9):932-42.

108. Savaskan NE, Borchert A, Brauer AU, Kuhn H. Role for glutathione

peroxidase-4 in brain development and neuronal apoptosis: specific induction of enzyme expression in reactive astrocytes following brain injury. Free Radic Biol Med. 2007;43(2):191-201.

109. Savaskan NE, Ufer C, Kuhn H, Borchert A. Molecular biology of glutathione peroxidase 4: from genomic structure to developmental expression and neural function. Biol Chem. 2007;388(10):1007-17.

110. Liu J, Du J, Zhang Y, Sun W, Smith BJ, Oberley LW, et al. Suppression of the malignant phenotype in pancreatic cancer by overexpression of phospholipid hydroperoxide glutathione peroxidase. Hum Gene Ther. 2006;17(1):105-16.

111. Cejas P, Garcia-Cabezas MA, Casado E, Belda-Iniesta C, De Castro J, Fresno JA, et al. Phospholipid hydroperoxide glutathione peroxidase (PHGPx) expression is downregulated in poorly differentiated breast invasive ductal carcinoma. Free radical research. 2007;41(6):681-7.

112. Guerriero E, Capone F, Accardo M, Sorice A, Costantini M, Colonna G, et al. GPX4 and GPX7 over-expression in human hepatocellular carcinoma tissues. Eur J Histochem. 2015;59(4):2540.

113. Meplan C, Hughes DJ, Pardini B, Naccarati A, Soucek P, Vodickova L, et al. Genetic variants in selenoprotein genes increase risk of colorectal cancer. Carcinogenesis. 2010;31(6):1074-9.

114. Meplan C, Dragsted LO, Ravn-Haren G, Tjonneland A, Vogel U, Hesketh J. Association between polymorphisms in glutathione peroxidase and selenoprotein P genes, glutathione peroxidase activity, HRT use and breast cancer risk. PloS one.

2013;8(9):e73316.

115. Geybels MS, Hutter CM, Kwon EM, Ostrander EA, Fu R, Feng Z, et al. Variation in selenoenzyme genes and prostate cancer risk and survival. Prostate. 2013;73(7):734-42.

116. Rejraji H, Vernet P, Drevet JR. GPX5 is present in the mouse caput and cauda epididymidis lumen at three different locations. Mol Reprod Dev. 2002;63(1):96-103.

117. Chabory E, Damon C, Lenoir A, Kauselmann G, Kern H, Zevnik B, et al. Epididymis seleno-independent glutathione peroxidase 5 maintains sperm DNA integrity in mice. J Clin Invest. 2009;119(7):2074-85.

118. Vernet P, Faure J, Dufaure JP, Drevet JR. Tissue and developmental distribution, dependence upon testicular factors and attachment to spermatozoa of GPX5, a murine epididymis-specific glutathione peroxidase. Mol Reprod Dev. 1997;47(1):87-98.

119. Li Y, Sun Z, Cunningham JM, Aubry MC, Wampfler JA, Croghan GA, et al. Genetic variations in multiple drug action pathways and survival in advanced stage non-small cell lung cancer treated with chemotherapy. Clin Cancer Res. 2011;17(11):3830-40.

120. Rusolo F, Capone F, Pasquale R, Angiolillo A, Colonna G, Castello G, et al. Comparison of the seleno-transcriptome expression between human non-cancerous mammary epithelial cells and two human breast cancer cell lines. Oncology letters. 2017;13(4):2411-7.

121. Kryukov GV, Castellano S, Novoselov SV, Lobanov AV, Zehtab O, Guigo R, et al. Characterization of mammalian selenoproteomes. Science. 2003;300(5624):1439-43.

122. Cao L, Tang J, Li Q, Xu J, Jia G, Liu G, et al. Expression of Selenoprotein Genes Is Affected by Heat Stress in IPEC-J2 Cells. Biol Trace Elem Res. 2016;172(2):354-60.

123. Shema R, Kulicke R, Cowley GS, Stein R, Root DE, Heiman M. Synthetic lethal screening in the mammalian central nervous system identifies Gpx6 as a modulator of Huntington's disease. Proc Natl Acad Sci U S A. 2015;112(1):268-72.

124. Kuchenbaecker KB, Ramus SJ, Tyrer J, Lee A, Shen HC, Beesley J, et al. Identification of six new susceptibility loci for invasive epithelial ovarian cancer. Nat Genet. 2015;47(2):164-71.

125. Utomo A, Jiang X, Furuta S, Yun J, Levin DS, Wang YC, et al. Identification of a novel putative non-selenocysteine containing phospholipid hydroperoxide glutathione peroxidase (NPGPx) essential for alleviating oxidative stress generated from polyunsaturated fatty acids in breast cancer cells. The Journal of biological chemistry. 2004;279(42):43522-9.

126. Nguyen VD, Saaranen MJ, Karala AR, Lappi AK, Wang L, Raykhel IB, et al. Two endoplasmic reticulum PDI peroxidases increase the efficiency of the use of peroxide during disulfide bond formation. J Mol Biol. 2011;406(3):503-15.

127. Wei PC, Hsieh YH, Su MI, Jiang X, Hsu PH, Lo WT, et al. Loss of the

oxidative stress sensor NPGPx compromises GRP78 chaperone activity and induces systemic disease. Mol Cell. 2012;48(5):747-59.

128. Chang YC, Yu YH, Shew JY, Lee WJ, Hwang JJ, Chen YH, et al. Deficiency of NPGPx, an oxidative stress sensor, leads to obesity in mice and human. EMBO Mol Med. 2013;5(8):1165-79.

129. Olsson AH, Volkov P, Bacos K, Dayeh T, Hall E, Nilsson EA, et al. Genome-wide associations between genetic and epigenetic variation influence mRNA expression and insulin secretion in human pancreatic islets. PLoS Genet. 2014;10(11):e1004735.

130. Johnson C, Pankratz VS, Velazquez AI, Aakre JA, Loprinzi CL, Staff NP, et al. Candidate pathway-based genetic association study of platinum and platinum-taxane related toxicity in a cohort of primary lung cancer patients. J Neurol Sci. 2015;349(1-2):124-8.

131. Guariniello S, Di Bernardo G, Colonna G, Cammarota M, Castello G, Costantini S. Evaluation of the selenotranscriptome expression in two hepatocellular carcinoma cell lines. Anal Cell Pathol (Amst). 2015;2015:419561.

132. Peng DF, Hu TL, Soutto M, Belkhiri A, El-Rifai W. Loss of glutathione peroxidase 7 promotes TNF-alpha-induced NF-kappaB activation in Barrett's carcinogenesis. Carcinogenesis. 2014;35(7):1620-8.

133. Toppo S, Vanin S, Bosello V, Tosatto SC. Evolutionary and structural insights into the multifaceted glutathione peroxidase (Gpx) superfamily. Antioxidants & redox signaling. 2008;10(9):1501-14.

134. Yamada Y, Limmon GV, Zheng D, Li N, Li L, Yin L, et al. Major shifts in the spatio-temporal distribution of lung antioxidant enzymes during influenza pneumonia. PloS one. 2012;7(2):e31494.

135. Morikawa K, Gouttenoire J, Hernandez C, Dao Thi VL, Tran HT, Lange CM, et al. Quantitative proteomics identifies the membrane-associated peroxidase GPx8 as a cellular substrate of the hepatitis C virus NS3-4A protease. Hepatology. 2014;59(2):423-33.

136. Lin DW, Porter M, Montgomery B. Treatment and survival outcomes in young men diagnosed with prostate cancer: a Population-based Cohort Study. Cancer. 2009;115(13):2863-71.

137. Welch HG, Albertsen PC. Prostate cancer diagnosis and treatment after the introduction of prostate-specific antigen screening: 1986-2005. J Natl Cancer Inst. 2009;101(19):1325-9.

138. Lemarchand L, Kolonel LN, Wilkens LR, Myers BC, Hirohata T. Animal Fat Consumption and Prostate-Cancer - a Prospective-Study in Hawaii. Epidemiology. 1994;5(3):276-82.

139. Lophatananon A, Archer J, Easton D, Pocock R, Dearnaley D, Guy M, et al. Dietary fat and early-onset prostate cancer risk. Brit J Nutr. 2010;103(9):1375-80.

140. Rohrmann S, Roberts WW, Walsh PC, Platz EA. Family history of prostate cancer and obesity in relation to high-grade disease and extraprostatic extension in young men with prostate cancer. Prostate. 2003;55(2):140-6.

141. Gong ZH, Agalliu I, Lin DW, Stanford JL, Kristal AR. Obesity is associated with increased risks of prostate cancer metastasis and death after initial cancer diagnosis in middle-aged men. Cancer. 2007;109(6):1192-202.

142. Jemal A, Bray F, Center MM, Ferlay J, Ward E, Forman D. Global Cancer Statistics. Ca-Cancer J Clin. 2011;61(2):69-90.

143. Bray F, Ren JS, Masuyer E, Ferlay J. Global estimates of cancer prevalence for 27 sites in the adult population in 2008. Int J Cancer. 2013;132(5):1133-45.

144. Zhang JJ, Dhakal IB, Zhao ZJ, Li L. Trends in mortality from cancers of the breast, colon, prostate, esophagus, and stomach in East Asia: role of nutrition transition. Eur J Cancer Prev. 2012;21(5):480-9.

145. Shimizu H, Ross RK, Bernstein L, Yatani R, Henderson BE, Mack TM. Cancers of the Prostate and Breast among Japanese and White Immigrants in Los-Angeles-County. Brit J Cancer. 1991;63(6):963-6.

146. Cook LS, Goldoft M, Schwartz SM, Weiss NS. Incidence of adenocarcinoma of the prostate in Asian immigrants to the United States and their descendants. J Urology. 1999;161(1):152-5.

147. Gronberg H. Prostate cancer epidemiology. Lancet. 2003;361(9360):859-64.

148. Klassen AC, Platz EA. What can geography tell us about prostate cancer? Am J Prev Med. 2006;30(2):S7-S15.

149. Hori S, Butler E, McLoughlin J. Prostate cancer and diet: food for

thought? Bju Int. 2011;107(9):1348-59.

150. Takahashi K, Avissar N, Whitin J, Cohen H. Purification and characterization of human plasma glutathione peroxidase: a selenoglycoprotein distinct from the known cellular enzyme. Arch Biochem Biophys. 1987;256(2):677-86.

151. Zhang X, Yang JJ, Kim YS, Kim KY, Ahn WS, Yang S. An 8-gene signature, including methylated and down-regulated glutathione peroxidase 3, of gastric cancer. Int J Oncol. 2010;36(2):405-14.

152. Lodygin D, Epanchintsev A, Menssen A, Diebold J, Hermeking H. Functional epigenomics identifies genes frequently silenced in prostate cancer. Cancer Res. 2005;65(10):4218-27.

153. Chen BS, Rao X, House MG, Nephew KP, Cullen KJ, Guo ZM. GPx3 promoter hypermethylation is a frequent event in human cancer and is associated with tumorigenesis and chemotherapy response. Cancer Lett. 2011;309(1):37-45.

154. Scholtysek C, Krukiewicz AA, Alonso JL, Sharma KP, Sharma PC, Goldmann WH. Characterizing components of the Saw Palmetto Berry Extract (SPBE) on prostate cancer cell growth and traction. Biochem Bioph Res Co. 2009;379(3):795-8.

155. Livak KJ, Schmittgen TD. Analysis of relative gene expression data using real-time quantitative PCR and the 2(T)(-Delta Delta C) method. Methods. 2001;25(4):402-8.

156. Park J-H, Walls JE, Galvez JJ, Kim M, Abate-Shen C, Shen MM, et al.

Prostatic Intraepithelial Neoplasia in Genetically Engineered Mice. The American Journal of Pathology. 2002;161(2):727-35.

157. Gingrich JR, Barrios RJ, Morton RA, Boyce BF, DeMayo FJ, Finegold MJ, et al. Metastatic prostate cancer in a transgenic mouse. Cancer Res. 1996;56(18):4096-102.

158. Greenberg NM, Demayo F, Finegold MJ, Medina D, Tilley WD, Aspinall JO, et al. Prostate-Cancer in a Transgenic Mouse. P Natl Acad Sci USA. 1995;92(8):3439-43.

159. Kaplan-Lefko PJ, Chen TM, Ittmann MM, Barrios RJ, Ayala GE, Huss WJ, et al. Pathobiology of autochthonous prostate cancer in a pre-clinical transgenic mouse model. The Prostate. 2003;55(3):219-37.

160. Park SH, Chang SN, Baek MW, Kim DJ, Na YR, Seok SH, et al. Effects of dietary high fat on prostate intraepithelial neoplasia in TRAMP mice. Lab Anim Res. 2013;29(1):39-47.

161. Fouladiun M, Korner U, Bosaeus I, Daneryd P, Hyltander A, Lundholm KG. Body composition and time course changes in regional distribution of fat and lean tissue in unselected cancer patients on palliative care - Correlations with food intake, metabolism, exercise capacity, and hormones. Cancer. 2005;103(10):2189-98.

162. Bosaeus I, Daneryd P, Svanberg E, Lundholm K. Dietary intake and resting energy expenditure in relation to weight loss in unselected cancer patients. Int J Cancer. 2001;93(3):380-3.

163. Tuxhorn JA, Ayala GE, Smith MJ, Smith VC, Dang TD, Rowley DR. Reactive stroma in human prostate cancer: Induction of myofibroblast phenotype and extracellular matrix remodeling. Clin Cancer Res. 2002;8(9):2912-23.

164. Grommes C, Landreth GE, Heneka MT. Antineoplastic effects of peroxisome proliferatoractivated receptor γ agonists. The lancet oncology. 2004;5(7):419-29.

165. Weng J, Chen C, Pinzone J, Ringel M, Chen C. Beyond peroxisome proliferator-activated receptor γ signaling: the multi-facets of the antitumor effect of thiazolidinediones. Endocrine-Related Cancer. 2006;13(2):401-13.

166. Sikka S, Chen L, Sethi G, Kumar AP. Targeting PPARγ signaling cascade for the prevention and treatment of prostate cancer. PPAR research. 2012;2012.

167. Kohler BA, Sherman RL, Howlader N, Jemal A, Ryerson AB, Henry KA, et al. Annual Report to the Nation on the Status of Cancer, 1975-2011, Featuring Incidence of Breast Cancer Subtypes by Race/Ethnicity, Poverty, and State. J Natl Cancer Inst. 2015;107(6):djv048.

168. Center MM, Jemal A, Lortet-Tieulent J, Ward E, Ferlay J, Brawley O, et al. International variation in prostate cancer incidence and mortality rates. European urology. 2012;61(6):1079-92.

169. Sohal RS, Weindruch R. Oxidative stress, caloric restriction, and aging. Science. 1996;273(5271):59-63.

170. Takebe G, Yarimizu J, Saito Y, Hayashi T, Nakamura H, Yodoi J, et al. A comparative study on the hydroperoxide and thiol specificity of the glutathione

peroxidase family and selenoprotein P. The Journal of biological chemistry. 2002;277(43):41254-8.

171. Barrett CW, Ning W, Chen X, Smith JJ, Washington MK, Hill KE, et al. Tumor suppressor function of the plasma glutathione peroxidase gpx3 in colitis-associated carcinoma. Cancer Res. 2013;73(3):1245-55.

172. Wang H, Luo K, Tan LZ, Ren BG, Gu LQ, Michalopoulos G, et al. p53-induced gene 3 mediates cell death induced by glutathione peroxidase 3. The Journal of biological chemistry. 2012;287(20):16890-902.

173. Sekine Y, Osei-Hwedieh D, Matsuda K, Raghavachari N, Liu D, Furuya Y, et al. High fat diet reduces the expression of glutathione peroxidase 3 in mouse prostate. The Prostate. 2011;71(14):1499-509.

174. Petkov PM, Cassell MA, Sargent EE, Donnelly CJ, Robinson P, Crew V, et al. Development of a SNP genotyping panel for genetic monitoring of the laboratory mouse. Genomics. 2004;83(5):902-11.

175. Kaplan-Lefko PJ, Chen TM, Ittmann MM, Barrios RJ, Ayala GE, Huss WJ, et al. Pathobiology of autochthonous prostate cancer in a pre-clinical transgenic mouse model. The Prostate. 2003;55(3):219-37.

176. Berman-Booty LD, Sargeant AM, Rosol TJ, Rengel RC, Clinton SK, Chen CS, et al. A review of the existing grading schemes and a proposal for a modified grading scheme for prostatic lesions in TRAMP mice. Toxicologic pathology. 2012;40(1):5-17.

177. Greenberg N, DeMayo F, Finegold M, Medina D, Tilley W, Aspinall J, et

al. Prostate cancer in a transgenic mouse. Proceedings of the National Academy of Sciences. 1995;92(8):3439-43.

178. Gingrich J, Barrios R, Foster B, Greenberg N. Pathologic progression of autochthonous prostate cancer in the TRAMP model. Prostate cancer and prostatic diseases. 1999;2(2):70-5.

179. Hurwitz AA, Foster BA, Allison JP, Greenberg NM, Kwon ED. The TRAMP mouse as a model for prostate cancer. Current protocols in immunology. 2001:20.5. 1-.5. 3.

180. Kaplan-Lefko PJ, Chen TM, Ittmann MM, Barrios RJ, Ayala GE, Huss WJ, et al. Pathobiology of autochthonous prostate cancer in a pre-clinical transgenic mouse model. Prostate. 2003;55(3):219-37.

181. Kypta RM, Waxman J. Wnt/beta-catenin signalling in prostate cancer. Nat Rev Urol. 2012;9(8):418-28.

182. Lu W, Tinsley HN, Keeton A, Qu Z, Piazza GA, Li Y. Suppression of Wnt/beta-catenin signaling inhibits prostate cancer cell proliferation. European journal of pharmacology. 2009;602(1):8-14.

183. Je E-C, Lca BS, Ga GA. The role of transcription factor TWIST in cancer cells. Journal of Genetic Syndromes & Gene therapy. 2013.

184. Wallerand H, Robert G, Pasticier G, Ravaud A, Ballanger P, Reiter RE, et al. The epithelial-mesenchymal transition-inducing factor TWIST is an attractive target in advanced and/or metastatic bladder and prostate cancers. Urologic oncology. 2010;28(5):473-9.

185. Kwok WK, Ling MT, Lee TW, Lau TC, Zhou C, Zhang X, et al. Up-regulation of TWIST in prostate cancer and its implication as a therapeutic target. Cancer Res. 2005;65(12):5153-62.

186. Miyake H, Hara I, Kamidono S, Eto H. Oxidative DNA damage in patients with prostate cancer and its response to treatment. The Journal of urology. 2004;171(4):1533-6.

187. Norman HA, Butrum RR, Feldman E, Heber D, Nixon D, Picciano MF, et al. The role of dietary supplements during cancer therapy. J Nutr. 2003;133(11):3794s-9s.

188. Prasad KN, Kumar A, Kochupillai V, Cole WC. High doses of multiple antioxidant vitamins: Essential ingredients in improving the efficacy of standard cancer therapy. J Am Coll Nutr. 1999;18(1):13-25.

189. Park JH, Davis KR, Lee G, Jung M, Jung Y, Park J, et al. Ascorbic acid alleviates toxicity of paclitaxel without interfering with the anticancer efficacy in mice. Nutr Res. 2012;32(11):873-83.

190. Siegel RL, Miller KD, Jemal A. Cancer statistics, 2015. CA: a cancer journal for clinicians. 2015;65(1):5-29.

191. Chi KN, Bjartell A, Dearnaley D, Saad F, Schroder FH, Sternberg C, et al. Castration-resistant prostate cancer: from new pathophysiology to new treatment targets. European urology. 2009;56(4):594-605.

192. Sun Y, Wang BE, Leong KG, Yue P, Li L, Jhunjhunwala S, et al. Androgen deprivation causes epithelial-mesenchymal transition in the prostate: implications

for androgen-deprivation therapy. Cancer Res. 2012;72(2):527-36.

193. Grommes C, Landreth GE, Heneka MT. Antineoplastic effects of peroxisome proliferator-activated receptor gamma agonists. The Lancet Oncology. 2004;5(7):419-29.

194. Weng JR, Chen CY, Pinzone JJ, Ringel MD, Chen CS. Beyond peroxisome proliferator-activated receptor gamma signaling: the multi-facets of the antitumor effect of thiazolidinediones. Endocrine-related cancer. 2006;13(2):401-13.

195. Wei S, Yang J, Lee SL, Kulp SK, Chen CS. PPARgamma-independent antitumor effects of thiazolidinediones. Cancer Lett. 2009;276(2):119-24.

196. Yu HN, Lee YR, Noh EM, Lee KS, Kim JS, Song EK, et al. Induction of G1 phase arrest and apoptosis in MDA-MB-231 breast cancer cells by troglitazone, a synthetic peroxisome proliferator-activated receptor gamma (PPARgamma) ligand. Cell biology international. 2008;32(8):906-12.

197. Colin-Cassin C, Yao X, Cerella C, Chbicheb S, Kuntz S, Mazerbourg S, et al. PPARgamma-inactive Delta2-troglitazone independently triggers ER stress and apoptosis in breast cancer cells. Molecular carcinogenesis. 2015;54(5):393-404.

198. Ye J, Yin L, Xie P, Wu J, Huang J, Zhou G, et al. Antiproliferative effects and molecular mechanisms of troglitazone in human cervical cancer in vitro. OncoTargets and therapy. 2015;8:1211-8.

199. Li MY, Deng H, Zhao JM, Dai D, Tan XY. PPARgamma pathway activation results in apoptosis and COX-2 inhibition in HepG2 cells. World journal

of gastroenterology. 2003;9(6):1220-6.

200. Shiau CW, Yang CC, Kulp SK, Chen KF, Chen CS, Huang JW, et al. Thiazolidenediones mediate apoptosis in prostate cancer cells in part through inhibition of Bcl-xL/Bcl-2 functions independently of PPARgamma. Cancer Res. 2005;65(4):1561-9.

201. Santha S, Viswakarma N, Das S, Rana A, Rana B. Tumor Necrosis Factor-related Apoptosis-inducing Ligand (TRAIL)-Troglitazone-induced Apoptosis in Prostate Cancer Cells Involve AMP-activated Protein Kinase. The Journal of biological chemistry. 2015;290(36):21865-75.

202. Mueller E, Smith M, Sarraf P, Kroll T, Aiyer A, Kaufman DS, et al. Effects of ligand activation of peroxisome proliferator-activated receptor gamma in human prostate cancer. Proc Natl Acad Sci U S A. 2000;97(20):10990-5.

203. Burstein HJ, Demetri GD, Mueller E, Sarraf P, Spiegelman BM, Winer EP. Use of the peroxisome proliferator-activated receptor (PPAR) gamma ligand troglitazone as treatment for refractory breast cancer: a phase II study. Breast cancer research and treatment. 2003;79(3):391-7.

204. Kulke MH, Demetri GD, Sharpless NE, Ryan DP, Shivdasani R, Clark JS, et al. A phase II study of troglitazone, an activator of the PPARgamma receptor, in patients with chemotherapy-resistant metastatic colorectal cancer. Cancer journal. 2002;8(5):395-9.

205. Thiery JP. Epithelial-mesenchymal transitions in tumour progression. Nature reviews Cancer. 2002;2(6):442-54.

206. Christofori G. New signals from the invasive front. Nature. 2006;441(7092):444-50.

207. Yang J, Weinberg RA. Epithelial-mesenchymal transition: at the crossroads of development and tumor metastasis. Developmental cell. 2008;14(6):818-29.

208. Frixen UH, Behrens J, Sachs M, Eberle G, Voss B, Warda A, et al. E-cadherin-mediated cell-cell adhesion prevents invasiveness of human carcinoma cells. The Journal of cell biology. 1991;113(1):173-85.

209. Ikezoe T, Miller CW, Kawano S, Heaney A, Williamson EA, Hisatake J, et al. Mutational analysis of the peroxisome proliferator-activated receptor gamma gene in human malignancies. Cancer Res. 2001;61(13):5307-10.

210. Matsuyama M, Yoshimura R. Peroxisome Proliferator-Activated Receptor-gamma Is a Potent Target for Prevention and Treatment in Human Prostate and Testicular Cancer. PPAR Res. 2008;2008:249849.

211. Sikka S, Chen L, Sethi G, Kumar AP. Targeting PPARgamma Signaling Cascade for the Prevention and Treatment of Prostate Cancer. PPAR research. 2012;2012:968040.

212. Yoshizumi T, Ohta T, Ninomiya I, Terada I, Fushida S, Fujimura T, et al. Thiazolidinedione, a peroxisome proliferator-activated receptor-gamma ligand, inhibits growth and metastasis of HT-29 human colon cancer cells through differentiation-promoting effects. Int J Oncol. 2004;25(3):631-9.

213. Takano S, Kubota T, Nishibori H, Hasegawa H, Ishii Y, Nitori N, et al.

Pioglitazone, a ligand for peroxisome proliferator-activated receptor-gamma acts as an inhibitor of colon cancer liver metastasis. Anticancer research. 2008;28(6A):3593-9.

214. Shen B, Chu ES, Zhao G, Man K, Wu CW, Cheng JT, et al. PPARgamma inhibits hepatocellular carcinoma metastases in vitro and in mice. Br J Cancer. 2012;106(9):1486-94.

215. Lee HJ, Su Y, Yin PH, Lee HC, Chi CW. PPAR(gamma)/PGC-1(alpha) pathway in E-cadherin expression and motility of HepG2 cells. Anticancer research. 2009;29(12):5057-63.

216. Magenta G, Borenstein X, Rolando R, Jasnis MA. Rosiglitazone inhibits metastasis development of a murine mammary tumor cell line LMM3. BMC cancer. 2008;8:47.

217. Liu H, Zang C, Fenner MH, Possinger K, Elstner E. PPARgamma ligands and ATRA inhibit the invasion of human breast cancer cells in vitro. Breast cancer research and treatment. 2003;79(1):63-74.

218. Yoo JY, Yang SH, Lee JE, Cho DG, Kim HK, Kim SH, et al. E-cadherin as a predictive marker of brain metastasis in non-small-cell lung cancer, and its regulation by pioglitazone in a preclinical model. Journal of neuro-oncology. 2012;109(2):219-27.

219. Yang DR, Lin SJ, Ding XF, Miyamoto H, Messing E, Li LQ, et al. Higher expression of peroxisome proliferator-activated receptor gamma or its activation by agonist thiazolidinedione-rosiglitazone promotes bladder cancer cell migration and

invasion. Urology. 2013;81(5):1109 e1-6.

220. Qin L, Gong C, Chen AM, Guo FJ, Xu F, Ren Y, et al. Peroxisome proliferatoractivated receptor gamma agonist rosiglitazone inhibits migration and invasion of prostate cancer cells through inhibition of the CXCR4/CXCL12 axis. Molecular medicine reports. 2014;10(2):695-700.

221. Lee JM, Dedhar S, Kalluri R, Thompson EW. The epithelial-mesenchymal transition: new insights in signaling, development, and disease. The Journal of cell biology. 2006;172(7):973-81.

222. Peng DF, Hu TL, Schneider BG, Chen Z, Xu ZK, El-Rifai W. Silencing of Glutathione Peroxidase 3 through DNA Hypermethylation Is Associated with Lymph Node Metastasis in Gastric Carcinomas. PloS one. 2012;7(10).

223. Agnani D, Camacho-Vanegas O, Camacho C, Lele S, Odunsi K, Cohen S, et al. Decreased levels of serum glutathione peroxidase 3 are associated with papillary serous ovarian cancer and disease progression. J Ovarian Res. 2011;4.

224. Brigelius-Flohe R, Kipp A. Glutathione peroxidases in different stages of carcinogenesis. Bba-Gen Subjects. 2009;1790(11):1555-68.

225. He YL, Wang YJ, Li P, Zhu ST, Wang JX, Zhang ST. Identification of GPX3 Epigenetically Silenced by CpG Methylation in Human Esophageal Squamous Cell Carcinoma. Digestive diseases and sciences. 2011;56(3):681-8.

226. Mohamed MM, Sabet S, Peng DF, Nouh MA, El-Shinawi M, El-Rifai W. Promoter Hypermethylation and Suppression of Glutathione Peroxidase 3 Are Associated with Inflammatory Breast Carcinogenesis. Oxid Med Cell Longev.

2014.

227. Chang SN, Lee JM, Oh H, Park JH. Glutathione peroxidase 3 inhibits prostate tumorigenesis in TRAMP mice. Prostate. 2016.

국문 초록

전립선암에서 GPx3의
종양 억제 유전자로서의 기능에 관한 연구

서울대학교 대학원

수의학과 수의병인생물학 및 예방수의학 전공

(실험동물의학)

장 서 나

(지도교수: 박재학)

전립선암은 서양 남성암 중 가장 흔한 암으로 높은 발생 빈도를 보이며, 최근에는 젊은 층에서도 많이 나타나고 있다. 이러한 전립선암의 원인으로서 동물성 지방이 높게 함유된 서구화된 식단이 발병의 중요한 위

험인자로 알려져 있다. 동물성 지방은 신체 내 산화스트레스 및 반응성 산소종 정도를 증가시키는데, 산화스트레스를 감소시키는 항산화 효소 중 GPx3 유전자가 세포내 항산화 시스템에서 중요한 역할을 하고 있다. GPx3는 산화적 손상으로부터 세포를 보호하는 것뿐만 아니라 전립선암 조직에서 발현이 감소되어 있는 것으로 보고된 바 있다. 그러나 이러한 GPx3 유전자의 발현이 전립선암 발생, 진행, 발달에 미치는 영향과 관련 기전의 연구가 보고되지 않았으며, 나아가서 전립선암 전이에서의 역할 또한 거의 보고된 바가 없다. 이에 본 연구에서는 전립선암 세포 및 전립선암 형질전환 마우스 모델을 이용하여 GPx3의 종양 억제 유전자로서의 역할에 대한 연구를 진행하였다.

첫 번째 장에서는 전립선암 자연발생 형질전환 마우스인 TRAMP 마우스를 이용하여 전립선암 발생 초기 단계에서부터 고지방 식이가 항산화 효소 GPx3 유전자의 발현에 미치는 영향을 평가하였다. 이를 위하여 6주령 마우스에 고지방 식이(45% Kcal 지방 함유) 및 정상 식이(10% Kcal 지방 함유)를 각각 5주 및 10주간 급이하였다. 그 결과 마우스의 연령이 높을수록 또한 고지방 식이를 급이한 경우에 조직병리학적으로 전립선암 정도가 높게 나타났으며, 고지방 식이를 급이한 마우스의 전립선 조직에서 GPx3 유전자의 mRNA 및 단백질 발현이 감소된 것이 관찰되었다. PC-3 사람 전립선암 세포에 콜레스테롤을 처치한 경우에는

암세포의 증식이 증가되면서 GPx3 유전자의 mRNA 및 단백질 발현이 감소되고, 배양 배지 내 H_2O_2 정도가 높게 나타났다. 또한 TGZ 처치에 의하여 GPx3 mRNA 발현이 증가된 경우에는 PC-3 전립선암 세포의 증식이 감소하고 H_2O_2는 감소되었다. 이는 동물성 지방 식이가 GPx3 유전자의 발현을 억제하고 전립선암 세포의 증식을 유도함으로써 전립선암 발생 및 진행을 촉진할 수 있음을 보여준다.

두 번째 장에서는 GPx3 유전자 발현이 감소된 TRAMP 마우스를 제작함으로써, 전립선암 발달 과정에서 GPx3 유전자 발현의 억제가 미치는 영향을 직접적으로 평가하고자 하였다. 8주, 16주, 20주령의 TRAMP, TRAMP / GPx3 HET, TRAMP / GPx3 KO 마우스에서 전립선암 발생 빈도와 정도를 비교 및 분석하였다. TRAMP 마우스에서 GPx3 발현은 감소되었으며, 제작된 GPx3 KO 마우스에서는 mRNA 및 단백질 수준에서 GPx3 발현이 검출되지 않았다. TRAMP 마우스에서 GPx3 발현을 억제 시킨 경우, 비뇨생식기계의 무게가 증가되었고, 조직병리학적으로 전립선암 정도가 높게 나타났으며, 조직 내 세포 증식률도 높게 관찰되었다. 또한 TRAMP / GPx3 HET 및 KO 모두에서 전립선암 발생률이 증가되었으며, 이는 Wnt/β-catenin 경로의 활성화를 동반하였다. 이러한 연구 결과는 GPx3가 전립선암 발달 과정에서 종양 억제 유전자로서의 기능을 가질 수 있다는 것을 보여주며, 처음으로 마우스 모델을 이용

하여 분자 유전적 증거를 제시했다는 점에서 그 의의를 갖는다.

세 번째 장에서는 TGZ가 세포의 성장, 이주, 침윤에 미치는 영향과 이와 관련된 기전을 PC-3 사람 전립선암 세포를 이용하여 밝히고자 하였다. TGZ는 합성 PPARγ 작용제로서 전립선암을 포함한 다양한 암에서 항암제로서의 잠재성을 갖고 있는 것으로 보고되고 있다. PC-3 전립선암 세포에 TGZ를 처치한 경우, 농도 의존적으로 암세포의 이주와 침윤을 억제함을 보였다. 또한 TGZ 처치는 E-cadherin과 GPx3 유전자의 mRNA 및 단백질 발현 증가를 유도하였다. 여기에 PPARγ 길항제인 GW9662를 처치한 경우 이러한 효과가 경감되는 것으로 관찰되었으며, 이는 PPARγ 의존적인 경로가 연관되어 있음을 나타낸다. 이를 통하여 PC-3 전립선암 세포에서 TGZ에 의한 암세포 이주 억제 및 침윤 억제 효과는 E-cadherin 및 GPx3 유전자의 발현 증가를 통하여 나타날 수 있음을 제시하였다.

본 연구에서는 동물성 지방에 의하여 전립선암 진행이 더 심화되며, 이때 GPx3 유전자 발현이 감소한다는 것을 PC-3 전립선암세포 및 TRAMP 마우스를 이용하여 확인하였다. 그리고 TRAMP 마우스에서 GPx3 유전자 발현을 억제하였을 때 전립선암 발달에 직접적으로 영향을 미친다는 것을 보임으로써, GPx3 유전자 발현이 전립선암 발생, 진행, 발달에 미치는 영향을 규명하였다. 또한 첫 번째 연구에서 사용하였

던 TGZ를 PC-3 전립선암 세포에 처치한 연구에서는 E-cadherin과 GPx3 유전자 발현이 증가되었을 때 전립선암 세포의 이주 및 침윤이 억제됨을 보임으로써, GPx3 유전자와 전립선암 전이와의 연관성을 확인하였다. 따라서 본 연구를 통해 궁극적으로 GPx3가 종양 억제 유전자로서 중요한 역할을 할 수 있음을 제시하였다. 본 연구가 전립선암에 미치는 산화스트레스의 영향에 대한 이해를 높이는데 활용되고, 새로운 전립선암 치료제 개발에 활용될 수 있을 것으로 기대한다.

주요어: 전립선암, GPx3, TRAMP, 종양 억제 유전자, 종양 발생, 종양 전이

학 번: 2010-21652